Performance Analysis of Network-Coded Cooperation Systems

by

Ali Reza Heidarpour

A thesis submitted in partial fulfillment of the requirements for the degree of

Doctor of Philosophy

in

Communications

Department of Electrical and Computer Engineering
University of Alberta

Abstract

Today's wireless networks face scarcity and expense of the radio spectrum, unprecedented increase in data traffic, and excessive energy consumption. The vision of the next generation of wireless networks is to overcome these challenges and provide seamless and ubiquitous wireless connectivity.

Cooperative communication (CC) and network coding (NC), referred to as network-coded cooperation (NCC), appears to be the ideal architecture for future wireless networks. The main focus of this thesis is to propose and analyze new NCC transmission strategies and study their performance under practical implementation issues.

The first part of this thesis focuses on design and analysis of new transmission strategies in single-antenna NCC systems. Firstly, we propose a two-step user-relay selection in multiuser multirelay NCC systems to exploit both multiuser diversity (MUD) and cooperative diversity (CD). Taking into account practical constraints, we suggest the most generalized user-relay selection (GURS) scheme. It selects any arbitrary subsets of users and any arbitrary subsets of relays. Our analytical results and design guidelines generalize and subsume all existing results as special cases. Secondly, we investigate the performance of a NCC system in an underlay cognitive radio network (CRN). Compared to the existing literature, the proposed CRN NCC has four main distinguishable features: i) it is applicable to general CRN NCC network settings with arbitrary number of sources and relays; ii) it considers general relay selection (RS) and independent and non-identically distributed (i.n.i.d.) Nakagami-m fading channels; iii) it accounts for maximum transmit power at the secondary network (SN) and assumes

secondary-to-primary (S2P) and primary-to-secondary (P2S) interference links; and iv) it provides a generalized version of previous works and includes existing results in the literature as special cases.

Despite the rich literature on NCC, all existing works have predominantly been focused on relay networks with single-antenna terminals. The applications of multiple-input multiple-output (MIMO) techniques on NCC networks are also interesting, which have been lacking in the literature. Furthermore, not only MIMO NCC is not studied in the literature, but also the existing NCC RS strategies rely on the "*max-min*" end-to-end (E2E) criterion. This RS strategy will be too complicated even for a network with single-antenna terminals as it requires global channel state information (CSI). Such high signaling overhead leads to difficult implementation of NCC system with RS, especially for a network with a large number of branches. Attracted by the benefits of multi-antenna techniques in enhancing NCC system performance, in the second part of the thesis, we firstly extend single-antenna NCC to a multi-antenna scenario. A new RS strategy for NCC systems is also proposed and analyzed. It can substantially reduce the required signaling overhead for RS-based NCC, without sacrificing the performance. Secondly, we investigate the performance of RS MIMO NCC systems under practical implementation issues such as co-channel interference (CCI) and outdated CSI.

Preface

The results of **Chapter** 2 were published in the following papers:

A. R. Heidarpour, M. Ardakani, C. Tellambura, M. Di Renzo, and M. Uysal, "**Network-coded cooperative systems with generalized user-relay selection**," *IEEE Trans. Wireless Commun.*, vol. 19, no. 11, pp. 7251–7264, 2020.

A. R. Heidarpour, M. Ardakani, and C. Tellambura, "**Generalized relay selection for network-coded cooperation systems**," *IEEE Commun. Lett.*, vol. 21, no. 12, pp.2742–2745, Dec. 2017.

A. R. Heidarpour, M. Ardakani, C. Tellambura, and M. Di Renzo, "**Generalized user-relay selection in network-coded cooperation systems**," in *Proc. IEEE Int .Conf. on Commun. (ICC)*, Shanghai, China, May 2019, pp. 1-6.

The results of **Chapter** 3 will be presented in the IEEE Intl. Conf. on Commun. (ICC) 2021 as:

A. R. Heidarpour, M. Ardakani and C. Tellambura, "**Underlay cognitive network-coded cooperation over Nakagami-m fading channels**," to be presented in the *Proc. IEEE Intl. Conf. on Commun. (ICC)*, Montreal, Canada, Jun. 2021.

The results of **Chapter** 4 were published in the following papers:

A. R. Heidarpour, M. Ardakani, C. Tellambura and M. Di Renzo, "**Relay selection in network-coded cooperative MIMO systems**," *IEEE Trans.*

Commun., vol. 67, no. 8, pp. 5346-5361, Aug. 2019.

A. R. Heidarpour and M. Ardakani, "**Diversity analysis of MIMO network coded cooperation systems with relay selection**," in *Proc. 86th Veh. Technol. Conf. (VTC Fall)*, Toronto, Canada, Sep. 2017, pp. 1-6.

The results of **Chapter** 5 were published in the following paper:

A. R. Heidarpour, M. Ardakani and C. Tellambura, "**Network-coded cooperative MIMO with outdated CSI and CCI**," in *Proc. 92nd Veh. Technol. Conf. (VTC Fall)*, Victoria, BC Canada, Nov. 2020, pp. 1-5.

To Mom, Dad,
and Maryam.

Acknowledgements

First and foremost, I express my utmost gratitude and respect to my supervisors, Dr. Masoud Ardakani and Dr. Chintha Tellambura who gave me the complete freedom to pursue my research interests and provided invaluable guidance, excellent mentorship, and continuous support which have been pivotal in the progress of my PhD study. I owed an inestimable debt to them for my professional and academic development.

I would also wish to thank Dr. Marco Di Renzo and Dr. Murat Uysal for their invaluable feedback and collaboration while coauthoring publications.

I extend my sincere gratitude to my PhD examining committee; Dr. Yindi Jing, Dr. Majid Khabbazian, and Dr. Raviraj Adve dedicating their precious time to read my thesis and providing useful feedback. I would also thank Dr. Behrad Gholipour for chairing my final PhD defense.

I am also especially grateful to the faculty and the staff of the ECE for their support and for creating a wonderful environment for teaching and research excellence. My special thanks goes to Ms. Pinder Bains, the ECE graduate student advisor. I would also like to gratefully acknowledge the generous financial support I received from a three-year Alberta Innovates Graduate Student Scholarship which made the completion of this work possible.

A special thank to my beloved parents, my sister, and my brother for their immeasurable support and encouragement in every facet of my life.

Finally, but most importantly, I am completely indebted to the most precious earning in my life, my wife Maryam, for her inspiration and unconditional support during my PhD journey. I owe to you all I have ever accomplished.

Acronyms

5G   fifth generation

6G   sixth generation

ABEP   average bit error probability

AF   amplify-and-forward

ANC   analog network coding

AWGN   additive white Gaussian noise

BS   base station

CC   cooperative communication

CCI   co-channel interference

CD   cooperative diversity

CDF   cumulative distribution function

CRN   cognitive radio network

CSI   channel state information

DF   decode-and-forward

DMT   diversity-multiplexing tradeoff

DNC   digital network coding

E2E   end-to-end

EH   energy harvesting

GF   Galois field

GURS   generalized user-relay selection

HetNet   heterogeneous network

i.i.d.   independent and identically distributed

i.n.i.d.   independent and non-identically distributed

LTE   long term evolution

MDS   maximum distance separable

MIMO   multiple-input multiple-output

ML   maximum likelihood

MRC   maximal ratio combining

MRS   multiple relay selection

MUD   multiuser diversity

NC   network coding

NCC   network-coded cooperation

NOMA   non-orthogonal multiple access

OMA   orthogonal multiple access

OP   outage probability

P2S   primary-to-secondary

PDF   probability density function

PN   primary network

PR   primary receiver

PT   primary transmitter

QoS   quality of service

RAS   random antenna selection

RF   radio frequency

RS   relay selection

RV   random variable

S2P   secondary-to-primary

SINR   signal-to-interference-plus-noise ratio

SN   secondary network

SNR   signal-to-noise ratio

SRS   single relay selection

SWIPT   simultaneous wireless information and power transfer

TAS   transmit antenna selection

Table of Contents

List of Tables

List of Figures

Chapter 1

Introduction

Over the past few years, the demand for new audio, video, and data services has snowballed and continues growing from year to year. Billions of devices are connected to wireless networks, and simultaneously each device requires high data rates to support data-hungry applications, including high-definition video streaming, online gaming, virtual reality, and social networks. It is predicted that the number of Internet-connected devices will exceed 125 billion worldwide by 2030 [1, 2]. These connected devices will transform the quality of our lives. Smart homes, smart cities, automated transportation and water distribution, environmental monitoring, and urban security are only a few examples of how the future wireless networks will improve our lives' quality, efficiency, and safety.

The next generation of wireless networks is expected to offer high data rates, ultra-reliable low latency, and improved energy efficiency to accommodate the massive data traffic. The fifth-generation (5G) wireless technologies are under development worldwide. 5G can handle billions of heterogeneous devices with very high data rates at very low latency [3]. While 5G is still at an early stage, efforts from academia and industry have started to conceptualize the next generation of wireless communication systems (6G), aiming at providing high-quality communication services for the future requirements of the 2030s. 6G vision is to deliver up to 1 Tb/s peak data rates, less than 1 ms end-to-end (E2E) latency, very high energy efficiency improvement, and

operate over vast frequency bands (73 GHz-140 GHz and 1 THz-3 THz) [4]. Achieving these goals requires developing novel wireless system architectures and transmission techniques to efficiently use spectrum and energy to satisfy future wireless requirements.

1.1 Cooperative Relay Networks

Cooperative communication (CC), also called cooperative diversity (CD), exploits spatial diversity by forming a virtual antenna array through the spatially distributed relay nodes [5,6]. Cooperative relay networks have been thus adopted by several wireless system standards [7] and are also considered as a key enabler technology for future wireless communications [8].

In general, CC systems require two phases to transmit a message from the source to the destination: i) the broadcasting phase; and ii) the relaying phase. During the former, the source transmits its information, while the relays and the destination listen. During the latter, one or multiple relay(s) process the received signal and then retransmit to the destination. However, in conventional multisource multirelay CC systems, each relay transmission must be coupled with a source transmission. Thus, each relay utilizes multiple resource blocks when forwarding messages for different sources. This time-slot usage results in throughput loss and becomes a significant performance-limiting factor for multisource CC networks. Inspired by the seminal work on network coding (NC) for wired networks [9], the joint use of CC and NC, which is referred to as network-coded cooperation (NCC), has been proposed to improve the spectral efficiency of CC systems [10–12]. The main idea is that the relay node invokes NC by linearly combining data packets received from multiple sources and then forwards the resulting signal to the destination. Thus, this transmission paradigm reduces the number of relay transmissions, which in turn significantly improves the spectral efficiency.

NCC can be classified according to the processing strategy at the relays. The most frequently used NCC relaying strategies are the amplify-and-forward (AF) and the decode-and-forward (DF) protocols. In what follows, we briefly explain the

2
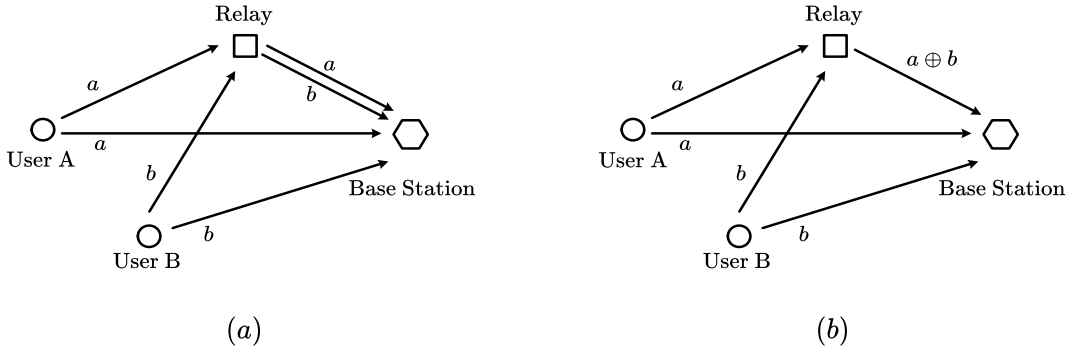
Fig. 1.1: A simple network where two mobile users transmit on the uplink to the BS: (a) conventional CC and (b) NCC.

underlying differences between these two NCC relaying strategies: **DF-based NCC:** DF-based NCC is frequently used for "*unidirectional*" (one-way) NCC networks where multiple sources transmit their messages to a single destination using both direct source-destination links and indirect source-relay-destination links. This scheme is usually referred to as "*digital*" NC (DNC) [13], since each relay performs NC at the bit (or symbol) level in the Galois field (GF).

AF-based NCC: AF-based NCC is widely used in "*bidirectional*" (two-way) NCC networks where two sources exchange their messages through the aid of one or multiple relays and NC is applied on signal level, rather than estimated bits or symbols. This scheme is referred to as "*analog*" NC (ANC) [14–17].

Therefore, DF-based NCC has a different system model and applications and works quite differently when compared to AF-based scheme. In this thesis, we focus on multisource multirelay unidirectional DF-based NCC systems.

Fig. 1.1 depicts a simple network where two mobile users transmit on the uplink to the base station (BS). In the first phase (broadcasting phase), two mobile users forward their messages in orthogonal channels while the relay overhears and decodes the message. In the second phase (relaying phase), the relay forwards the users' messages to the BS in orthogonal channels. Thus, four time-slots are required for two users. On the other hand, in NCC, the relay combines the messages from two users by employing NC and then forwards the coded message to the BS. Thus, a total of three time-slots are required for one round of cooperation; two time-slots for the broadcasting phase
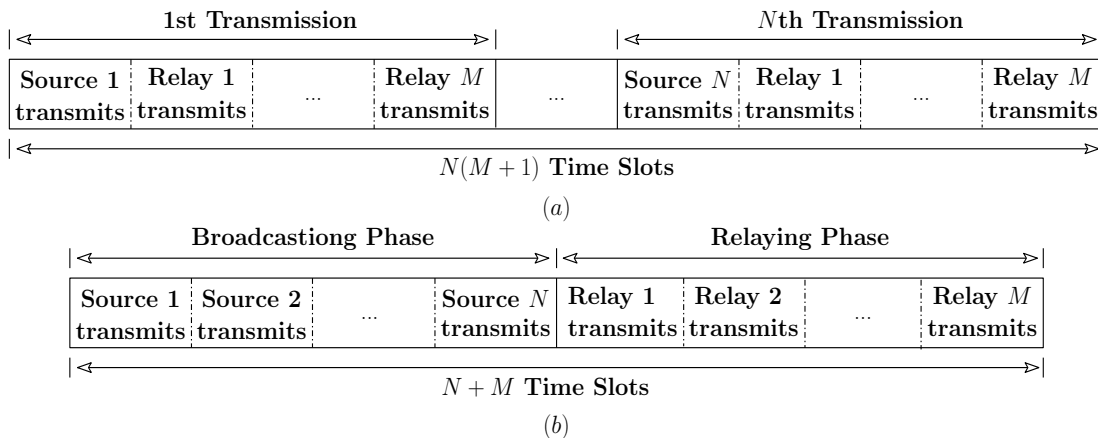
Fig. 1.2: Time-resource allocation for general N-source, M-relay cooperative networks: (*a*) conventional CC and (*b*) NCC.

and one time-slot for the relaying phase.

Now, consider the general case of multisource multirelay cooperative network. Fig. 1.2 illustrates the time-resource allocation for an N-source, M-relay cooperative network. In CC, each message of a single source is transmitted in $M + 1$ time-slots. Thus, a total number of $N(M + 1)$ time-slots are required. On the other hand, in NCC, N sources are able to benefit from each relay transmission. In particular, during the broadcasting phase, the sources transmit their information to the destination in N orthogonal time-slots and the relays overhear the transmissions. During the relaying phase, each relay linearly combines the received packets from the N sources and then forwards the resulting network-coded packet to the destination in a single time-slot. As a result, only $N + M$ time-slots are required, which is much smaller than $N(M + 1)$ time-slots consumed by CC. Since NCC reduces the total transmission time, network throughput is significantly increased.

1.2 Performance Metrics

1.2.1 Outage Probability

In N-source M-relay NCC networks, the destination receives $N + M$ packets; N packets from the sources and M network-coded packets from the relays. Due to the severe

channel fading some of the links might be in outage and thereby only a subset of packets can be successfully recovered by the destination. If the destination receives at least N error-free packets, either from the sources or from the relays, it is capable of recovering N original packets; otherwise, an outage occurs.

The overall outage probability (OP) of NCC thus depends upon the outage events of single-hop links. Therefore, the OP calculation for each single-hop link is required to evaluate the E2E performance.

The single-hop link $i \to j$ is in outage if it cannot support the fixed transmission rate R_0 (in bits per channel use). The corresponding OP is given by

$$\mathcal{P}_{o_{ij}}(R_0) = \mathsf{Pr}\{\mathcal{I}(\gamma_{ij}) < R_0\}, \tag{1.1}$$

where $\mathcal{I}(\gamma_{ij})$ is the instantaneous mutual information corresponding to the received signal-to-noise ratio (SNR) γ_{ij}. Noting that $\mathcal{I}(\gamma_{ij}) = \log_2(1+\gamma_{ij})$, (1.1) can be rewritten as

$$\mathcal{P}_{o_{ij}} = \mathsf{Pr}\{\gamma_{ij} < \gamma_{th}\} = F_{\gamma_{ij}}(\gamma_{th}), \tag{1.2}$$

where $\gamma_{th} = 2^{R_0} - 1$.

1.2.2 Diversity Order

In asymptotically high-SNR regime ($\rho \to \infty$), the OP of the system can be written as

$$\lim_{\rho \to \infty} \mathcal{P}_{\text{out}} \overset{\rho \to \infty}{\approx} (G_c.\rho)^{-G_d}, \tag{1.3}$$

where the variable G_d in (1.3) denotes the diversity order and determines the slope of the OP curve. This is given by

$$G_d = - \lim_{\rho \to \infty} \frac{\log(\mathcal{P}_{\text{out}})}{\log(\rho)}. \tag{1.4}$$

On the other hand, G_c represents the coding gain and quantify the SNR advantage of the asymptotic OP with respect to the reference curve ρ^{-G_d}.

5

1.3 Related Literature on NCC

The design and analysis of NCC, in general, build upon two error propagation models: i) the "*erasure channel*" model; and ii) the "*error channel*" model. In the former, the erroneous sources' packets are discarded at the relays and thus no error propagation occurs. In the latter, however, the erroneous packets are allowed to propagate through the network, but error propagation is counteracted at the destination with the aid of appropriate "*error-aware*" demodulators. In what follows, we will provide a summary of research works under these two channel models.

1.3.1 Erasure Channel Model

The performance analysis of NCC under the erasure channel model has been studied in the literature. In particular, in [18] the authors investigate network codes design for general N-source, M-relay wireless networks with a single destination, where codes are constructed in q-ary GF NC and relays use DF protocol. Their results reveal that binary NC is not optimal to achieve full diversity order in a cooperative network with $M > 1$. Instead, a non-binary NC based on maximum distance separable (MDS) codes is shown to provide the full diversity order of $M + 1$ for any arbitrary M and N. Furthermore, the diversity order of $M - N + 1$ can be achieved if direct source-to-destination channels are not available, which is equivalent to achieving Singleton bound in error correction codes. The OP and diversity-multiplexing tradeoff (DMT) [19] of NCC based on DF relaying has been further studied in [20], showing that NCC is capable of achieving full diversity order and outperforms cooperative space-time coding [6] and relay selection (RS) based CC [21] in terms of DMT. These works have triggered other research efforts to investigate the performance of NCC systems for various system models (see e.g., [22–25]).

1.3.2 Error Propagation Model

Several other seminal works have also studied the performance of NCC under error channel model. For instance, [26, 27] investigated the performance of NCC with binary

modulation and binary NC. In particular, the average bit error probability (ABEP) was computed for two types of demodulaters; a hard decision based demodulator [26] and a NCC maximal ratio combining (MRC) demodulator [27]. Furthermore, guidelines for network code design were developed and the impact of error propagation on the diversity order and coding gain was quantified. In [28], the performance of the XOR-based NCC with RS for multiple source-destination pairs was analyzed. Later, the performance of repetition-based and RS-based NCC protocols were investigated in [29], assuming NCC-MRC demodulator and arbitrary modulation order and arbitrary GF size. Following [29], the exact and asymptotic expressions of the OP for single RS (SRS) and multiple RS (MRS) protocols were further derived in [30]. More specifically, SRS protocol selects the relay with the highest E2E SNR out of M available relays. On the other hand, in MRS protocol L highest-SNR relays are selected. The results revealed that SRS achieves diversity order of only two [29,30]. This contrasts with conventional CC systems where SRS achieves the full diversity order of $M+1$ [21,31]. Further, MRS achieves full diversity order under a restrictive condition where the number of selected relays must be at least equal to the number of sources [29,30].

1.4   Motivations and Contributions

Multiuser diversity (MUD) is inherent in a network of spatially separated users and provides a form of diversity against fading [19]. The basic premise of MUD is to exploit channel variations among those users by allocating resources to the best users experiencing good channel qualities. The application of MUD to conventional CC has been studied [32–34], demonstrating that MUD-based CC with RS exploits both MUD and CD gains and thus offers substantial performance improvement. The application of MUD to NCC has tremendous potential to improve the performance of NCC systems further [35,36]. Therefore, we propose MUD-based NCC in an N-user M-relay network where subsets of users and relays are selected to exploit both MUD and CD in a multiuser multirelay NCC system.

Effective resource allocation strategies are key design considerations in 5G and

beyond. The best solution is to allocate a resource block to the best user experiencing the highest SNR, which maximizes the cell throughput from a spectral efficiency perspective. However, scheduling based on max-SNR does not account for other important factors such as fairness, cell-edge coverage, and energy efficiency. This necessitates a flexible resource allocation mechanism that provides a good trade-off among different performance objectives (e.g., throughput, delay, or energy). On the other hand, traffic load disparity, inherited from scheduling schemes based on the max-SNR criterion, inevitably leads to sub-optimal resource allocations across the network, particularly in Long Term Evolution-Advanced (LTE-Advanced) heterogeneous networks (HetNets) with diverse quality of service (QoS) requirements. Under these circumstances, user/relay selection may be based on factors other than SNR. Furthermore, there are several practical scenarios that selecting the best-SNR users/relays might be inefficient or even infeasible. For instance, the scheduler may fail to select the best-SNR users/relays in the presence of imperfect channel state information (CSI); the best-SNR users may not have any data packet to transmit, and the best-SNR users/relays might run out of the battery at the time of transmission. These observations suggest that the ability to select an arbitrary set of users and/or relays is beneficial. Thus, the performance of generalized user selection [37–39] and generalized RS [40–42] have been separately and extensively studied recently. However, the performance analysis of generalized user-relay selection (GURS) has not been investigated in the literature. Thus, we propose the most GURS scheme that selects any arbitrary subsets of users and any arbitrary subsets of relays subject to any practical constraints [43, 44]. Our analysis evaluates the performance loss incurred when sub-optimal user-relay selection is performed and hence provides the basis for better scheduling and efficient resource management algorithms in 5G and beyond.

Rapid evolution in wireless communications and new data services necessitate a large increase in data rates coupled with higher demands for the radio spectrum. The radio spectrum, however, is a scarce and expensive natural resource and is regulated by governmental agencies. Cognitive radio networks (CRNs), which enable dynamic and flexible spectrum sharing between the primary (licensed) and secondary (non-licensed)

8

systems, have been acknowledged as a promising technique to ease the scarcity of radio spectrum resources. The most common paradigms in spectrum sharing systems are the interweave, overlay, and underlay [45]. The underlay paradigm is of particular interest since both primary and secondary users transmit concurrently under regulatory constraints over a given spectrum slot; thereby achieving high spectral efficiency and improved spectrum utilization. These benefits, however, may be limited, since the secondary transmitters have to reduce their transmit power to satisfy strict interference constraints in the primary network (PN). And the secondary receivers are being subject to interference incurred by the primary transmitter (PT). Therefore, when designing spectrum sharing underlay systems, there are two conflicting objectives: i) protecting the PN from the secondary network (SN) interference by keeping the secondary transmit powers below the interference threshold; and ii) preserving the QoS of the SN. The former is of higher priority, imposing strict regulation on the secondary transmit powers, leading to a limited E2E performance and unacceptable link quality at the SN. The latter necessitates an efficient mechanism for the SNs that are subject to power and interference constraints. One promising candidate of such a mechanism is NCC systems that exploit NC and CC systems' benefits. While CRNs with conventional CC have been widely studied in the literature [46–49], the application of NCC to CRNs is limited to a few studies, focusing mainly on simple network topologies and Rayleigh fading channels [50–53]. However, modern wireless networks are composed of a massive number of nodes with complicated network topologies. Further, compared to Rayleigh fading, the Nakagami-m model has greater accuracy in matching the experimental data and includes Rayleigh fading ($m = 1$) a special case. Thus, we investigate the performance of an underlay cognitive multisource multirelay NCC with general RS. Our analysis can apply to many network settings, and more importantly, subsumes the case of generalized channels, ranging from independent and identically distributed (i.i.d.) Rayleigh fading to independent and non-identically distributed (i.n.i.d.) Nakagami-m fading.

Despite the rich literature on NCC, all existing works have predominantly been focused on relay networks with single-antenna terminals. Employing multiple antennas

at the transmitter and/or receiver has been identified as a key enabling technique for future generation of wireless networks and has been broadly investigated in the context of CC systems [54–57]. The applications of multiple-input multiple-output (MIMO) techniques on NCC networks are also interesting, which have been lacking in the literature. Furthermore, not only MIMO NCC is not studied in the literature, but also the existing NCC RS strategies rely on the "*max-min*" E2E criterion. This selection strategy (called Strategy $\mathcal{A}$) will be too complicated even for a network with single-antenna terminals as it requires global CSI. Such high signaling overhead leads to difficult implementation of NCC system with RS, especially for a network with a large number of branches. It is thus important to devise efficient RS schemes with limited overhead. One of the key contributions of our work here is to propose and analyze a new RS strategy (Strategy $\mathcal{B}$) based on the local CSI of the relay-to-destination channels (rather than global CSI), resulting in a significantly reduced signaling overhead [58].

Many prior works on NCC build upon the assumption that the direct links between the sources and the destination are available. This might not be a realistic assumption, in particular, when the sources are far from the destination and the direct links experience heavy path-loss and shadowing. This thesis studies the performance of RS NCC in the absence of direct source-destination links. Further, so far, only one paper investigated the impact of outdated CSI on the performance of single-antenna RS NCC [59]. But this work has not been extended to RS MIMO NCC. Beside, the performance of NCC subjected to co-channel interference (CCI) is not available. However, because of the aggressive frequency reuse, CCI (e.g., CCI from neighboring cells) is an important constraint for 5G and beyond. Thus, it is of both theoretical and practical interest to study the impact of outdated CSI and CCI on the performance of RS MIMO NCC. Therefore, we study the adverse effect of outdated CSI and CCI on the performance of RS MIMO NCC systems [60].

1.5 Thesis Outline

Motivated by key observations in Section 1.4, this thesis consists of two parts. The first part of this thesis (**Chapter** 2 and 3) focuses on design and analysis of new transmission strategies for single-antenna NCC and presents: i) the most GURS scheme in the literature; ii) the application of NCC to CRNs.

Attracted by the benefits of multi-antenna techniques in enhancing NCC system performance, in the second part of the thesis (**Chapter** 4 and 5), i) we extend single-antenna NCC to a multi-antenna scenario; and ii) investigate the performance of RS MIMO NCC systems under practical implementation issues.

Finally, **Chapter** 6 presents the conclusions and suggests directions for future works.

1.6 Contributions not Included in the Thesis

The following publications are some extensions/special cases of the above problems and are not included in the thesis.

A. R. Heidarpour, M. Ardakani and C. Tellambura, "**Multiuser diversity in network-coded cooperation: outage and diversity analysis**," *IEEE Commun. Lett.*, vol. 23, no. 3, pp. 550-553, Mar. 2019.

A. R. Heidarpour, M. Ardakani and C. Tellambura, "**Network-coded cooperation with outdated CSI**," *IEEE Commun. Lett.*, vol. 22, no. 8, pp. 1720-1723, Aug. 2018.

A. R. Heidarpour, M. Ardakani and C. Tellambura, "**Network coded cooperation based on relay selection with imperfect CSI**," in *Proc. IEEE 86th Vehicular Technology Conference (VTC-Fall)*, Toronto, Canada, Sep. 2017, pp. 1-5.

A. R. Heidarpour, M. Ardakani and C. Tellambura, "**Opportunistic scheduling in network-coded cooperative systems**," in *Proc. IEEE*

Notations: Throughout the thesis, the following notations are used: $\Pr\{A\}$, $\binom{n}{k} = \mathcal{C}_k^n = \frac{n!}{(n-k)!k!}$, and $\lceil \cdot \rceil$ denote the probability of an event A, binomial coefficient, and ceiling function, respectively. $\mathbb{F}_q$ denotes GF with size q. Addition and multiplication in $\mathbb{F}_q$ are denoted by $\oplus$ and $\otimes$, respectively. $F_X(\cdot)$ and $f_X(\cdot)$, respectively, denote the cumulative distribution function (CDF) and probability density function (PDF) of X. Finally, $\Gamma(\beta)$ and $\Gamma(\alpha, \beta)$ represent Gamma function and upper incomplete Gamma function, respectively.

Chapter 2

Network-Coded Cooperative Systems With Generalized User-Relay Selection

This chapter considers a dual-hop multiuser multirelay cooperative network that consists of $N \geq 2$ sources, $M \geq 1$ relays, and a single destination. The relays use DF relaying and apply NC on received sources' symbols, either correctly or incorrectly demodulated, using the weighting coefficients forming an MDS code. For the system under consideration, we propose the most GURS scheme in the literature that selects any arbitrary subsets of K (out of N) users and any arbitrary subsets of L (out of M) relays subject to any practical constraints such as load balancing conditions, scheduling policy, and other factors.

The main contributions of this chapter are summarized as follows:

- A new closed-form OP expression is derived, assuming i.n.i.d. Rayleigh fading over all the wireless links.

- We derive a concise high-SNR OP expression, based on which the achievable diversity order and coding gain are quantified; the two system-design parameters that govern the OP in the high-SNR regime.

- We show that our performance analysis and design guidelines apply to many situations and generalize and subsume all existing results in the literature as special cases.

- We further confirm our theoretical findings through extensive Monte-Carlo simulations.

The rest of this chapter is organized as follows: Section 2.1 describes the system and channel models. Section 2.2 presents the detailed analysis of outage performance of GURS NCC. Asymptotic analysis is provided in Section 2.3. Numerical results are presented in Section 2.4. Finally, we conclude in Section 2.5.

2.1 System Model and Transmission Scheme

This section first explains the system and channel models and after that describes the signal model and transmission protocol in detail.

2.1.1 System and Channel Models

Consider a dual-hop multiuser multirelay network with N sources $\mathcal{S} = \{S_n\}_{n=1}^{N}$, one destination D, and M DF relays $\mathcal{R} = \{R_m\}_{m=1}^{M}$. The direct links between sources and the destination are available, and the relays assist the sources in delivering the information packets to the destination. Each node is equipped with a single antenna, transmits with power ρ, and operates in the half-duplex fashion. The transmissions occur in different orthogonal time-slots, and the cooperation takes place in two phases, namely i) the broadcasting phase; and ii) the relaying phase. Fig. 2.1 depicts the timing diagram for the GURS NCC system. In the broadcasting phase, the $i_1^{\text{th}}, i_2^{\text{th}}, ..., i_K^{\text{th}}$ best sources $\{S_{(i_k)}\}_{k=1}^{K}$ (amongst N sources) are selected to transmit their messages to the destination in a round-robin fashion. The source selection might include a set of K highest-SNR sources or any other possible selection. This phase lasts K time-slots. Thanks to the broadcast nature of the wireless medium, the M relays also overhear the transmissions. In the relaying phase, any arbitrary subset of relays of size L (out

14

Broadcasting Phase				Relaying Phase			
$S_{(i_1)}$ transmits	$S_{(i_2)}$ transmits	...	$S_{(i_K)}$ transmits	$R_{(j_1)}$ transmits	$R_{(j_2)}$ transmits	...	$R_{(j_L)}$ transmits

$K + L$ time-slots
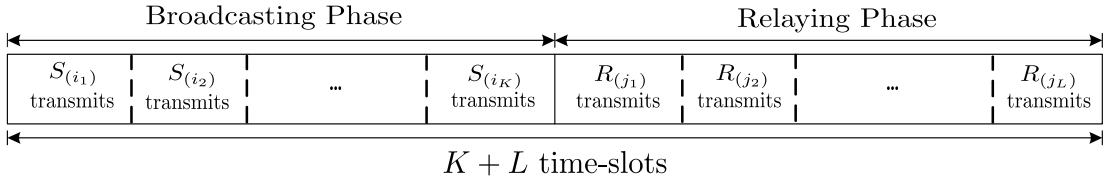
Fig. 2.1: Timing diagram for GURS NCC.

of M available relays), the $j_1^{\text{th}}, j_2^{\text{th}}, ..., j_L^{\text{th}}$ best relays $\{R_{(j_l)}\}_{l=1}^L$, can be selected. More specifically, the selected L relays employ NC to linearly combine K received packets and then are assigned orthogonal channels to forward the resulting network-coded packets to the destination sequentially. This phase thus takes place in L orthogonal time-slots.

The network subchannels are subjected to independent slow and frequency non-selective Rayleigh fading. We consider i.n.i.d. (i.e., asymmetric) Rayleigh fading channels over all the wireless links. In particular, the channel coefficient of link $i \to j$ is denoted by h_{ij} and follows $h_{ij} \sim \mathcal{CN}(0, \sigma_{ij}^2)$; a circularly-symmetric complex Gaussian random variable (RV) whose mean is zero and whose variance is equal to σ_{ij}^2. Furthermore, the additive white Gaussian noise (AWGN) term of link $i \to j$ is denoted by w_{ij} and has mean zero and unit variance i.e., $w_{ij} \sim \mathcal{CN}(0, 1)$. We remark that although the transmit power and the noise variance are set to be symmetric throughout the network, asymmetry cases can be lumped into the fading variances.

In GURS NCC, $\binom{N}{K}\binom{M}{L}$ different source-relay selections are possible. It is customary to assume a centralized selection method where the source-relay selection process is performed by a central unit (this could also be the destination). This entity requires instantaneous CSI of the source-to-destination links for source selection. In contrast, it requires the CSI of source-to-relay and relay-to-destination links for the RS process.[1]

The CSI of the indirect source-to-relay links are estimated by the relays using pilot sequences sent by selected K sources and then are forwarded to the destination. The selection depends on load balancing conditions, scheduling policy, and other factors.

[1]In time-varying fading channels, due to delayed feedback, the instantaneous CSI used in user/relay selection may substantially differ from the CSI at the data transmission instant. The outdated CSI may result in wrong selections and hence impact the system performance. The effect of the outdated CSI on GURS NCC's performance is an exciting research topic and is left as future work.

15

2.1.2 Signal Model and Transmission Scheme

2.1.2.1 Broadcasting Phase

In this phase, the destination selects K sources $\{S_{(i_k)}\}_{k=1}^K$ for data transmission. The source selection criterion is based on the instantaneous SNR of the direct source-to-destination links. We define $\gamma_{(n)}$ as the nth largest SNR of the source-to-destination SNRs. Specifically, $\gamma_{(n)}$ can be written as

$$\gamma_{(n)} = n^{\text{th}} \max_{1 \leq n \leq N} \{\gamma_{S_n D}\}. \tag{2.1}$$

Let $\{\gamma_{(i_k)}\}_{k=1}^K$ denote the ordered SNRs of any arbitrary subset of $\{\gamma_{(n)}\}_{n=1}^N$ and $\mathcal{I} = \{i_k\}_{k=1}^K$ being the set of indexes of the elements in $\{\gamma_{(i_k)}\}_{k=1}^K$ where $i_1 < i_2 < ... < i_K$. For the special case when the source selection includes the K highest-SNR source-to-destination links, we have $\mathcal{I} = \{1, 2, ..., K\}$.

Denoting $\epsilon_{S_{(k)}} \in \mathbb{F}_q$ as the symbol transmitted by the selected source $S_{(k)}$, $k \in \mathcal{I}$, the received signal at relay R_m ($\forall m$) and D can be expressed as

$$y_{S_{(k)}D} = \sqrt{\rho} h_{S_{(k)}D} x_{S_{(k)}} + w_{S_{(k)}D}, \tag{2.2}$$

$$y_{S_{(k)}R_m} = \sqrt{\rho} h_{S_{(k)}R_m} x_{S_{(k)}} + w_{S_{(k)}R_m}, \tag{2.3}$$

where $x_{S_{(k)}}$ is the modulated version of $\epsilon_{S_{(k)}}$.

2.1.2.2 Relaying Phase

This phase is based on the RS policy, which minimizes the possible error of network-coded symbols. Under this selection strategy, the equivalent channel for relay R_m is determined by the worst channel in the two-hop source-relay-destination links [29, 30, 61, 62]. Let $\mathcal{A}$ denote the set of indexes of the selected sources. The cardinality of $\mathcal{A}$ is K and the number of all possible $\mathcal{A}$'s is $\binom{N}{K}$. The "*equivalent SNR*" of the channels between K selected sources, relay R_m, and the destination can then be expressed as

$$\gamma_{m|\mathcal{A}}^{\min} = \min \left\{ \gamma_{S_{(i_1)}R_m}, \gamma_{S_{(i_2)}R_m}, ..., \gamma_{S_{(i_K)}R_m}, \gamma_{R_m D} \right\}. \tag{2.4}$$

16

Define $g_{(m)}$ as the mth largest equivalent SNRs of relays. Mathematically, this can be expressed as

$$g_{(m)} = m^{\text{th}} \max_{1 \leq m \leq M} \{\gamma_{m|\mathcal{A}}^{\min}\}. \tag{2.5}$$

In the relaying phase, relays $\{R_{(j_l)}\}_{l=1}^{L}$ take part in cooperation. Let $\{g_{(j_l)}\}_{l=1}^{L}$ denote the ordered SNRs of any arbitrary subset of $\{g_{(m)}\}_{m=1}^{M}$, where $j_1 < j_2 < ... < j_L$. As an example, assume that the number of relays $M = 10$ and $\mathcal{J} = \{j_l\}_{l=1}^{L} = \{1, 3, 7, 9\}$. This implies that four relays out of ten relays are selected whose SNRs are the first, third, seventh, and ninth largest SNRs in $\{g_{(m)}\}_{m=1}^{M}$.

The selected relays $R_{(l)}$, $l \in \mathcal{J}$, first decode the data received from the K selected sources using the maximum likelihood (ML) detector as follows

$$\hat{\epsilon}_{S_{(k)}R_{(l)}} = \arg \min_{\epsilon_{S_{(k)}} \in \mathbb{F}_q} \left\{ \left| y_{S_{(k)}R_{(l)}} - \sqrt{\rho} h_{S_{(k)}R_{(l)}} x_{S_{(k)}} \right|^2 \right\}, \tag{2.6}$$

and then sequentially transmit their network-coded symbols to the destination. The NC operation is applied to all correct or incorrect received symbols [29]. In particular, relay $R_{(l)}$ linearly combines estimated symbols in $\mathbb{F}_q$ using the weighting coefficients $\alpha_{S_{(k)}R_{(l)}}$ forming an MDS code. MDS codes always exist if the field size is sufficiently large and are proven to be maximal-diversity-achievable in the uplink multiple-source, multiple-relay cooperative systems. Such network codes satisfy the Singleton bound and minimize the total number of packets required at the destination to decode the sources' packets. The network-coded symbol generated by relay $R_{(l)}$ can then be expressed as

$$\hat{\epsilon}_{R_{(l)}} = \sum_{k \in \mathcal{I}} \bigoplus \left(\alpha_{S_{(k)}R_{(l)}} \bigotimes \hat{\epsilon}_{S_{(k)}R_{(l)}} \right). \tag{2.7}$$

Modulating $\hat{\epsilon}_{R_{(l)}}$ to $\hat{x}_{R_{(l)}}$, the received signal from relay $R_{(l)}$, $l \in \mathcal{J}$, at D can be expressed as

$$y_{R_{(l)}D} = \sqrt{\rho} h_{R_{(l)}D} \hat{x}_{R_{(l)}} + w_{R_{(l)}D}. \tag{2.8}$$

Fig. 2.2 shows an example of GURS NCC scheme when $N = 5$, $K = 3$, $M = 3$, $L = 2$, $\gamma_{S_5 D} > \gamma_{S_2 D} > \gamma_{S_1 D} > \gamma_{S_3 D} > \gamma_{S_4 D}$, $\mathcal{I} = \{1, 4, 5\}$, $\gamma_{2|\{3,5,4\}}^{\min} > \gamma_{3|\{3,5,4\}}^{\min} > \gamma_{1|\{3,5,4\}}^{\min}$, and $\mathcal{J} = \{1, 3\}$.
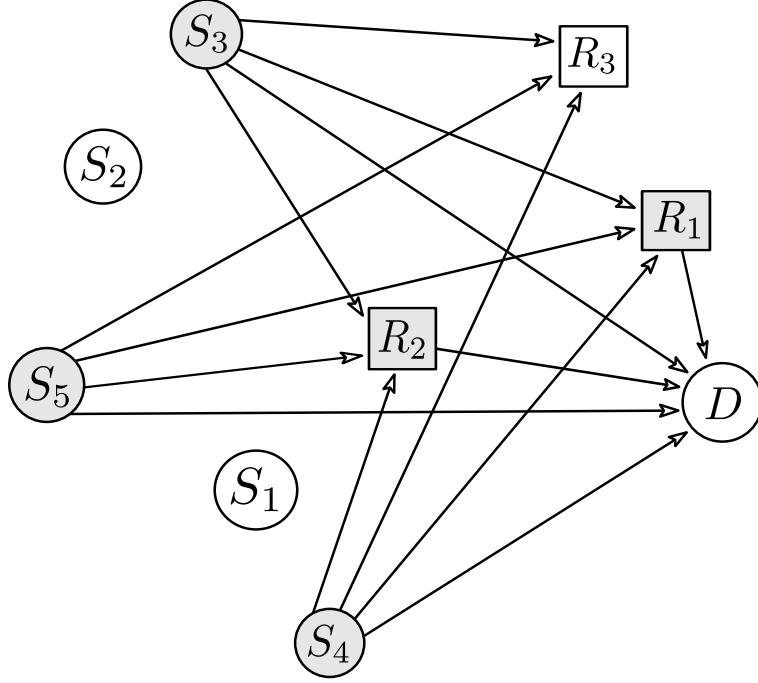
Fig. 2.2: System model for GURS NCC scheme. Example with $N = 5$, $K = 3$, $M = 3$, $L = 2$, $\gamma_{S_5 D} > \gamma_{S_2 D} > \gamma_{S_1 D} > \gamma_{S_3 D} > \gamma_{S_4 D}$, $\mathcal{I} = \{1, 4, 5\}$, $\gamma_{2|\{3,5,4\}}^{\min} > \gamma_{3|\{3,5,4\}}^{\min} > \gamma_{1|\{3,5,4\}}^{\min}$, and $\mathcal{J} = \{1, 3\}$.

2.2 Outage Probability

In this section, we derive a closed-form expression for the GURS NCC system OP, assuming i.n.i.d. Rayleigh fading channels over all wireless channels.

The following lemma is of importance when it provides the closed-form expression of the OP.

Lemma 2.1. *Let $X_1, X_2, ..., X_n$ be n independent and non-identical RVs with PDF $f_{X_i}(x_i) = \lambda_i e^{-\lambda_i x_i}$. Then,*

$$\Pr\{X_1 > X_2 > ... > X_n\} = \prod_{v=2}^{n} \left[\frac{\lambda_v}{\lambda_1 + \sum_{i=2}^{v} \lambda_i} \right]. \tag{2.9}$$

Proof. The proof is by induction.

- **Base Case:** The probability in (2.9) can be written in the integral form as

$$\Pr\{X_1 > X_2 > ... > X_n\} =$$

$$\underbrace{\int_0^\infty \int_0^{x_1} \int_0^{x_2} ... \int_0^{x_{n-1}}}_{n} \prod_{i=1}^n [f_{X_i}(x_i)]\, dx_n dx_{n-1}...dx_1. \tag{2.10}$$

We begin by verifying equation (2.9) for $n = 2$. For $n = 2$, (2.10) can be obtaied as

$$\begin{aligned}
\Pr\{X_1 > X_2\} &= \int_0^\infty \int_0^{x_1} \lambda_1 e^{-\lambda_1 x_1} \lambda_2 e^{-\lambda_2 x_2} dx_2 dx_1 \\
&= \int_0^\infty \lambda_1 e^{-\lambda_1 x_1} \left(1 - e^{-\lambda_2 x_1}\right) dx_1 \\
&= \frac{\lambda_2}{\lambda_1 + \lambda_2},
\end{aligned} \tag{2.11}$$

which verifies that (2.9) is true for $n = 2$.

- **Induction Hypothesis:** Assume that (2.9) holds when $n = k$ i.e.,

$$\Pr\{X_1 > X_2 > ... > X_k\} = \prod_{v=2}^k \left[\frac{\lambda_v}{\lambda_1 + \sum_{i=2}^v \lambda_i}\right]. \tag{2.12}$$

- **Inductive Step:** Now, we need to prove that (2.9) holds when $n = k+1$ using the assumption in (2.12):

$$\Pr\{X_1 > X_2 > ... > X_{k+1}\} =$$

$$\Pr\{X_1 > X_2 > ... > X_k\} \underbrace{\Pr\{X_{k+1} < X_1, X_2, ..., X_k\}}_{\mathcal{B}}. \tag{2.13}$$

The probability $\mathcal{B}$ in (2.13) can be derived as follows

$$\begin{aligned}
\mathcal{B} &= \underbrace{\int_0^\infty \int_{x_{k+1}}^\infty \int_{x_{k+1}}^\infty ... \int_{x_{k+1}}^\infty}_{k+1} \prod_{i=1}^{k+1} [f_{X_i}(x_i)]\, dx_1...dx_{k+1} \\
&= \lambda_{k+1} \int_0^\infty e^{-(\lambda_1 + \lambda_2 + ... + \lambda_{k+1})x_{k+1}} dx_{k+1} \\
&= \frac{\lambda_{k+1}}{\lambda_1 + \lambda_2 + ... + \lambda_{k+1}}.
\end{aligned} \tag{2.14}$$

19

Substituting (2.14) into (2.13), we have

$$\mathsf{Pr}\{X_1 > X_2 > ... > X_{k+1}\}$$

$$= \prod_{v=2}^{k} \left[\frac{\lambda_v}{\lambda_1 + \sum_{i=2}^{v} \lambda_i} \right] \left[\frac{\lambda_{k+1}}{\lambda_1 + \lambda_2 + ... + \lambda_{k+1}} \right]$$

$$= \prod_{v=2}^{k+1} \left[\frac{\lambda_v}{\lambda_1 + \sum_{i=2}^{v} \lambda_i} \right]. \tag{2.15}$$

Thus, (2.9) holds for $n = k + 1$, and the proof of the induction step is complete.

By the principle of induction, (2.9) is true for all $n \geq 2$ which concludes the proof.[2]

$\square$

Special Case 2.1. *For the special case of i.i.d. RVs i.e., $\lambda_i = \lambda$, $\forall i$, (2.9) is simplified to*

$$\mathsf{Pr}\{X_1 > X_2 > ... > X_n\} = \frac{1}{n!}. \tag{2.16}$$

Theorem 2.1. *Consider a cooperative network that consists of N users, M relays, and one destination. Assume the relays use DF protocol and apply NC on the received users' symbols. If the destination selects the i_1^{th}, i_2^{th}, ..., i_K^{th} best users and the j_1^{th}, j_2^{th},..., j_L^{th} best relays, the OP of the system when $K > L$ can be formulated as*

$$\mathcal{P}_{\text{out}_1} = \sum_{\eta=0}^{K-L-1} \mathsf{Pr}\{\mathcal{E}_\eta\} + \sum_{\eta=1}^{L} \left(\mathsf{Pr}\{\mathcal{E}_{K-\eta}\} \sum_{\ell=0}^{\eta-1} \mathrm{Pr}\{\mathcal{V}_\ell\} \right). \tag{2.17}$$

On the other hand, the OP when $K \leq L$ is given by

$$\mathcal{P}_{\text{out}_2} = \sum_{\eta=1}^{K} \left(\mathsf{Pr}\{\mathcal{E}_{K-\eta}\} \sum_{\ell=0}^{\eta-1} \mathrm{Pr}\{\mathcal{V}_\ell\} \right), \tag{2.18}$$

---

[2]We note that the result in Lemma 1 can be directly obtained using n-fold integrals given by (2.10). The direct proof of the obtained result, however, requires lengthy mathematical manipulations that do not bring much insight. In the interest of space, we chose to provide the shorter proof based on induction. In doing so, we first derived the results for small values of n using (2.10). We noted that with mathematical manipulations they can be represented in the simple form of (2.9), where we proved (2.9) by induction.

where $\Pr\{\mathcal{E}_\eta\}$ and $\Pr\{\mathcal{V}_\ell\}$ are, respectively, given by

$$\Pr\{\mathcal{E}_\eta\} =$$

$$\sum_{v=N-i_{\eta+1}+1}^{N-i_\eta} \left(\sum_{\substack{a_1,\cdots,a_v\in\{1,\ldots,N\} \\ a_1\neq\cdots\neq a_v}} \left[\prod_{n=a_1}^{a_v} \Pr\{\mathcal{O}_{S_nD}\} \prod_{\substack{n'=1 \\ n'\neq\{a_1,\ldots,a_v\}}}^{N} \left(1 - \Pr\left\{\mathcal{O}_{S_{n'}D}\right\}\right) \right] \right), \tag{2.19}$$

$$\Pr\{\mathcal{V}_\ell\} =$$

$$\sum_{\mathcal{A}} \left(\sum_{v=M-j_{\ell+1}+1}^{M-j_\ell} \left(\sum_{\substack{a_1,\cdots,a_v\in\{1,\ldots,M\} \\ a_1\neq\ldots\neq a_v}} \left[\prod_{m=a_1}^{a_v} \Pr\{\mathcal{O}_m|\mathcal{A}\} \prod_{\substack{m'=1 \\ m'\neq\{a_1,\ldots,a_v\}}}^{M} \left(1 - \Pr\{\mathcal{O}_{m'}|\mathcal{A}\}\right) \right] \right) \right.$$

$$\left. \times \sum_{\substack{z_1,\ldots,z_N\in\{1,\ldots,N\} \\ z_1\neq\ldots\neq z_N \\ z_{i_1},\ldots,z_{i_K}\in\mathcal{A}}} \left(\prod_{n=2}^{N} \left[\frac{\lambda_{S_{z_n}D}}{\lambda_{S_{z_1}D} + \sum_{i=2}^{n} \lambda_{S_{z_i}D}} \right] \right) \right), \tag{2.20}$$

in which

$$\Pr\{\mathcal{O}_{S_nD}\} = 1 - e^{-\lambda_{S_nD}\gamma_{th}}, \tag{2.21}$$

with $\lambda_{ij} = \frac{1}{\rho\sigma_{ij}^2}$.

Furthermore, $\Pr\{\mathcal{O}_m|\mathcal{A}\}$ is given by

$$\Pr\{\mathcal{O}_m|\mathcal{A}\} = 1 - e^{-\lambda_{m|\mathcal{A}}\gamma_{th}}, \tag{2.22}$$

with $\lambda_{m|\mathcal{A}}$ being

$$\lambda_{m|\mathcal{A}} = \lambda_{S_{(i_1)}R_m} + \ldots + \lambda_{S_{(i_K)}R_m} + \lambda_{R_mD}. \tag{2.23}$$

Proof. In GURS NCC, the destination receives $K + L$ packets; K packets from selected users and L network-coded packets from selected relays. If the destination receives at least K error-free packets, either from the selected users or from the selected relays, it is capable of recovering K original packets; otherwise, an outage occurs.

The overall OP of GURS NCC thus depends upon the outage events of direct user-to-destination links and dual-hop indirect user-to-relay-to-destination links. Let $\mathcal{E}_\eta$ and $\mathcal{V}_\ell$ denote the set of non-outage selected users and relays with cardinality η and ℓ, respectively. Mathematically, $\mathcal{E}_\eta$ and $\mathcal{V}_\ell$ can be written, respectively, as

$$\mathcal{E}_\eta \triangleq \left\{ S_{(k)} \in \mathcal{S} : \gamma_{S_{(k)}D} > \gamma_{th} \right\}, \tag{2.24}$$

$$\mathcal{V}_\ell|\mathcal{A} \triangleq \left\{ R_{(l)} \in \mathcal{R} : \gamma_{(l)|\mathcal{A}}^{\min} > \gamma_{th} \right\}. \tag{2.25}$$

where γ_{th} is the threshold SNR.

The overall outage events of GURS NCC can then be expressed as

$$\mathcal{O} = \mathcal{O}' \bigcup \mathcal{O}'', \tag{2.26}$$

where $\mathcal{O}'$ corresponds to the outage events when $K > L$ and there are not enough non-outage selected users, η, such that even if $\ell = L$, the destination is still in outage i.e., $\eta < K - L$. On the other hand, $\mathcal{O}''$ stands for the outage events where $\eta \geq K - L$, but the sum of non-outage selected users and relays is less than K i.e., $\eta + \ell < K$.

Now, we proceed to obtain $\Pr\{\mathcal{E}_\eta\}$ and $\Pr\{\mathcal{V}_\ell\}$, based on which, $\Pr\{\mathcal{O}'\}$ and $\Pr\{\mathcal{O}''\}$ can be derived.

An outage event occurs in a given link when its corresponding instantaneous SNR falls below γ_{th}. The threshold SNR γ_{th} can be written in terms of the transmission rate R_0 (in bits per channel use) as $\gamma_{th} = 2^{R_0} - 1$. Let $\mathcal{O}_{ij}$ denote the outage event of link $i \to j$. The OP of $i \to j$ link can be then written as

$$\Pr\{\mathcal{O}_{ij}\} = \Pr\{\gamma_{ij} < \gamma_{th}\}, \tag{2.27}$$

where $\gamma_{ij} = \rho|h_{ij}|^2$ is the instantaneous SNR of link $i \to j$. Noting that γ_{ij} is exponentially distributed, (2.27) is readily solved as

$$\Pr\{\mathcal{O}_{ij}\} = 1 - \int_{\gamma_{th}}^{\infty} \lambda_{ij} e^{-\lambda_{ij}y} dy = 1 - e^{-\lambda_{ij}\gamma_{th}}, \tag{2.28}$$

Applying order statistics properties and using (2.28), $\Pr\{\mathcal{E}_\eta\}$ can be written as (2.19). On the other hand, $\Pr\{\mathcal{V}_\ell\}$ can be formulated using total probability theorem

as follows

$$\Pr\{\mathcal{V}_\ell\} = \sum_{\mathcal{A}} \Pr\{\mathcal{V}_\ell|\mathcal{A}\}\Pr\{\mathcal{A}\}, \tag{2.29}$$

where the sum spans over all $\binom{N}{K}$ possible $\mathcal{A}$'s from the set of N candidate users and $\Pr\{\mathcal{V}_\ell|\mathcal{A}\}$ is given by

$$\Pr\{\mathcal{V}_\ell|\mathcal{A}\} =$$

$$\sum_{v=M-j_{\ell+1}+1}^{M-j_\ell} \left(\sum_{\substack{a_1,\cdots,a_v \in \{1,\ldots,M\} \\ a_1 \neq \ldots \neq a_v}} \left[\prod_{m=a_1}^{a_v} \Pr\{\mathcal{O}_m|\mathcal{A}\} \prod_{\substack{m'=1 \\ m' \neq \{a_1,\ldots,a_v\}}}^{M} (1 - \Pr\{\mathcal{O}_{m'}|\mathcal{A}\}) \right] \right). \tag{2.30}$$

Further, $\Pr\{\mathcal{A}\}$ can be derived as (2.31) using Lemma 2.1. Note that the sum in (2.31) spans over $(N-K)!K!$ possibilities. For the special case of $\lambda_{S_n D} \approx \lambda_{SD}$, $\forall n$, we have $\Pr\{\mathcal{A}\} \approx \frac{1}{\binom{N}{K}}$.

$$\Pr\{\mathcal{A}\} = \sum_{\substack{z_1,\ldots,z_N \in \{1,\ldots,N\} \\ z_1 \neq \ldots \neq z_N \\ z_{i_1},\ldots,z_{i_K} \in \mathcal{A}}} \left(\prod_{n=2}^{N} \left[\frac{\lambda_{S_{z_n} D}}{\lambda_{S_{z_1} D} + \sum_{i=2}^{n} \lambda_{S_{z_i} D}} \right] \right). \tag{2.31}$$

Now, plugging (2.30) and (2.31) into (2.29), the closed-form expression of $\Pr\{\mathcal{V}_\ell\}$ can be obtained as (2.20).

Finally, using (2.19), (2.20), and (2.26) one can obtain the closed-form expression for the OP as given by (2.17) and (2.18). Thus, we complete the proof. □

Special Case 2.2. *The derived OP expression in* (2.17) *and* (2.18) *is based on the assumption of asymmetric i.n.i.d. Rayleigh fading channels over all wireless links and can be treated as the generalized versions of semi-symmetric i.n.i.d. channels or symmetric i.i.d. channels.*[3] *Furthermore, it subsumes all existing results in the literature as special cases. In particular, for* $K = N$ *and* $L = M$ *(NCC without user-relay selection) and asymmetric i.n.i.d. channels, it reduces to (34) in [30]. When*

[3]Semi-symmetric i.n.i.d. subchannels refers to the case when $\lambda_{S_n D} \approx \lambda_{SD}$, $\forall n$, and $\lambda_{R_m D} \approx \lambda_{RD}$, $\forall m$. This assumption can be applicable to cooperative uplink cellular systems [35,44] where the mobile users and relays are formed as clusters. On the other hand, the channels are said symmetric i.i.d. when $\lambda_{S_n D} = \lambda_{R_m D} = \lambda_{S_n R_m}$, $\forall n, m$.

$K = N$ and L highest-SNR relays are selected, it reduces to (21) and (22) in [30]. For i.i.d. channels with $K = N$ and any arbitrary RS, it coincides to (4) and (7) in [61].

2.3 Asymptotic Analysis

In this section, we first derive the asymptotic outage expression at the high-SNR regime to quantify the achievable diversity order and coding gain. Then, we provide some insights and guidelines that can be drawn from our diversity analysis.

2.3.1 Asymptotic Outage Probability

In the previous section, the closed-form expression of the OP has been derived, which is still too complicated to learn the relationship between OP and different system parameters. To gain deeper insights about how the system parameters impact on the outage performance, we now characterize the asymptotic behavior of the OP in the high-SNR regime. From the asymptotic expression, we extract two important system design parameters, namely the diversity order and the coding gain.

Theorem 2.2. *Consider a cooperative network that consists of N users, M relays, and one destination. Assume the relays use DF protocol and apply NC on the received users' symbols. If the destination selects the i_1^{th}, i_2^{th}, ..., i_K^{th} best users and the j_1^{th}, j_2^{th},..., j_L^{th} best relays, the achievable diversity order when $K > L$ can be obtained as*

$$
G_{d_1} = \begin{cases} N - i_{K-L} + 1, \\ \qquad\qquad \psi_L^{\max} < M + i_{K-L} + 1 \\ N + M - \psi_L^{\max} + 2, \\ \qquad\qquad \psi_L^{\max} > M + i_{K-L} + 1 \end{cases} \tag{2.32}
$$

and the the coding gain is given by

$$
G_{c_1} = \begin{cases}
\dfrac{\Psi_1'^{-\frac{1}{N-i_{K-L}+1}}}{\gamma_{th}}, \\
\qquad\qquad \psi_L^{\max} < M + i_{K-L} + 1 \\[2mm]
\dfrac{\Psi_1''^{-\frac{1}{N+M-\psi_L^{\max}+2}}}{\gamma_{th}}, \\
\qquad\qquad \psi_L^{\max} > M + i_{K-L} + 1 \\[2mm]
\dfrac{\left(\Psi_1' + \Psi_1''\right)^{-\frac{1}{N-i_{K-L}+1}}}{\gamma_{th}}, \\
\qquad\qquad \psi_L^{\max} = M + i_{K-L} + 1
\end{cases}
\tag{2.33}
$$

where $\psi_\delta^{\max} = \max\{\psi_\eta\}_{\eta=1}^{\delta}$ with $\psi_\eta = i_{K-\eta+1} + j_\eta$. Further,

$$
\Psi_1' = \sum_{\substack{a_1,\cdots,a_{N-i_{K-L}+1} \\ a_1 \neq \cdots \neq a_{N-i_{K-L}+1}}} \left(\prod_{n=a_1}^{a_{N-i_{K-L}+1}} \left(\frac{1}{\sigma_{S_n D}^2} \right) \right),
\tag{2.34}
$$

and

$$
\Psi_1'' = \sum_{\eta:\psi_\eta=\psi_L^{\max}} Q_\eta,
\tag{2.35}
$$

where Q_q is given by (2.36) and $\frac{1}{\sigma_{m|\mathcal{A}}^2} = \frac{1}{\sigma_{S_{(i_1)} R_m}^2} + \ldots + \frac{1}{\sigma_{S_{(i_K)} R_m}^2} + \frac{1}{\sigma_{R_m D}^2}$.

$$
\begin{aligned}
Q_\eta = &\sum_{\substack{a_1,\cdots,a_{N-i_{K-\eta+1}+1} \\ a_1\neq\cdots\neq a_{N-i_{K-\eta+1}+1}}} \prod_{n=a_1}^{a_{N-i_{K-\eta+1}+1}} \left(\frac{1}{\sigma_{S_n D}^2} \right) \sum_{\mathcal{A}} \left(\sum_{\substack{a_1,\cdots,a_{M-j_\eta+1} \\ a_1\neq\ldots\neq a_{M-j_\eta+1}}} \prod_{m=a_1}^{a_{M-j_\eta+1}} \left(\frac{1}{\sigma_{m|\mathcal{A}}^2} \right) \right. \\
&\left. \times \sum_{\substack{z_1,\ldots,z_N \in \{1,\ldots,N\} \\ z_1\neq\ldots\neq z_N \\ z_{i_1},\ldots,z_{i_K} \in \mathcal{A}}} \prod_{n=2}^{N} \left[\frac{\lambda_{S_{z_n} D}}{\lambda_{S_{z_1} D} + \sum_{i=2}^{n} \lambda_{S_{z_i} D}} \right] \right).
\end{aligned}
\tag{2.36}
$$

On the other hand, the achievable diversity order and the coding gain when $K \leq L$ can be obtained as

$$
G_{d_2} = N + M - \psi_K^{\max} + 2,
\tag{2.37}
$$

and

$$G_{c_2} = \frac{\Psi_2^{-\frac{1}{N+M-\psi_K^{\max}+2}}}{\gamma_{th}},$$ (2.38)

where

$$\Psi_2 = \sum_{\eta:\psi_\eta=\psi_K^{\max}} Q_\eta.$$ (2.39)

Proof. To find the asymptotic expressions in the high-SNR regime, we use Taylor series expansion of the exponential function given by $e^{-x} = \sum_{k=0}^{\infty} \frac{(-x)^k}{k!}$. Plugging this expression in (2.21), we have

$$\mathsf{Pr}^\infty\{\mathcal{O}_{S_nD}\} = \lambda_{S_nD}\gamma_{th}.$$ (2.40)

Similarly, (2.22) can be approximated as

$$\mathsf{Pr}^\infty\{\mathcal{O}_m|\mathcal{A}\} = \lambda_{m|\mathcal{A}}\gamma_{th}.$$ (2.41)

Substituting (2.40) and (2.41) into (2.19) and (2.20), and then keeping dominant terms, we respectively have

$$\mathsf{Pr}^\infty\{\mathcal{E}_\eta\} = \sum_{\substack{a_1,\cdots,a_{N-i_{\eta+1}+1} \\ a_1\neq\cdots\neq a_{N-i_{\eta+1}+1}}} \left(\prod_{n=a_1}^{a_{N-i_{\eta+1}+1}} \lambda_{S_nD}\gamma_{th}\right),$$ (2.42)

and

$$\mathsf{Pr}^\infty\{\mathcal{V}_\ell\} = \sum_{\mathcal{A}} \left(\sum_{\substack{a_1,\cdots,a_{M-j_{\ell+1}+1} \\ a_1\neq\cdots\neq a_{M-j_{\ell+1}+1}}} \prod_{m=a_1}^{a_{M-j_{\ell+1}+1}} \lambda_{m|\mathcal{A}}\gamma_{th}\right.$$

$$\left. \cdot \sum_{\substack{z_1,\ldots,z_N \\ z_1\neq\ldots\neq z_N \\ z_{i_1},\ldots,z_{i_K}\in\mathcal{A}}} \left(\prod_{n=2}^{N} \left[\frac{\lambda_{S_{z_n}D}}{\lambda_{S_{z_1}D} + \sum_{i=2}^{n}\lambda_{S_{z_i}D}}\right]\right)\right).$$ (2.43)

By plugging (2.42), (2.43) into (2.17) and then retaining the dominant terms, (2.17) can be approximated as

$$\mathcal{P}_{\text{out}_1}^\infty = \mathsf{Pr}^\infty\{\mathcal{E}_{K-L-1}\} + \sum_{\eta:\psi_\eta=\psi_L^{\max}} \mathsf{Pr}^\infty\{\mathcal{E}_{K-\eta}\}\mathsf{Pr}^\infty\{\mathcal{V}_{\eta-1}\}.$$ (2.44)

Now, based on the relationship between $\psi_L^{\max}$ and $M+i_{K-L}+1$, (2.44) in high SNRs can be derived as follows

26

- **Case 1:** $\psi_L^{\max} < M + i_{K-L} + 1$. In this case, $\mathcal{P}_{\text{out}_1}^\infty$ is determined by the first term in (2.44) and is given by

$$\mathcal{P}_{\text{out}_1}^\infty = \Psi_1' \left(\frac{\gamma_{th}}{\rho} \right)^{N-i_{K-L}+1}. \tag{2.45}$$

- **Case 2:** $\psi_L^{\max} > M + i_{K-L} + 1$. In this case, $\mathcal{P}_{\text{out}_1}^\infty$ is determined by the second term in (2.44) and can be expressed as

$$\mathcal{P}_{\text{out}_1}^\infty = \Psi_1'' \left(\frac{\gamma_{th}}{\rho} \right)^{N+M-\psi_L^{\max}+2}. \tag{2.46}$$

- **Case 3:** $\psi_L^{\max} = M + i_{K-L} + 1$. In this case, $\mathcal{P}_{\text{out}_1}^\infty$ is determined by the first and second terms in (2.44). The asymptotic outage expression can then be written as

$$\mathcal{P}_{\text{out}_1}^\infty = \left(\Psi_1' + \Psi_1'' \right) \left(\frac{\gamma_{th}}{\rho} \right)^{N-i_{K-L}+1}. \tag{2.47}$$

Finally, using (1.3), the diversity order and coding gain of GURS NCC system when $K > L$ are, respectively, given by (2.32) and (2.33).

Now, we proceed to obtain the asymptotic outage expression for $K \leq L$. Substituting (2.42), (2.43) into (2.18) and then retaining the dominant terms, (2.18) in high SNRs can be written as

$$\mathcal{P}_{\text{out}_2}^\infty = \Psi_2 \left(\frac{\gamma_{th}}{\rho} \right)^{N+M-\psi_K^{\max}+2}. \tag{2.48}$$

Based on (1.3) and (2.48), the achievable diversity order and the coding gain when $K \leq L$ are, respectively, given by (2.37) and (2.38). This concludes the proof. $\qquad\square$

Special Case 2.3. *The derived diversity order in* (2.32) *and* (2.37) *is the most generic expression in the literature and includes all existing results as special cases. More specifically, for $K = N$ (no user selection) and $L = M$ (no RS), it reduces to $G_d = M + 1$ [18, 20, 29, 30]. When $K = N$ and L highest-SNR relays are selected, the diversity order for $N > L$ and $N \leq L$ reduces to $G_{d_1} = L + 1$ and $G_{d_2} = M + 1$. This coincides with the diversity order reported in [29, 30]. Finally, when K best users and L best relays are selected, it coincides to the results in [35].*

Special Case 2.4. *When $K = N$ and arbitrary relays are selected, the diversity order reduces to the diversity order of $G_{d_1} = L + 1$ and $G_{d_2} = N + M - j_N + 1$ for $N > L$ and $N \leq L$, respectively. Therefore, if the number of sources exceeds the number of selected relays, we find:*

- *The diversity order is always limited by the number of selected relays and is equal to $G_{d_1} = L + 1$. This implies that other system parameters such as number of sources N, number of relays M, and any arbitrary RS do not impact the achievable diversity order. Further, as long as the lowest-SNR relay is not selected (i.e., the set of selected relays does not include the worst relay), the outage performance for any arbitrary RS is identical to that of the best RS in the high-SNR regime.*

- *Any arbitrary SRS is a special case when $L = 1$. Hence, unlike the SRS in conventional CC systems where the j_1^{th} highest-SNR relay achieves the diversity gain of $G_d = M - j_1 + 2$ [40], the same relay in NCC system always achieves the diversity order of only two.*

On the other hand, if the number of selected relays is greater than or equal to the number of sources, we find:

- *The diversity order is now equal to $G_{d_2} = N + M - j_N + 1$. This indicates that the full diversity order of $G_{d_2} = M + 1$ is preserved where $j_N = N$. This condition is only satisfied when N best relays be in the set of selected relays. Otherwise, the diversity order of the system is only determined by the Nth element in $\mathcal{J}$ i.e., j_N.*

- *$j_1, j_2, ..., j_{N-1}$ in $\mathcal{J}$ affect on the coding gain rather than the diversity order.*

- *Interestingly but counter intuitively, $j_{N+1}, ..., j_L$ do not impact either the diversity or the coding gains. Indeed, the performance of $L > N$ is exactly the same to that of $L = N$. This reveals that selecting more than N relays not only does not bring further performance gain over the configuration with $L = N$, but also reduces the throughput of the system.*

- *If $j_{N+1} = j_N + 1$, increasing sources from N to $N + 1$ does not change the diversity order of the system. However, when $j_{N+1} \neq j_N + 1$ the diversity order decreases by a*

factor of $j_{N+1} - j_N - 1$. This is in contrast to the best RS where the number of sources does not change the diversity order and the full diversity order of $G_{d_2} = M + 1$ is always achieved.

Special Case 2.5. *The derived diversity order can also be thought as a generalization of the all results available in the non-NCC literature. For $K = 1$ and $M = 0$ (non-cooprative multiuser case), the diversity order reduces to $G_{d_1} = N - i_1 + 1$ which coincides to that of [39]. For $N = 1$ and the best RS, it reduces to $G_{d_2} = M + 1$ [21]. For $N = 1$ and the j_1^{th} best relay is selected, it reduces to $G_{d_2} = M - j_1 + 2$ which agrees with that of in [40]. When the best user and the best relay are selected, it reduces to $G_{d_2} = N + M$. This diversity order is identical to that of [32, 33]. For $N = 1$ and any arbitrary RS, it reduces to $G_{d_2} = M - j_1 + 2$. This result is in agreement with the diversity order reported in [42].*

2.3.2 Insights and Guidelines

Here, we provide some insights and guidelines that can be drawn from our diversity analysis and can help the understanding and the design of practical NCC systems with user-relay selection protocols.

From (2.32), the following remarks and guidelines can be drawn:

Remark 2.1. *From $\binom{N}{K}\binom{M}{L}$ different user-relay selections, $\Delta_1 = N - K + 1$ distinct diversity orders can be achieved. Therefore, the number of achievable diversity orders is a function of the number of users N, number of selected users K, but it is independent of the number of relays M and the number of selected relays L.*

Remark 2.2. *The maximum and minimum diversity orders are given by*

$$\begin{cases} G_{d_1}^{\max} = N - K + L + 1, \\ G_{d_1}^{\min} = L + 1 \end{cases} \tag{2.49}$$

The condition $i_{K-L} = K - L$ is the necessary (but not sufficient) condition for achieving maximum diversity $G_{d_1}^{\max}$. Other user selections with $i_{K-L} \neq K - L$ cannot provide $G_{d_1}^{\max}$. The condition $i_{K-L} = K - L$ is satisfied if and only if the set of selected users

includes $K - L$ highest-SNR users. On the other hand, the system has the minimum diversity $G_{d_1}^{\min}$ if $i_{K-L} = N - L$ or $\psi_L^{\max} = N + M - L + 1$.

Remark 2.3. When $\psi_L^{\max} < M + i_{K-L} + 1$, the diversity is determined by $G_{d_1} = N - i_{K-L} + 1$ which only depends on the number of users N and the i_{K-L}^{th} best user. This indicates that other system parameters such as number of relays M, number of selected relays L, and any arbitrary RS do not impact the achievable diversity order.

Remark 2.4. The number of user selections that always guarantee the diversity order of $G_{d_1} = N - i_{K-L} + 1$, no matter how the RS proceeds, can be expressed as

$$\xi = \binom{i_{K-L} - 1}{K - L - 1}. \tag{2.50}$$

If user selection includes $K - L$ highest-SNR users, we have $i_{K-L} = K - L$ which yields the maximum diversity order of $G_{d_1}^{\max} = N - K + L + 1$ and $\xi = 1$. This implies that only one user selection always guarantees maximum diversity $G_{d_1}^{\max}$, no matter which of L relays are selected. This user selection is indeed the best user selection that includes K highest-SNR users. On the other hand, when $i_{K-L} = N - L$, we have the minimum diversity order of $G_{d_1}^{\min} = L + 1$ and $\xi = \binom{N-L-1}{K-L-1}$. This suggests that $\binom{N-L-1}{K-L-1}$ number of user selections, including the worst user selection, have always minimum diversity $G_{d_1}^{\min}$ irrespective of RS process. Note that the order of the selected relays only manifests its effect on the coding gain, rather than the diversity. According to (2.33), if the set of selected relays does not include the lowest-SNR relay (i.e., $j_L \neq M$), the coding gain of any arbitrary RS is identical to that of the best RS leading to the same outage performance in the high-SNR regime.

Remark 2.5. When $\psi_L^{\max} > M + i_{K-L} + 1$, the diversity is determined by $G_{d_1} = N + M - \psi_L^{\max} + 2$. In this case, the diversity is a function of the number of users N, number of relays M, the $j_1^{\text{th}}, j_2^{\text{th}}, ..., j_L^{\text{th}}$ best relays and the $i_{K-L+1}^{\text{th}}, i_{K-L+2}^{\text{th}}, ..., i_K^{\text{th}}$ best users. This implies that all the system parameters impact the achievable diversity except the $i_1^{\text{th}}, i_2^{\text{th}}, ..., i_{K-L}^{\text{th}}$ best users.

Example 2.1. Consider a network with $N = 6$, $K = 4$, $M = 4$, and $L = 2$. These system parameters satisfy the condition $K > L$. All $\binom{6}{4}\binom{4}{2} = 90$ user-relay selections

Table 2.1: Diversity Orders for All Possible User-Relay Selections: $N = 6$, $K = 4$, $M = 4$, $L = 2$.

	$\mathcal{I} = \{1,2,3,4\}$	$\mathcal{I} = \{1,2,3,5\}$	$\mathcal{I} = \{1,2,3,6\}$	$\mathcal{I} = \{1,2,4,5\}$	$\mathcal{I} = \{1,2,4,6\}$	$\mathcal{I} = \{1,2,5,6\}$	$\mathcal{I} = \{1,3,4,5\}$	$\mathcal{I} = \{1,3,4,6\}$	$\mathcal{I} = \{1,3,5,6\}$	$\mathcal{I} = \{1,4,5,6\}$	$\mathcal{I} = \{2,3,4,5\}$	$\mathcal{I} = \{2,3,4,6\}$	$\mathcal{I} = \{2,3,5,6\}$	$\mathcal{I} = \{2,4,5,6\}$	$\mathcal{I} = \{3,4,5,6\}$
$\mathcal{J} = \{1,2\}$	5	5	5	5	5	5	4	4	4	3	4	4	4	3	3
$\mathcal{J} = \{1,3\}$	5	5	5	5	5	4	4	4	4	3	4	4	4	3	3
$\mathcal{J} = \{1,4\}$	5	5	5	4	4	3	4	4	3	3	4	4	3	3	3
$\mathcal{J} = \{2,3\}$	5	5	4	5	4	4	4	4	4	3	4	4	4	3	3
$\mathcal{J} = \{2,4\}$	5	5	4	4	4	3	4	4	3	3	4	4	3	3	3
$\mathcal{J} = \{3,4\}$	5	4	3	4	3	3	4	3	3	3	4	3	3	3	3

with their corresponding achievable diversity orders (2.32) are reported in Table 2.1. As can be seen, there are $\Delta_1 = N - K + 1 = 3$ different diversity orders ranging from minimum diversity $G_{d_1}^{\min} = L + 1 = 3$ to maximum diversity $G_{d_1}^{\max} = N - K + L + 1 = 5$. This confirms the statements in Remarks 2.1, 2.2. In addition, the user selections with $i_2 \neq 2$ i.e., $i_2 = 3$, 4 are not capable of achieving the maximum diversity of five even if the best RS is performed, confirming Remark 2.2. Furthermore, there are six user selections that always achieve the diversity order of $G_{d_1} = N - i_{K-L} + 1$, no matter which of two relays are selected. More precisely, the best user selection $\mathcal{I} = \{1, 2, 3, 4\}$ guarantees the maximum diversity of five. There are also $\xi = \binom{2}{1} = 2$ (2.50) number of user selections that always achieve the diversity of four i.e., $\mathcal{I} = \{1, 3, 4, 5\}$ and $\mathcal{I} = \{2, 3, 4, 5\}$. Besides, $\xi = \binom{3}{1} = 3$ user selections always have the minimum diversity of three. They are $\mathcal{I} = \{1, 4, 5, 6\}$, $\mathcal{I} = \{2, 4, 5, 6\}$ and the worst user selection $\mathcal{I} = \{3, 4, 5, 6\}$. This confirms the statements in Remark 2.4.

On the other hand, based on (2.37), we have the following design insights and remarks.

Remark 2.6. *All possible user-relay selections provide $\Delta_2 = N + M - K - L + 1$ different diversities. Accordingly, the number of diversity orders is a function of all system parameters.*

Remark 2.7. *The diversity order depends on N, M, the $i_1^{\text{th}}, i_2^{\text{th}}, ..., i_K^{\text{th}}$ best users and the $j_1^{\text{th}}, j_2^{\text{th}}, ..., j_K^{\text{th}}$ best relays. Therefore, the $j_{K+1}^{\text{th}}, j_2^{\text{th}}, ..., j_L^{\text{th}}$ best relays do not change the achievable diversity order.*

Remark 2.8. *The maximum and minimum diversity orders are given by (2.51). The diversity order of $G_{d_2}^{\max} = N - K + M + 1$ can be achieved if and only if $\psi_K^{\max} = K + 1$, implying that the set of selected users and relays must include K highest-SNR users and K highest-SNR relays. On the other hand, the system has the minimum diversity order of $G_{d_2}^{\min} = L + 1$ if and only if $\psi_K^{\max} = N + M - L + 1$.*

$$\begin{cases} G_{d_2}^{\max} = N - K + M + 1, \\ G_{d_2}^{\min} = L + 1 \end{cases} \tag{2.51}$$

Remark 2.9. *The number of RSs that achieve full diversity order $G_{d_2}^{\max}$ is given by*

$$\zeta = \binom{M - K}{L - K}. \tag{2.52}$$

Remark 2.10. *The RSs that include K highest-SNR relays have the minimum diversity of $M+1$ when the lowest-SNR user is in the set of selected users or equivalently $i_K = N$. Similarly, the worst RS has the minimum diversity of $L + 1$ when $i_K = N$.*

Remark 2.11. *The term $N - K + 1$ in $G_{d_v}^{\max}$ ($v = 1, 2$) (2.49) and (2.51) corresponds to the MUD and the remaining terms L and M correspond to the CD. It can be readily checked that $G_{d_v}^{\max}$ increases when the number of users N increases. Further, it decreases when the number of selected users K increases. Obviously, when $K = N$ the MUD gain vanishes and only the CD gain can be achieved [35].*

Example 2.2. *Now, consider a network with $N = 4$, $K = 2$, $M = 6$, and $L = 4$. These system parameters satisfy the condition $K \leq L$. The achievable diversity orders (2.37) for all $\binom{4}{2}\binom{6}{4} = 90$ user-relay selections are provided in Table 2.2. It can be*

Table 2.2: Diversity Orders for All Possible User-Relay Selections: $N = 4$, $K = 2$, $M = 6$, $L = 4$.

	$\mathcal{J}=\{1,2,3,4\}$	$\mathcal{J}=\{1,2,3,5\}$	$\mathcal{J}=\{1,2,3,6\}$	$\mathcal{J}=\{1,2,4,5\}$	$\mathcal{J}=\{1,2,4,6\}$	$\mathcal{J}=\{1,2,5,6\}$	$\mathcal{J}=\{1,3,4,5\}$	$\mathcal{J}=\{1,3,4,6\}$	$\mathcal{J}=\{1,3,5,6\}$	$\mathcal{J}=\{1,4,5,6\}$	$\mathcal{J}=\{2,3,4,5\}$	$\mathcal{J}=\{2,3,4,6\}$	$\mathcal{J}=\{2,3,5,6\}$	$\mathcal{J}=\{2,4,5,6\}$	$\mathcal{J}=\{3,4,5,6\}$
$\mathcal{I}=\{1,2\}$	9	9	9	9	9	9	8	8	8	7	8	8	8	7	7
$\mathcal{I}=\{1,3\}$	8	8	8	8	8	8	8	8	8	7	7	7	7	7	6
$\mathcal{I}=\{1,4\}$	7	7	7	7	7	7	7	7	7	7	6	6	6	6	5
$\mathcal{I}=\{2,3\}$	8	8	8	8	8	8	7	7	7	6	7	7	7	6	6
$\mathcal{I}=\{2,4\}$	7	7	7	7	7	7	7	7	7	6	6	6	6	6	5
$\mathcal{I}=\{3,4\}$	7	7	7	7	7	7	6	6	6	5	6	6	6	5	5

seen that there are $\Delta_2 = N + M - K - L + 1 = 5$ different achievable diversity orders; from the minimum diversity of $G_{d_2}^{\min} = L + 1 = 5$ to the maximum diversity of $G_{d_2}^{\max} = N - K + M + 1 = 9$ i.e., $G_{d_2} = 5, 6, 7, 8, 9$. This confirms Remarks 2.6, 2.8. Besides, $\zeta = \binom{4}{2} = 6$ (2.52) RSs achieve maximum diversity $G_{d_2}^{\max} = 9$. Furthermore, the RSs that include $K = 2$ highest-SNR relays have the minimum diversity of $M + 1 = 7$ when $i_2 = 4$ i.e., $\mathcal{I} = \{1,4\}$, $\mathcal{I} = \{2,4\}$, and $\mathcal{I} = \{3,4\}$. Similarly, the worst RS $\mathcal{J} = \{3,4,5,6\}$ has the minimum diversity of $L + 1 = 5$ when $i_2 = 4$. This confirms the statements in Remarks 2.9 and 2.10.

2.4 Numerical Results and Discussions

In this section, we provide numerical and simulation results to verify the derived analytical expressions.

Fig. 2.3 illustrates outage versus ρ for $N = K = 3$, $M = 5$, $L = 2$, $R_0 = 1$, assuming i.i.d. Rayleigh fading channels. The selections satisfy the condition $N > L$. As a benchmark, the selection of two highest-SNR relays (i.e., when $\mathcal{J} = \{1,2\}$) is
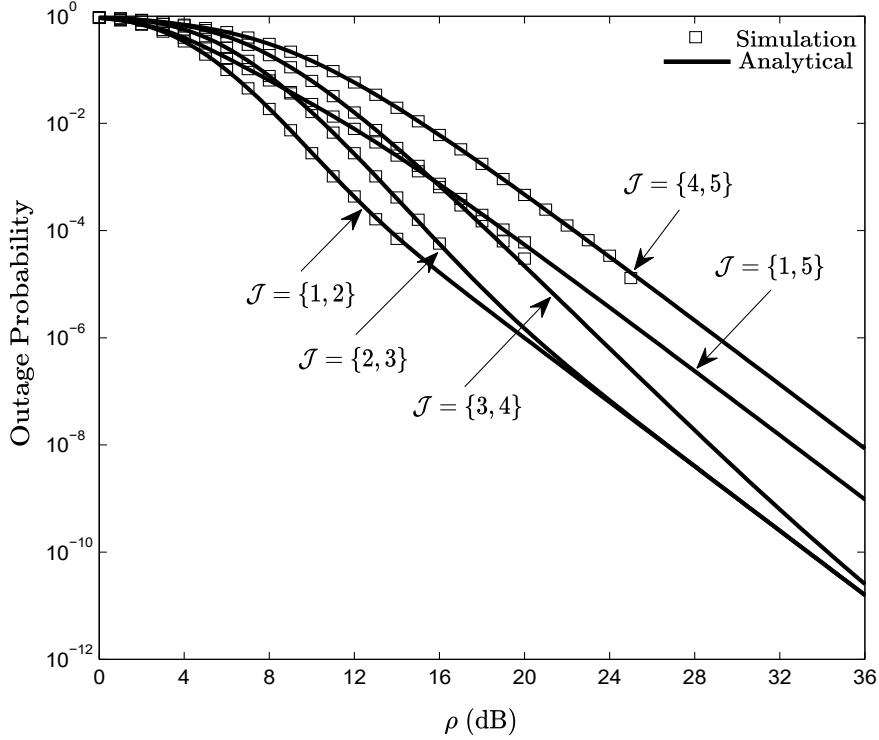
Fig. 2.3: OP versus SNR when $N = K = 3$, $M = 5$, $L = 2$, $R_0 = 1$, assuming i.i.d. Rayleigh fading channels.

also plotted. We observe that the exact closed-form outage completely agrees with simulation results. Furthermore, the slopes of the curves clearly reveal that the diversity order is determined by the number of relays selected L and is always equal to $G_{d_1} = L + 1 = 3$. Interestingly, the diversity is preserved no matter which two relays are selected. However, an SNR loss is incurred. For example, consider the RSs $\mathcal{J} = \{1, 2\}$, $\mathcal{J} = \{2, 3\}$, $\mathcal{J} = \{3, 4\}$ and $\mathcal{J} = \{1, 5\}$. All these achieve the same diversity order, but for a target outage of 10^{-4}, the latter three need 2, 4.5 and 5.5 dB SNR more compared to $\mathcal{J} = \{1, 2\}$. This SNR loss increases for $\mathcal{J} = \{4, 5\}$ (i.e., the two lowest-SNR relays) and increases to 8.5 dB. In addition, when the worst relay is not selected, outage will eventually converge to that of the best RS as SNR increases. However, when the worst relay is indeed selected, the outage performance of the system is always worse than that of the best RS both in finite and asymptotic SNR regime.

In Fig. 2.4, we plot the OP versus ρ when $N = K = 3, 4$, $M = 10$, $L = 3, 4$,
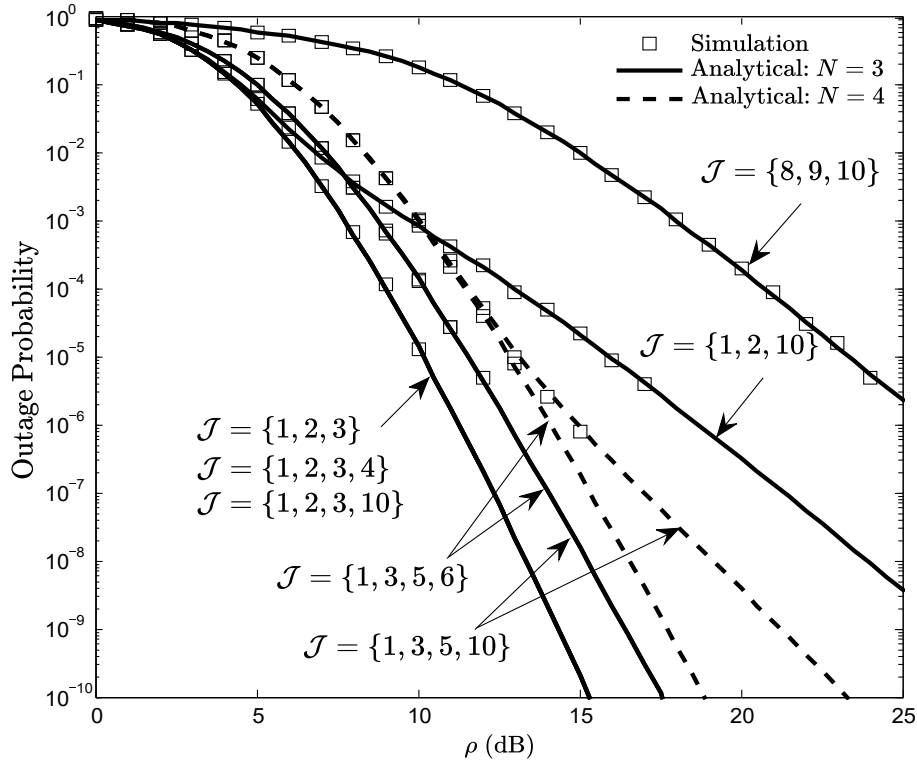
Fig. 2.4: OP versus ρ when $N = K = 3, 4$, $M = 10$, $L = 3, 4$, $R_0 = 1$, assuming i.i.d. Rayleigh fading channels.

$R_0 = 1$ and i.i.d. Rayleigh fading channels are assumed. Note that, these system parameters satisfy the condition $L \geq N$. Similar to Fig. 2.3 analytical curves perfectly match the simulation results. Furthermore, maximum achievable diversity order of $G_{d_2} = M + 1 = 11$ is only persevered when the condition $j_N = N$ holds. This in fact implies that the set $\mathcal{J}$ includes $N = 3$ best-SNR relays. On the other hand, when $j_N \neq \mathcal{N}$, the diversity gain of the system becomes a function of Nth best relay in $\mathcal{J}$ and is equal to $G_{d_2} = N + M - j_N + 1$. For example, when $\mathcal{J} = \{1, 3, 5, 6\}$ or $\mathcal{J} = \{1, 3, 5, 10\}$ the diversity order is equal to $G_{d_2} = M + N - j_N + 1 = 9$ which is less than the full diversity order of 11. In addition, the performance of $\mathcal{J} = \{1, 2, 3\}$ is exactly the same as that of $\mathcal{J} = \{1, 2, 3, 4\}$ and $\mathcal{J} = \{1, 2, 3, 10\}$ over the entire SNR regime. Similar behavior can also be seen for $\mathcal{J} = \{1, 3, 5, 6\}$ and $\mathcal{J} = \{1, 3, 5, 10\}$. Furthermore, although $\mathcal{J} = \{1, 2, 10\}$ significantly outperforms $\mathcal{J} = \{8, 9, 10\}$ in terms of the coding gain, the diversity order for both cases is identical and is equal to four.

In addition, since $j_4 = j_3 + 1$ holds for the set $\mathcal{J} = \{1, 3, 5, 6\}$, increasing the number of sources from $N = 3$ to $N = 4$ does not change the diversity order of the system. However, when $\mathcal{J} = \{1, 3, 5, 10\}$, changing $N = 3$ to $N = 4$ reduces the diversity order by a factor of $j_4 - j_3 - 1 = 4$ i.e., from nine to five.

Now, we consider the same system parameters as in Table 2.1 and i.n.i.d. Rayleigh fading channels. Specifically, we assume that number of users $N = 6$, number of selected users $K = 4$, number of relays $M = 4$, and number of selected relays $L = 2$. The transmission rate R_0 is set one. The randomly generated values for the channel variances of the user-to-relay links are given in (2.53). Note that the effect of different transmit power, noise variance, and path loss on the received signal can be lumped into the fading variances [5]. In particular, the element at the nth row and the mth column of matrix $\mathbf{\Sigma}_{SR}$ corresponds to the variance of the channel between user S_n and relay R_m.

$$\mathbf{\Sigma}_{SR} = \begin{bmatrix} 2.3 & 2.6 & 0.5 & 5.1 \\ 6.5 & 0.8 & 4.9 & 6.5 \\ 4.8 & 2.7 & 5.1 & 1.3 \\ 3.9 & 3.9 & 0.7 & 5.2 \\ 3.7 & 4.2 & 2.1 & 1.1 \\ 2.6 & 1.9 & 3.5 & 4.3 \end{bmatrix}. \tag{2.53}$$

Furthermore, the nth and m^{th} elements in the vector variances $\mathbf{\Sigma}_{SD}$ (2.54) and $\mathbf{\Sigma}_{RD}$ (2.55) correspond to the channel variance of the link from user S_n and Relay R_m to the destination D.

$$\mathbf{\Sigma}_{SD} = \begin{bmatrix} 0.7 & 0.8 & 1.2 & 1.3 & 0.9 & 2.3 \end{bmatrix}, \tag{2.54}$$

$$\mathbf{\Sigma}_{RD} = \begin{bmatrix} 2.3 & 1.2 & 3.8 & 4.9 \end{bmatrix}. \tag{2.55}$$

In what follows, the derived analytical expressions for the OP and diversity order are examined via representative numerical plots and Monte-Carlo simulations.

Fig. 2.5 plots the OP of GURS NCC versus SNR ρ with different sets of selected users and two highest-SNR relays ($\mathcal{J} = \{1, 2\}$). One can observe that the analytical curves perfectly match with simulation results, confirming the correctness of the derived

expression (2.17). Furthermore, the asymptotic curves accurately predict the behaviour of the outage provability in the high-SNR regime. More specifically, the slope of the asymptotic curves reveals that the maximum diversity order of $G_{d_1}^{\max} = N - K + L + 1 = 5$ can be achieved if $i_2 = 2$. This is verified as the diversity for $\mathcal{I} = \{1, 2, 3, 5\}$ and $\mathcal{I} = \{1, 2, 4, 6\}$ with $i_2 = 2$ is equal to $G_{d_1}^{\max} = 5$, while that of $\mathcal{I} = \{1, 3, 4, 5\}$ and $\mathcal{I} = \{1, 4, 5, 6\}$ with $i_2 = 3$ and $i_2 = 4$ is equal to four and three, respectively. In conclusion, the condition $i_{K-L} = K - L$ is the necessary condition for achieving maximum diversity $G_{d_1}^{\max}$, as shown in Table 2.1.
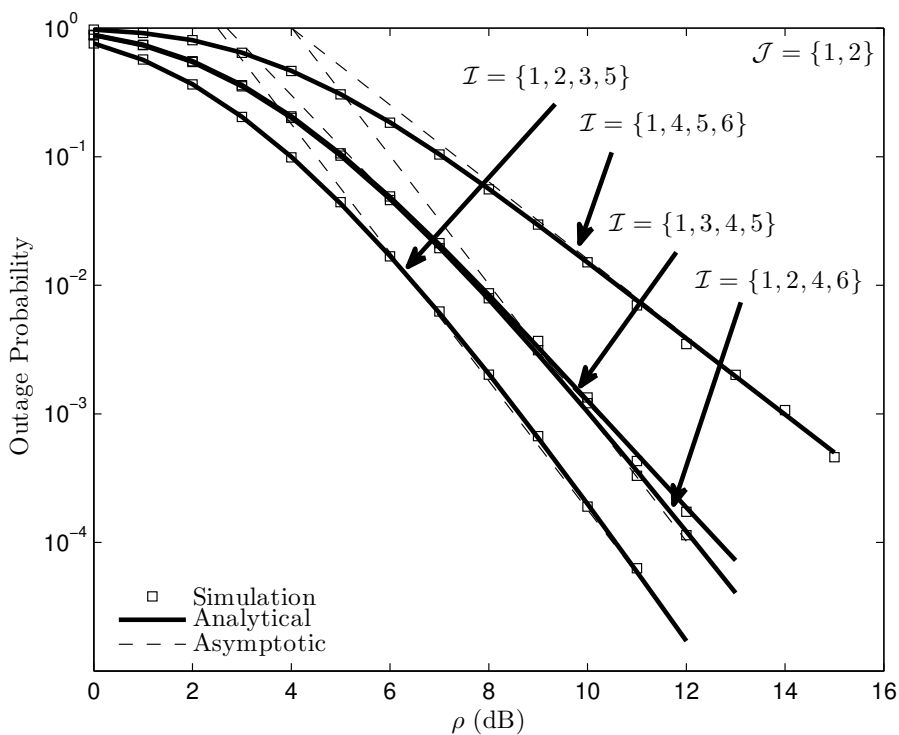
Fig. 2.5: OP versus ρ for $N = 6$, $K = 4$, $M = 4$, $L = 2$, $\mathcal{J} = \{1, 2\}$ with different user selections.

In Fig. 2.6, we plot the OP of GURS NCC for different user-relay selections. It can be seen, the best user selection with the highest- and lowest-SNR relays achieves the maximum diversity order of $G_{d_1}^{\max} = 5$. When $\mathcal{I} = \{1, 2, 3, 5\}$, however, the diversity order varies depending on the RS process. More precisely, the diversity order for $\mathcal{I} = \{1, 2, 3, 5\}$ with $\mathcal{J} = \{1, 2\}$ is equal to five, while that of $\mathcal{I} = \{1, 2, 3, 5\}$ with
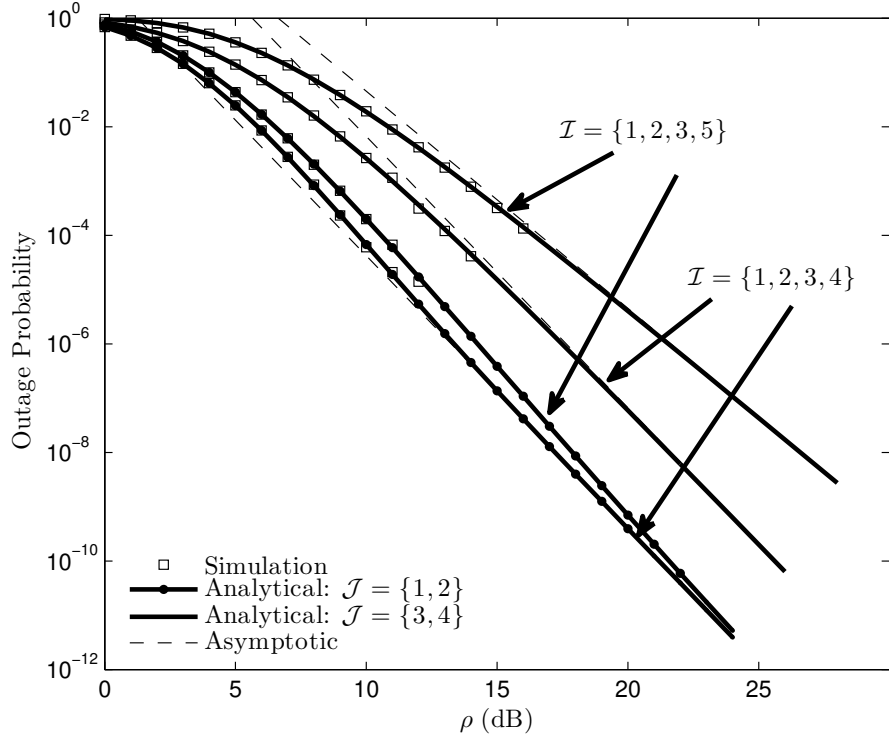
Fig. 2.6: OP versus ρ for $N = 6$, $K = 4$, $M = 4$, $L = 2$ with different user-relay selections.

$\mathcal{J} = \{3, 4\}$ is four. This indicates that the best user selection always guarantees the maximum diversity order $G_{d_1}^{\max}$, no matter how the RS proceeds, as shown in Table 2.1.

Fig. 2.7 illustrates the outage performance of GURS NCC for $\mathcal{I} = \{2, 4, 5, 6\}$ and different RSs. As can be seen, the slope of the curves is always proportional to the number of users N and the i_{K-L}^{th} best user which is reflected by the parallel slopes of the asymptotic lines. This verifies the theoretical observation that the diversity order is equal to $G_{d_1} = N - i_{K-L} + 1 = 3$ (cf. Table 2.1). Interestingly, this diversity is preserved, no matter which of two relays are selected. Furthermore, when the worst relay is not selected i.e., $j_2 \neq 4$, the outage performance is exactly the same as that of the best RS in the high-SNR regime. On the other hand, when the set of selected relays includes the worst relay ($j_2 = 4$), the outage is always worse than that of the best RS both in finite and asymptotic SNRs.

Here, the same system parameters as in Table 2.2 are considered. In particular, we
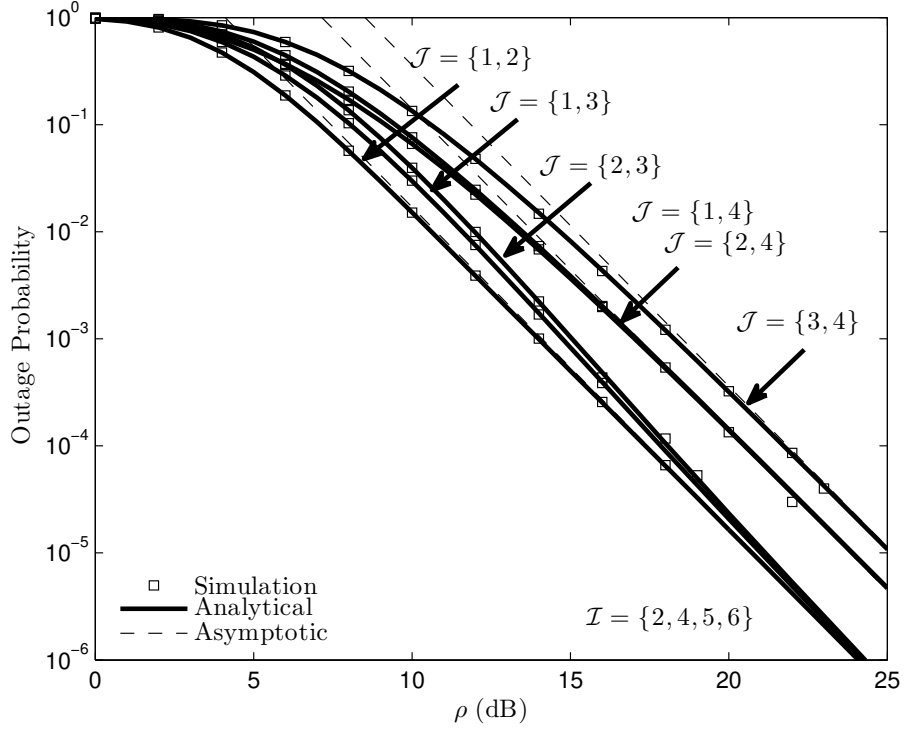
Fig. 2.7: OP versus ρ for $N = 6$, $K = 4$, $M = 4$, $L = 2$, $\mathcal{I} = \{2, 4, 5, 6\}$ and different RS sets.

assume $N = 4$, $K = 2$, $M = 6$, $L = 4$. These system parameters satisfies the condition $K \leq L$. The variances of the user-to-relay, user-to-destination, and relay-to-destination channels are generated randomly and are, respectively, given by (2.56), (2.57), and (2.58). We set the transmission rate as $R_0 = 2$.

$$\mathbf{\Sigma}_{SR} = \begin{bmatrix} 0.5 & 1.3 & 1.4 & 2.1 & 0.7 & 1.9 \\ 2.1 & 2.8 & 2.9 & 2.5 & 2.6 & 1.5 \\ 2.8 & 0.9 & 1.8 & 0.6 & 1.3 & 1.4 \\ 1.6 & 1.5 & 1.2 & 3.2 & 2.8 & 2.4 \end{bmatrix}, \tag{2.56}$$

$$\mathbf{\Sigma}_{SD} = \begin{bmatrix} 1.9 & 0.9 & 1.5 & 1.1 \end{bmatrix}, \tag{2.57}$$

$$\mathbf{\Sigma}_{RD} = \begin{bmatrix} 1.2 & 2.7 & 3.3 & 2.2 & 0.9 & 2.6 \end{bmatrix}. \tag{2.58}$$

Fig. 2.8 shows the outage performance of GURS NCC when the best/worst
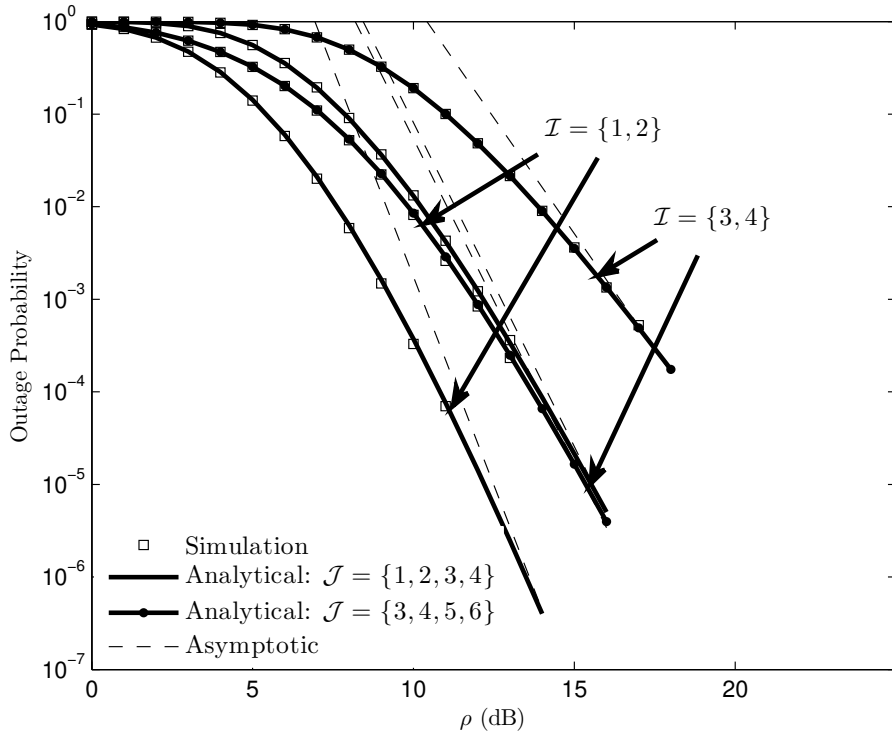
Fig. 2.8: OP versus ρ for $N = 4$, $K = 2$, $M = 6$, $L = 4$ with the best/worst user selection and the best/worst RS.

user and best/worst relay sets are selected. Once again, the analytical curves are confirmed by simulations to be exact and accurate. Furthermore, the asymptotic lines well approximate the exact curves in the high-SNR regime. In addition, we can readily see that the best user-relay selection achieves the maximum diversity of $G_{d_2}^{\max} = N - K + M + 1 = 9$. On the other hand, the worst user-relay selection has the minimum diversity of $G_{d_2}^{\min} = L + 1 = 5$. Besides, although the best-user worst-relay selection outperforms the best-relay worst-user selection in terms of the coding gain, the diversity order for both cases is identical and is equal to $G_{d_2} = M + 1 = 7$ (cf. Table 2.2).

Finally, Figs. 2.9 and 2.10 present the outage performance of GURS NCC for $\mathcal{J} = \{1, 2, 5, 6\}$ and $\mathcal{J} = \{3, 4, 5, 6\}$ when different sets of selected users are considered. As can be seen, three distinct diversities are achieved for $\mathcal{J} = \{1, 2, 5, 6\}$ and $\mathcal{J} = \{3, 4, 5, 6\}$ depending on the set of selected users. In particular, for $\mathcal{J} = \{1, 2, 5, 6\}$,
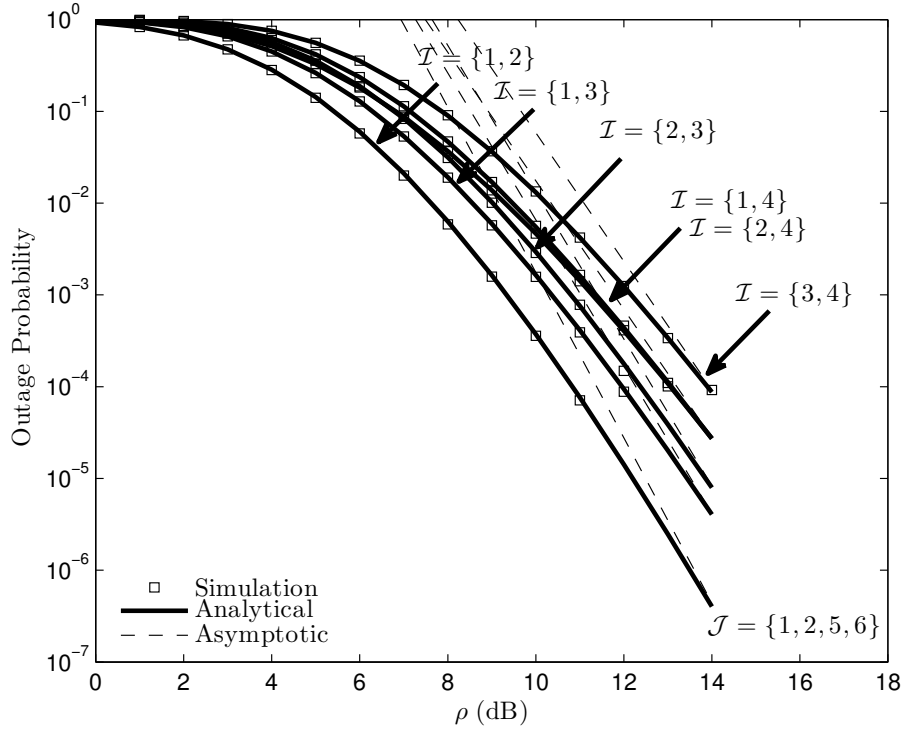
Fig. 2.9: OP versus ρ for $N = 4$, $K = 2$, $M = 6$, $L = 4$, $\mathcal{J} = \{1, 2, 5, 6\}$ and different user selections.

the maximum diversity of $G_{d_2}^{\max} = 9$ is achieved when the user selection includes two highest-SNR users. Furthermore, when the user selection includes the worst user (i.e., $i_2 = 4$), the minimum diversity order of $G_{d_2} = M + 1 = 7$ is achieved. Also, $\mathcal{I} = \{1, 3\}$ and $\mathcal{I} = \{2, 3\}$ have the diversity order of eight. On the other hand, from Fig. 2.10, we observe that in the case of $\mathcal{J} = \{3, 4, 5, 6\}$ the diversity of $G_{d_2} = M + 1 = 7$ is achieved for $\mathcal{I} = \{1, 2\}$. Besides, when $i_2 = 4$ the diversity order of $G_{d_2} = L + 1 = 5$ is achieved. For both $\mathcal{I} = \{1, 3\}$ and $\mathcal{I} = \{2, 3\}$ the diversity is identical and is equal to six. These observations are in agreement with the diversity orders reported in Table 2.2.

2.5   Conclusions

In this chapter, we proposed GURS in a multiuser multirelay NCC system. More specifically, we considered N sources, M relays, and a single destination. The

41
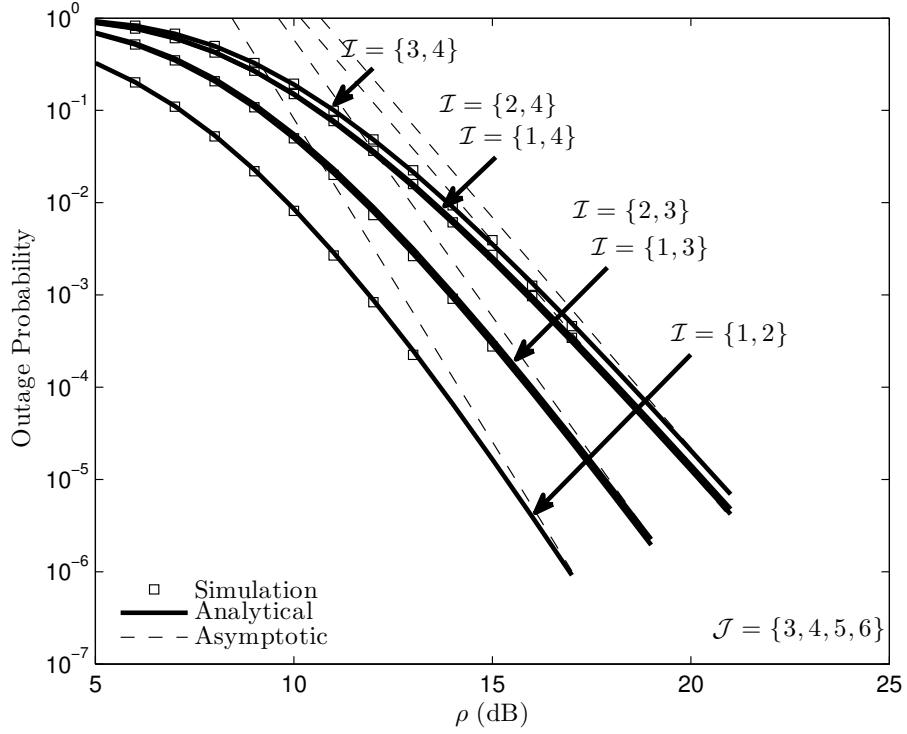
Fig. 2.10: OP versus ρ for $N = 4$, $K = 2$, $M = 6$ $L = 4$, $\mathcal{J} = \{3, 4, 5, 6\}$ and different user selections.

destination selects the $i_1^{\text{th}}, i_2^{\text{th}}, ..., i_K^{\text{th}}$ best sources and the $j_1^{\text{th}}, j_2^{\text{th}}, ..., j_L^{\text{th}}$ best relays subject to any practical considerations. Considering i.n.i.d. Rayleigh fading channels, generalized closed-form expression for the OP has been derived. Asymptotic analysis has been further performed to quantify the diversity order and coding gain of the considered system. We showed that the derived diversity order is the generalized version of the earlier results reported in the literature and thus subsume all existing results as special cases. The theoretical derivations were also validated through Monte-Carlo simulation.

Chapter 3

Underlay Cognitive Network-Coded Cooperation over Nakagami-m Fading Channels

In this chapter, we investigate the performance of an underlay cognitive multisource multirelay NCC with general RS.[1] In particular, the PN consists of a single transmitter-receiver pair, while the SN is composed of $N > 1$ sources, a single destination, and $M \geq 1$ DF relays, employing NC over non-binary GF. Our system models assume i.n.i.d. Nakagami-m fading channels, maximum transmit power at the SN, secondary-to-primary (S2P), and primary-to-secondary (P2S) interference links. For the SN, a closed-form expression and an asymptotically tight E2E OP are derived, and the diversity order is quantified. Our analysis can apply to many network settings and subsumes the case of generalized channels, ranging from i.i.d. Rayleigh fading to i.n.i.d. Nakagami-m fading. Simulation results are further provided to support the accuracy of our analysis.

This chapter is organized as follows: In Section 3.1, we describe the system and channel models. In Section 3.2, we derive the OP and the diversity order of the SN.

---

[1]In this chapter, we assume general RS. Our analysis can be extended to the GURS scenario. This task is left as future work.

Numerical results are provided in Section 3.3. Finally, we conclude in Section 3.4.

3.1   System and Channel Description

Consider a dual-hop cognitive multisource multirelay cooperative network that coexists with a PN with an underlay peak interference power constraint. The former may share the same spectrum band licensed as long as the interference imposed on the latter's receiver remains below a predefined threshold. The SN includes a set of N sources, a set of M DF relays, and a single destination, whereas the PN consists of a single transmitter-receiver pair. In the SN, the cooperation takes place in two phases. The goal is to deliver N sources' packets to the destination successfully. In the first phase, N sources broadcast their messages to the relays and the destination in N orthogonal time-slots. In the second phase, the destination selects a set of L (out of M) relays, the $j_1^{\text{th}}, j_2^{\text{th}}, ..., j_L^{\text{th}}$ best relays, to apply NC on the received N sources' packets and sequentially transmit L NC packets to the destination in L orthogonal time-slots. Specifically, each selected relay transmits a linear combination of sources' packets by decoding the N sources' messages, multiplying them with network-code coefficients drawn from GF, and adding the N products. Since the best relays may not be available due to the practical implementation restriction such as scheduling or load balancing [40], our setup covers all $\binom{M}{L}$ possible RSs.

We assume that the channels for all pertinent links are subject to quasi-static i.n.i.d. Nakagami-m fading. Further, the noise over all channels is zero-mean AWGN with variance one. Denote f_i, h_{ij}, and g_j, $i \in \{1, 2, ..., N\}$, $j \in \{1, 2, ..., M\}$, as the channel coefficients of the ith source-to-destination, ith source-to-jth relay, and jth relay-to-destination links. Besides, the interference channel coefficients of the ith source and jth relay to the primary receiver (PR) are denoted by α_i and α_j, respectively. Further, v_j and v_0 represent the interference channel coefficients of the PT to the jth relay and the destination. Let χ denote a generic channel coefficient between any pair of nodes. Since χ is Nakagami-m distributed, the channel power gain $|\chi|^2$ is modeled as independent RV, following Gamma distribution with integer shape parameter m_χ and

rate parameter $\beta_\chi = \frac{m_\chi}{\Omega_\chi}$ i.e., $|\chi|^2 \sim \mathcal{G}(m_\chi, \beta_\chi)$. The value m_χ measures the small-scale fading, while $\Omega_\chi = \mathbf{E}\{|\chi|^2\}$ quantifies the impact of large-scale fading.

Assume that the sources and the relays are power-limited terminals with maximum allowable transmit power ρ and that the PT has a transmit power of ρ_p. In the underlay scenario, the transmit power of the sources and relays must be adapted such that the interference at the PR is below Q; the maximum tolerable interference power at the PR to guarantee the communication of the PN. Accordingly, the transmit power of the ith source and jth relay are, respectively, adjusted to $\rho_i = \min(Q/Y_i, \rho)$ and $\rho_j = \min(Q/Y_j, \rho)$, where $Y_i \triangleq |\alpha_i|^2$ and $Y_j \triangleq |\alpha_j|^2$. Further, since the PN and SN share the same licensed band, the received signals at the relays and the destination are impacted by interference from the PT. The instantaneous received signal-to-interference-plus-noise ratio (SINR) of a generic single-hop is then given by

$$\gamma = \frac{\hat{\rho} X}{1 + Z}, \tag{3.1}$$

where $\gamma \in \{\gamma_i, \gamma_{ij}, \gamma_j\}$, $\hat{\rho} \in \{\rho_i, \rho_j\}$, $X \in \{X_i, X_{ij}, X_j\}$, $Z \in \{Z_0, Z_j\}$ with $X_i \triangleq |f_i|^2$, $X_{ij} \triangleq |h_{ij}|^2$, $X_j \triangleq |g_j|^2$, $Z_0 \triangleq \rho_p|v_0|^2$, and $Z_j \triangleq \rho_p|v_j|^2$.

3.2 Performance Analysis

3.2.1 Exact Outage Probability

Here, we present the CDF of γ (3.1), which will be invoked in the subsequent derivations.

Lemma 3.1. *The exact CDF of γ is given by*

$$F_\gamma(x, X, Y, Z) = 1 - F_Y(\mu)\left(1 - F_W(x/\rho)\right) - \frac{\beta_Y^{m_Y}\beta_Z^{m_Z}}{\Gamma(m_Y)\Gamma(m_Z)} \sum_{k=0}^{m_X-1} \sum_{l=0}^{k} \sum_{n=0}^{m_Y+k-1} \binom{k}{l}$$
$$\cdot \binom{m_Y + k - 1}{n} \frac{\Gamma(m_Z + l)\hat{\omega}^{m_Z+l-n-1}(-\beta_Z)^{m_Y+k-n-1}}{\omega^{m_Y+m_Z+l-n-1}k!}$$
$$\cdot \Gamma(-(m_Z + l) + n + 1, \hat{\omega}(\mu + \beta_Z/\omega))e^{\frac{\hat{\omega}\beta_Z}{\omega}}, \tag{3.2}$$

where $\mu = Q/\rho$, $\omega = \beta_X x/Q$, $\hat{\omega} = \omega + \beta_Y$,

$$F_W(w) = 1 - \frac{\beta_Z^{m_Z}}{\Gamma(m_Z)} \sum_{k=0}^{m_X-1} \sum_{l=0}^{k} \binom{k}{l} \frac{\Gamma(m_Z + l)}{k!} (\beta_X w)^k (\beta_X w + \beta_Z)^{-(m_Z+l)} e^{-\beta_X w},$$

$$(3.3)$$

$$F_Y(y) = 1 - \sum_{k=0}^{m_Y-1} \frac{(\beta_Y y)^k}{k!} e^{-\beta_Y y}, \tag{3.4}$$

with $m_Z \in \{m_{Z_0}, m_{Z_j}\}$, $\beta_Z \in \{\beta_{Z_0}, \beta_{Z_j}\}$, $m_Y \in \{m_{Y_i}, m_{Y_j}\}$, and $\beta_Y \in \{\beta_{Y_i}, \beta_{Y_j}\}$.

Proof. The CDF of γ (3.1) can be written as

$$F_\gamma(x) = \varpi_1 + \varpi_2, \tag{3.5}$$

where ϖ_1 is given by

$$\varpi_1 = \mathsf{Pr}\left(W < \frac{xY}{Q}, Y \geq \mu\right) = \int_\mu^\infty F_W\left(\frac{xy}{Q}\right) f_Y(y) dy, \tag{3.6}$$

and ϖ_2 can be expressed as

$$\varpi_2 = \mathsf{Pr}\left(W < \frac{x}{\rho}, Y < \mu\right) = F_W(x/\rho) F_Y(\mu), \tag{3.7}$$

where $W \triangleq X/(1+Z)$ and $f_Y(y)$ is given by

$$f_Y(y) = \frac{\beta_Y^{m_Y} y^{m_Y-1}}{\Gamma(m_Y)} e^{-\beta_Y y}. \tag{3.8}$$

To proceed, we need to derive the CDF of W, $F_W(w)$, which can be obtained using the following integral:

$$F_W(w) = \int_0^\infty F_X((1+z)w) f_Z(z) dz, \tag{3.9}$$

where

$$F_X(x) = 1 - \sum_{k=0}^{m_X-1} \frac{(\beta_X x)^k}{k!} e^{-\beta_X x}, \tag{3.10}$$

$$f_Z(z) = \frac{\beta_Z^{m_Z} z^{m_Z-1}}{\Gamma(m_Z)} e^{-\beta_Z z}, \tag{3.11}$$

with $m_X \in \{m_{X_i}, m_{X_{ij}}, m_{X_j}\}$, $\beta_X \in \{\beta_{X_i}, \beta_{X_{ij}}, \beta_{X_j}\}$.

Using (3.10) and the binomial expansion, we have

$$F_X\left((1+z)w\right) = 1 - \sum_{k=0}^{m_X-1} \sum_{l=0}^{k} \binom{k}{l} \frac{(\beta_X w)^k z^l}{k!} e^{-\beta_X(1+z)w}. \qquad (3.12)$$

Next, plugging (3.11) and (3.12) in (3.9), and solving the resultant integral, $F_W(w)$ can be derived as (3.3).

Now, by substituting (3.3) and (3.8) into (3.6), we have

$$\varpi_1 = 1 - F_Y(\mu) - \frac{\beta_Y^{m_Y} \beta_Z^{m_Z}}{\Gamma(m_Z)\Gamma(m_Y)} \sum_{k=0}^{m_X-1} \sum_{l=0}^{k} \binom{k}{l} \frac{\omega^k \Gamma(m_Z+l)}{k!} \hat{\varpi}, \qquad (3.13)$$

where $\hat{\varpi}$ is an integral given by

$$\hat{\varpi} = \int_{\mu}^{\infty} (\omega y + \beta_Z)^{-(m_Z+l)} y^{m_Y+k-1} e^{-\hat{\omega}y} dy. \qquad (3.14)$$

By changing variable $u = \omega y + \beta_Z$, we have

$$\hat{\varpi} = \int_{\omega\mu+\beta_Z}^{\infty} \omega^{-(m_Y+k)} (u - \beta_Z)^{m_Y+k-1} u^{-(m_Z+l)} e^{-\frac{\hat{\omega}(u-\beta_Z)}{\omega}} du. \qquad (3.15)$$

Solving the integral in (3.15) and then inserting the resultant expression in (3.13), the first summand in (3.5), ϖ_1, is obtained.

On the other hand, the second summand (3.7) can easily be obtained using (3.3) and (3.4). Finally, adding ϖ_1 with ϖ_2 yields the final expression in (3.2). This completes the proof. □

Special Case 3.1. *The derived closed-form CDF (3.2) is simplified to (16) of [50] when normalized i.i.d. Rayleigh fading channels are considered ($m_\chi = 1$, $\Omega_\chi = 1$).*

Theorem 3.1. *Consider an underlay cognitive N-source M-relay cooperative network. If the relays use DF protocol and apply NC on the received sources' packets and the destination selects L relays, the j_1^{th}, j_2^{th},..., j_L^{th} best relays, the OP of the SN, over i.n.i.d. Nakagami-m fading channels, is derived as*

$$P_{out}(\gamma_{th}) = \sum_{\tau=0}^{N-L-1} \Phi(\tau) + \sum_{\tau=1}^{L} \Phi(N-\tau) \sum_{\eta=0}^{\tau-1} \Upsilon(\eta), \qquad (3.16)$$

if $N > L$, otherwise it is given by

$$P_{out}(\gamma_{th}) = \sum_{\tau=1}^{N} \Phi(N-\tau) \sum_{\eta=0}^{\tau-1} \Upsilon(\eta), \qquad (3.17)$$

with

$$\Phi(\tau) = \sum_{1 \le a_1 < \cdots < a_\tau \le N} \left[\prod_{i=a_1}^{a_\tau} (1 - F_{\gamma_i}(\gamma_{th})) \prod_{\substack{i'=1 \\ i' \ne \{a_1,\ldots,a_\tau\}}}^{N} F_{\gamma_{i'}}(\gamma_{th}) \right], \qquad (3.18)$$

where

$$F_{\gamma_i}(\gamma_{th}) = F_\gamma(\gamma_{th}, X_i, Y_i, Z_0), \qquad (3.19)$$

and γ_{th} is the threshold SINR. Further, $\Upsilon(\eta)$ is formulated as

$$\Upsilon(\eta) = \sum_{v=M-j_{\eta+1}+1}^{M-j_\eta} \psi(v), \qquad (3.20)$$

in which

$$\psi(v) = \sum_{1 \le a_1 < \cdots < a_v \le M} \left[\prod_{j=a_1}^{a_v} F_{\hat\gamma_j}(\gamma_{th}) \prod_{\substack{j'=1 \\ j' \ne \{a_1,\ldots,a_v\}}}^{M} \left(1 - F_{\hat\gamma_{j'}}(\gamma_{th}) \right) \right], \qquad (3.21)$$

where

$$F_{\hat\gamma_j}(\gamma_{th}) = 1 - \prod_{i=1}^{N} \left[1 - F_{\gamma_{ij}}(\gamma_{th}) \right] \left[1 - F_{\gamma_j}(\gamma_{th}) \right], \qquad (3.22)$$

with

$$F_{\gamma_{ij}}(\gamma_{th}) = F_\gamma(\gamma_{th}, X_{ij}, Y_i, Z_j), \qquad (3.23)$$

$$F_{\gamma_j}(\gamma_{th}) = F_\gamma(\gamma_{th}, X_j, Y_j, Z_0). \qquad (3.24)$$

Proof. In NCC, each relay is connected to $N + 1$ links; N source-to-relay links and one relay-to-destination link. The E2E performance of dual-hop multi-source-to-relay-to-destination link is determined by the link whose SINR is less than that of other links. Accordingly, each dual-hop multi-source-to-relay-to-destination link can be treated as a single-hop link with

the SINR given by $\hat{\gamma}_j = \min \{\gamma_{ij}, \gamma_j\}_{i=1}^{N}$. The OP of the jth relay can then be written as

$$F_{\hat{\gamma}_j}(\gamma_{th}) = 1 - \Pr \{\hat{\gamma}_j > \gamma_{th}\}. \tag{3.25}$$

Since γ_{ij} ($\forall i$) and γ_j are mutually independent RVs, (3.25) can be written as (3.22).

At the end of the second phase, the destination receives $N + L$ packets; N original sources' packets through direct source-to-destination links and L NC packets through relay-to-destination links. The system is in outage if fewer than N packets are successfully delivered at the destination. Denote τ and η, respectively, as the number of successful transmissions from the N sources and L selected relays. The outage events of the system can then be formulated as

$$\mathcal{O} = \mathcal{O}_\mathcal{A} \bigcup \mathcal{O}_\mathcal{B}, \tag{3.26}$$

where i) $\mathcal{O}_\mathcal{A}$ represents the outage events when $N > L$ and there are not enough number of successful transmissions through source-to-destination links such that even if all the relay transmissions are successful i.e., $\eta = L$, the destination is still in outage i.e., $\tau < N - L$; and ii) $\mathcal{O}_\mathcal{B}$ stands for the outage events where $\tau \geq N - L$, but the sum of successful transmissions is less than N i.e., $\tau + \eta < N$.

The probability of $\mathcal{O}_\mathcal{A}$ in (3.26) can be written as

$$\Pr\{\mathcal{O}_\mathcal{A}\} = \sum_{\tau=0}^{N-L-1} \Phi(\tau), \tag{3.27}$$

where $\Phi(\tau)$ is given by (3.18) and is the probability that τ (out of N) direct transmissions are successful and the remaining $N - \tau$ direct transmissions are in outage.

On the other hand, the probability that v relays out of M available relays are in outage can be written as (3.21). Further, the probability that η transmissions from L relay transmissions are successful can be derived as (3.20). Next, with the aid of (3.18) and (3.20), the probability of $\mathcal{O}_\mathcal{B}$ in (3.26) is formulated as

$$\Pr\{\mathcal{O}_\mathcal{B}\} = \sum_{\tau=1}^{\delta} \Phi(N - \tau) \sum_{\eta=0}^{\tau-1} \Upsilon(\eta), \tag{3.28}$$

where $\delta = L$ if $N > L$ and $\delta = N$ if $N \leq L$.

Finally, using (3.27) and (3.28) along with (3.26), one can obtain (3.16) and (3.17), thus completing the proof. $\qquad\square$

3.2.2 Asymptotic Analysis

Here, we derive the asymptotic E2E OP in the high-SNR region ($\rho \to \infty$) for two cases: Case 1 when $Q = \mu\rho$, $\mu > 0$; and Case 2 when Q is fixed. The following theorem presents the diversity order and coding gain of the SN when Case 1 is considered.

Theorem 3.2. *When $Q = \mu\rho$, the diversity order is given by*

$$G_d = \begin{cases} \min\{G_{d_\mathcal{A}}, G_{d_\mathcal{B}}(L)\}, & N > L \\ G_{d_\mathcal{B}}(N), & N \leq L \end{cases} \tag{3.29}$$

with

$$G_{d_\mathcal{A}} = \min\{m_{f_{i_1}} + ... + m_{f_{i_{L+1}}} | 1 \leq i_1 < ... < i_{L+1} \leq N\}, \tag{3.30}$$

$$G_{d_\mathcal{B}}(\delta) = \min\{\mathcal{M}(\tau)\}_{\tau=1}^\delta, \tag{3.31}$$

$\mathcal{M}(\tau) = \mathcal{M}_1(\tau) + \mathcal{M}_2(\tau)$, $\mathcal{M}_1(\tau) = \min\{m_{f_{i_1}} + ... + m_{f_{i_\tau}} | 1 \leq i_1 < ... < i_\tau \leq N\}$, $\mathcal{M}_2(\tau) = \min\{m_{i_1} + ... + m_{i_{M-j_\tau+1}} | 1 \leq i_1 < ... < i_{M-j_\tau+1} \leq M\}$, $m_j = \min\{\hat{m}_j, m_{g_j}\}$, and $\hat{m}_j = \min\{m_{h_{ij}}\}_{i=1}^N$. Further, the coding gain is given by

$$G_c = \begin{cases} \dfrac{\mathcal{C}_1^{-\frac{1}{G_{d_\mathcal{A}}}}}{\gamma_{th}}, & G_{d_\mathcal{A}} < G_{d_\mathcal{B}}(L) \\[3mm] \dfrac{\mathcal{C}_2(L)^{-\frac{1}{G_{d_\mathcal{B}}(L)}}}{\gamma_{th}}, & G_{d_\mathcal{A}} > G_{d_\mathcal{B}}(L) \\[3mm] \dfrac{(\mathcal{C}_1 + \mathcal{C}_2(L))^{-\frac{1}{G_{d_\mathcal{A}}}}}{\gamma_{th}}, & G_{d_\mathcal{A}} = G_{d_\mathcal{B}}(L) \end{cases} \tag{3.32}$$

if $N > L$, otherwise it is

$$G_c = \frac{\mathcal{C}_2(N)^{-\frac{1}{G_{d_\mathcal{B}}(N)}}}{\gamma_{th}}, \tag{3.33}$$

where

$$\mathcal{C}_1 = \sum_{\substack{1 \leq a_1 < \cdots < a_{L+1} \leq N \\ m_{f_{a_1}} + ... + m_{f_{a_{L+1}}} = G_{d_\mathcal{A}}}} \left\{ \prod_{i=a_1}^{a_{L+1}} \Xi(X_i, Y_i, Z_0) \right\}, \tag{3.34}$$

$$\mathcal{C}_2(\delta) = \sum_{\substack{\mathcal{M}(\tau)=G_{d_{\mathcal{B}}}(\delta)}} \left\{ \sum_{\substack{1\leq a_1 < \cdots < a_\tau \leq N \\ m_{f_{a_1}} + \ldots + m_{f_{a_\tau}} = \mathcal{M}_1(\tau)}} \prod_{i=a_1}^{a_\tau} \Xi(X_i, Y_i, Z_0) \right.$$

$$\left. \sum_{\substack{1\leq a_1 < \cdots < a_{M-j_\tau+1} \leq M \\ m_{f_{a_1}} + \ldots + m_{f_{a_{M-j_\tau+1}}} = \mathcal{M}_2(\tau)}} \prod_{j=a_1}^{a_{M-j_\tau+1}} \mathcal{H}_j \right\}, \qquad (3.35)$$

with $\Xi(X, Y, Z) = \Xi_1(X, Y, Z) + \Xi_2(X, Y, Z)$, where

$$\Xi_1(X, Y, Z) = \frac{\beta_Y^{m_Y} \beta_Z^{m_Z}}{\Gamma(m_Z)\Gamma(m_Y)} \sum_{l=0}^{m_X} \binom{m_X}{l} \frac{(\beta_X/\mu)^{m_X}}{m_X!}$$

$$.\Gamma(m_Z + l)\Gamma(m_X + m_Y, \mu\beta_Y)\beta_Y^{-(m_X+m_Y)}\beta_Z^{-(m_Z+l)}, \qquad (3.36)$$

$$\Xi_2(X, Y, Z) = \frac{\beta_Z^{m_Z}}{\Gamma(m_Z)} \sum_{l=0}^{m_X} \binom{m_X}{l} \frac{\Gamma(m_Z + l)}{m_X!} \beta_X^{m_X} \beta_Z^{-(m_Z+l)} F_Y(\mu), \qquad (3.37)$$

$$\mathcal{H}_j = \begin{cases} \Xi(X_j, Y_j, Z_0), \\ \qquad\qquad\qquad\qquad \hat{m}_j > m_{g_j} \\ \sum_{i:m_{h_{ij}}=\hat{m}_j} \Xi(X_{ij}, Y_i, Z_j), \\ \qquad\qquad\qquad\qquad \hat{m}_j < m_{g_j} \\ \Xi(X_j, Y_j, Z_0) + \sum_{i:m_{h_{ij}}=\hat{m}_j} \Xi(X_{ij}, Y_i, Z_j), \\ \qquad\qquad\qquad\qquad \hat{m}_j = m_{g_j} \end{cases} \qquad (3.38)$$

Proof. The asymptotic expression of (3.3) can be derived as

$$F_W^\infty(w) = \frac{\beta_Z^{m_Z}}{\Gamma(m_Z)} \sum_{l=0}^{m_X} \binom{m_X}{l} \frac{\Gamma(m_Z + l)}{m_X!} (\beta_X w)^{m_X} \beta_Z^{-(m_Z+l)}. \qquad (3.39)$$

Substituting (3.39) into (3.6) and (3.7), we, respectively, obtain

$$\varpi_1^\infty = \Xi_1(X, Y, Z) \left(\frac{\gamma_{th}}{\rho}\right)^{m_X},$$

$$\varpi_2^\infty = \Xi_2(X, Y, Z) \left(\frac{\gamma_{th}}{\rho}\right)^{m_X}. \qquad (3.40)$$

Therefore, (3.2) can be expressed as

$$F_\gamma^\infty(\gamma_{th}, X, Y, Z) = \Xi(X, Y, Z) \left(\frac{\gamma_{th}}{\rho} \right)^{m_X}. \tag{3.41}$$

Using (3.41), the asymptotic expression of (3.19) is given by

$$F_{\gamma_i}^\infty(\gamma_{th}) = \Xi(X_i, Y_i, Z_0) \left(\frac{\gamma_{th}}{\rho} \right)^{m_{f_i}}. \tag{3.42}$$

Next, substituting (3.42) into (3.18) and then ignoring higher order terms, we find

$$\Phi^\infty(\tau) = \sum_{1 \le a_1 < \cdots < a_{N-\tau} \le N} \prod_{i=a_1}^{a_{N-\tau}} \Xi(X_i, Y_i, Z_0) \left(\frac{\gamma_{th}}{\rho} \right)^{m_{f_i}}. \tag{3.43}$$

Now, we proceed to find the asymptotic expression of (3.22). According to (3.41), we have

$$F_{\gamma_j}^\infty(\gamma_{th}) = \Xi(X_j, Y_j, Z_0) \left(\frac{\gamma_{th}}{\rho} \right)^{m_{g_j}}. \tag{3.44}$$

Further, based on the following multinomial expansion identity

$$\prod_{\ell=1}^T (1 - x_\ell) = 1 + \sum_{k=1}^T (-1)^k \sum_{1 \le a_1 < \cdots < a_k \le T} \prod_{m=a_1}^{a_k} x_m, \tag{3.45}$$

the term in (3.22) in the high-SNR regime can be written as

$$\prod_{i=1}^N \left[1 - F_{\gamma_{ij}}^\infty(\gamma_{th}) \right] = 1 + \sum_{k=1}^N (-1)^k \sum_{1 \le a_1 < \cdots < a_k \le N} \prod_{i=a_1}^{a_k} F_{\gamma_{ij}}^\infty(\gamma_{th}), \tag{3.46}$$

where

$$F_{\gamma_{ij}}^\infty(\gamma_{th}) = \Xi(X_{ij}, Y_i, Z_j) \left(\frac{\gamma_{th}}{\rho} \right)^{m_{h_{ij}}}. \tag{3.47}$$

Finally, keeping the dominant terms in (3.46) and then plugging the resultant expression and (3.44) in (3.22), we have

$$F_{\hat{\gamma}_j}^\infty(\gamma_{th}) = \mathcal{H}_j \left(\frac{\gamma_{th}}{\rho} \right)^{m_j}, \tag{3.48}$$

where $\mathcal{H}_j$ has been defined in (3.38).

Now, by plugging (3.48) into (3.21) and then keeping the dominant terms, we obtain

$$\psi^\infty(v) = \sum_{1 \le a_1 < \cdots < a_v \le M} \prod_{j=a_1}^{a_v} \mathcal{H}_j \left(\frac{\gamma_{th}}{\rho} \right)^{m_j}. \tag{3.49}$$

Substituting (3.43) in (3.27), and then ignoring higher order terms, (3.27) is approximated as

$$\Pr^{\infty}\{\mathcal{O}_{\mathcal{A}}\} = \mathcal{C}_1 \left(\frac{\gamma_{th}}{\rho}\right)^{G_{d_{\mathcal{A}}}}. \tag{3.50}$$

Further, (3.28) can be simplified to

$$\Pr^{\infty}\{\mathcal{O}_{\mathcal{B}}\} = \mathcal{C}_2(\delta) \left(\frac{\gamma_{th}}{\rho}\right)^{G_{d_{\mathcal{B}}}(\delta)}. \tag{3.51}$$

Finally, using (3.50), (3.51), and (1.3), the diversity order and coding gain can be obtained, thus completing the proof. □

Remark 3.1. *According to (3.29), the diversity is independent of the peak interference power constraint, Q, and the fading severity parameters $\{m_{\alpha_i}\}_{i=1}^{N}$, $\{m_{\alpha_j}\}_{j=1}^{M}$, $\{m_{v_j}\}_{j=1}^{M}$, and m_{v_0}. Instead, N, M, L, and the fading severity parameters in the SN $\{m_{f_i}\}_{i=1}^{N}$ and $\{m_j\}_{j=1}^{M}$ have a direct impact on the diversity. The interference power constraint manifests its effect on the coding gain.*

Special Case 3.2. *The diversity order (3.29) is a generalized version of the existing results in the NCC literature when Rayleigh fading channels are assumed ($m_{\chi} = 1$). In particular, for $L = M$ (no RS), it reduces to $G_d = M + 1$ [29, 30]. When L highest-SNR relays are selected, the diversity order for $N > L$ and $N \leq L$ reduces to $G_d = L+1$ and $G_d = M+1$, respectively. This is in line with the diversity order reported in [29, 30]. For any arbitrary RSs, it reduces to the diversity order of $G_d = L+1$ and $G_d = N + M - j_N + 1$ for $N > L$ and $N \leq L$ [61].*

Special Case 3.3. *The derived diversity order can also be seen as a generalization of several previous results presented in the non-NCC (conventional CC) literature. More specifically, assuming Rayleigh fading channels, $N = 1$, and the best RS, it reduces to $G_d = M + 1$ [21]. For $N = 1$ and the j_1^{th} best RS, it reduces to $G_d = M - j_1 + 2$ which coincides with that of in [40]. For $N = 1$ and any arbitrary RSs, it reduces to $G_d = M - j_1 + 2$ [42]. On the other hand, if Nakagami-m fading channels are assumed, it reduces to $G_d = m_f + \sum_{i=1}^{M} m_i$ [63] and $G_d = m_f + \min\{m_{i_1} + ... + m_{i_{M-j_1+1}} | 1 \leq i_1 < ... < i_{M-j_1+1} \leq M\}$ [64], when the best relay and the j_1^{th} best relay are selected.*

Theorem 3.3. *When Q is fixed, the OP saturates in the high-SNR regime, resulting in an error floor and a diversity order of zero.*

Proof. The proof follows similar steps as the proof of Theorem 3.2, hence omitted to save space. □

3.3 Numerical Results and Discussion

Herein, our preceding analysis is validated via representative numerical plots and simulations. In all figures, we assume that $N = 3$, $M = 5$, $\{m_{f_i}\}_{i=1}^3 = \{2, 3, 1\}$, $\{m_{h_{1j}}\}_{j=1}^5 = \{2, 2, 2, 1, 2\}$, $\{m_{h_{2j}}\}_{j=1}^5 = \{2, 1, 2, 3, 3\}$, $\{m_{h_{3j}}\}_{j=1}^5 = \{3, 2, 3, 2, 2\}$, $\{m_{g_j}\}_{j=1}^5 = \{2, 2, 1, 2, 1\}$, $\gamma_{th} = 0$ dB, $Q = 15$ dB, and $\rho_p = 3$ dB. For simplicity, we define $m_{\alpha_i} = 1$, $m_{\alpha_j} = 2$, $m_{v_j} = 1$, $m_{v_0} = 1$, and $\Omega_{f_i} = \Omega_{h_{ij}} = \Omega_{g_j} = \Omega_{\alpha_i} = \Omega_{\alpha_j} = \Omega_{v_j} = \Omega_{v_0} = 1$ ($\forall i, j$). All the figures clearly show that the analytical and simulation curves perfectly match. And, importantly, the asymptotic lines accurately predict the outage behavior in the high SNR regime.

Fig. 3.1 depicts the OP versus ρ for different RSs when $L = 2$ ($N > L$) and Q scales with ρ. As can be seen, the OP of the SN improves continuously with increasing ρ without any outage floor. Furthermore, the slope of the curves reveals that the SN achieves the maximum diversity of six when $\mathcal{J} = \{1, 2\}$ and $\mathcal{J} = \{1, 3\}$. The diversity for $\mathcal{J} = \{1, 4\}$, however, reduces to five. It further reduces to four when $\mathcal{J} = \{1, 5\}$ and $\mathcal{J} = \{3, 5\}$, while it takes its minimum value of three when the RS includes two-lowest SNR relays ($\mathcal{J} = \{4, 5\}$). This verifies the theoretical observation that the SN diversity is determined by (3.29) when Q scales with ρ.

In Figs. 3.2 and 3.3, we plot the OP versus ρ when $L = 3$ ($N \leq L$). Fig. 3.2 illustrates the OP when Q is proportional to ρ. As can be seen from Fig. 3.2, the OP improves substantially as ρ increases. Also, we can readily check that the maximum diversity of seven is achieved when the RS includes the highest-SNR relays (i.e., $\mathcal{J} = \{1, 2, 3\}$). In addition, the diversity for $\mathcal{J} = \{1, 3, 4\}$, $\mathcal{J} = \{2, 4, 5\}$, and $\mathcal{J} = \{3, 4, 5\}$ reduces to six, five, and four, respectively (3.29). Fig. 3.3 presents the OP when Q is fixed and is independent of ρ. The figure shows that an error floor
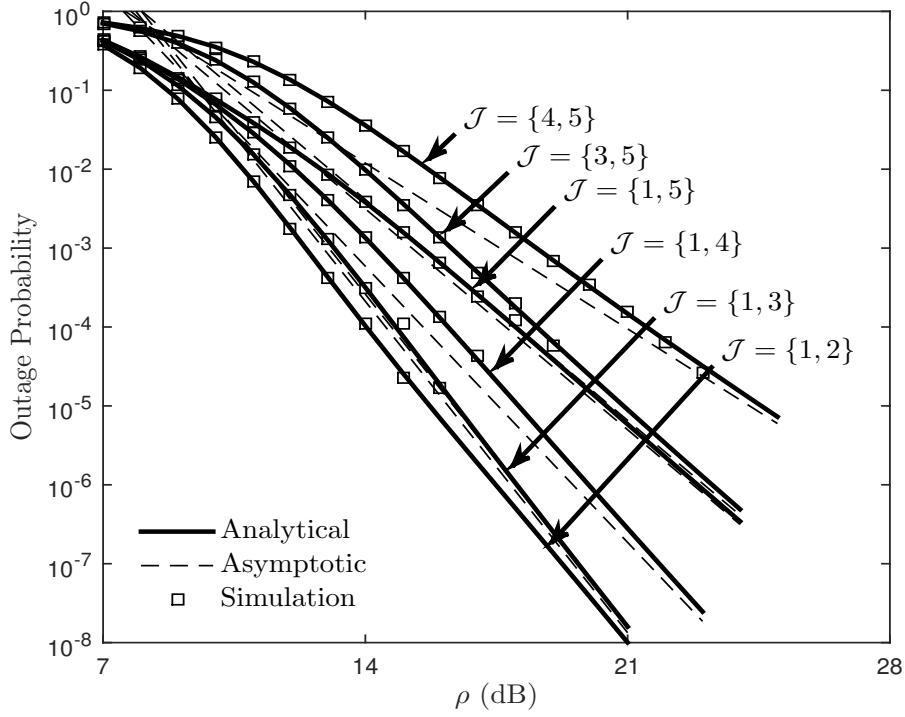
Fig. 3.1: OP versus ρ for different RSs when $N = 3$, $M = 5$, $L = 2$ $(N > L)$.

occurs, since the SN transmit power level is strictly constrained by Q as ρ grows large.

3.4 Conclusions

We studied the performance of a generic multisource multirelay NCC system in an underlay spectrum sharing. Considering i.n.i.d. Nakagami-m fading channels, new analytical expressions have been derived for the exact and asymptotic OP of the SN. The SN diversity order was quantified to provide valuable insights. Our results revealed that the diversity is only determined by the fading severity of the SN when Q scales with ρ. On the other hand, when Q is fixed, the OP saturates in the high-SNR regime, resulting in an error floor and a zero diversity order.
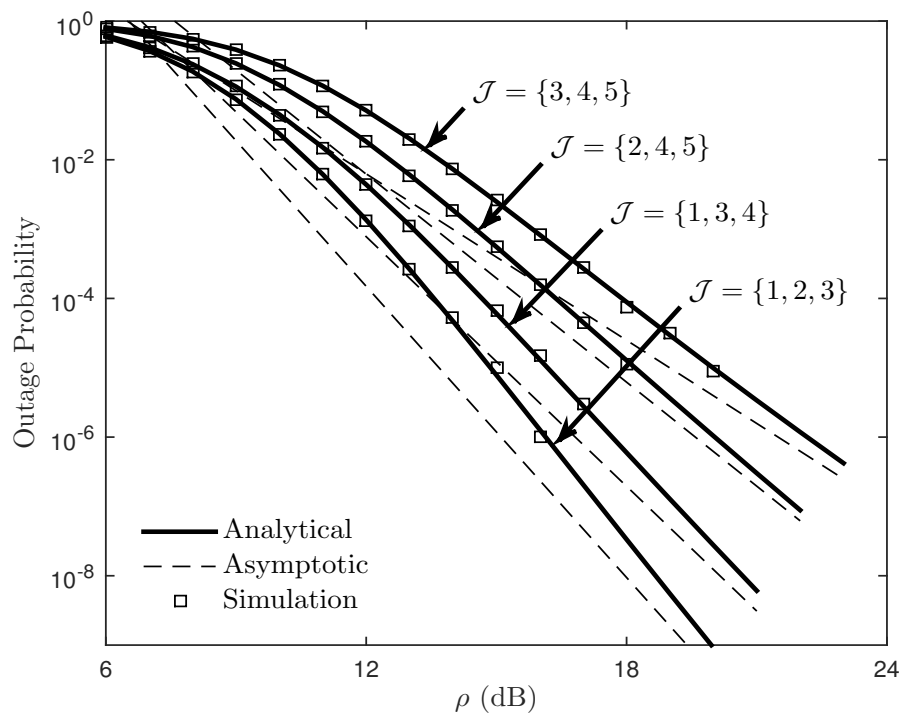
Fig. 3.2: OP versus ρ for different RSs when $N = 3$, $M = 5$, $L = 3$ ($N \leq L$).
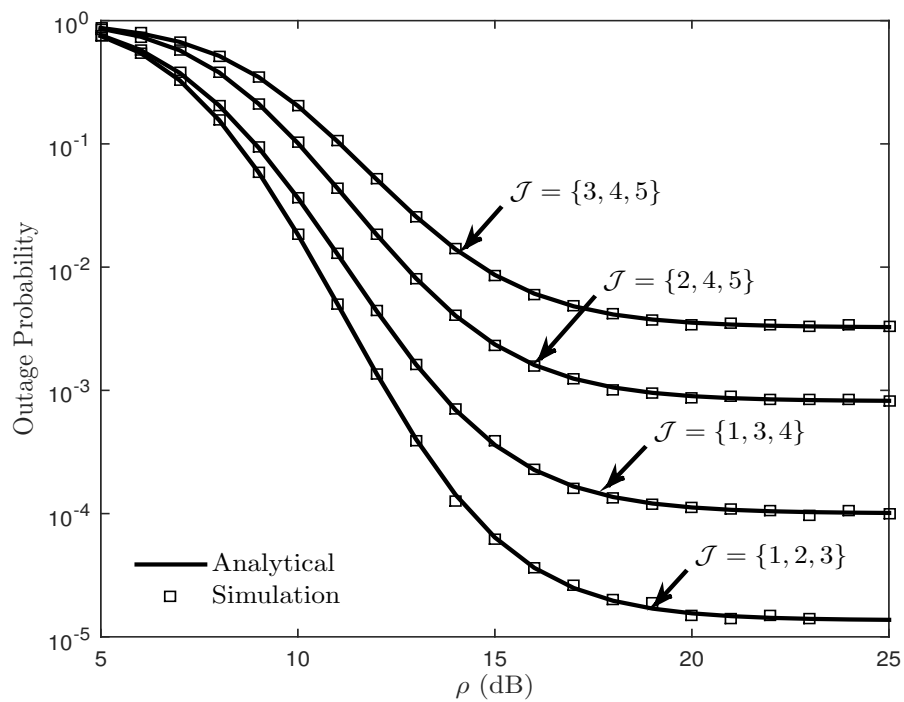
Fig. 3.3: OP versus ρ for different RSs when $N = 3$, $M = 5$, $L = 3$ ($N \leq L$).

Chapter 4

Relay Selection in Network Coded Cooperative MIMO Systems

In this chapter, we study the performance of a RS MIMO NCC system that consists of $N > 1$ single-antenna sources, a multiple-antenna destination, and $M \geq 1$ multiple-antenna relays. This scenario could be an instance of the cellular uplink, where single-antenna mobile terminals communicate with a multiple-antenna BS with infrastructure relays.[1] This is a realistic assumption, since the use of multiple antennas at the relays and the BS is reasonable. In contrast, multiple antennas at mobile terminals are restricted because of the size constraint, transmission power, and circuit complexity. Among various strategies to exploit multiple antennas, we consider transmit antenna selection (TAS) at the transmitter side. This choice is made because TAS is easy to implement with low feedback signaling [66]. On the other hand, MRC can maximize the diversity order and the received SNR at the receiver side. Therefore, in our system setup, the relays and destination use MRC for signal reception, and relays use TAS for forwarding the encoded signals to the destination. The contributions of

---

[1]Infrastructure relays are applicable in practice to infrastructure-based relay networks, where relays are fixed and therefore can be equipped with multiple antennas [65].

this work can be summarized as follows:

- Attracted by the benefits of multi-antenna techniques in enhancing NCC system performance, we extend single-antenna NCC to a multi-antenna scenario.

- A new RS strategy (Strategy $\mathcal{B}$) for NCC systems is proposed and analyzed. It can substantially reduce the required signaling overhead for RS-based NCC, particularly in a network with a large number of branches without sacrificing the performance. RS Strategy $\mathcal{B}$ is different from those based on "*max-min*" criterion (called Strategy $\mathcal{A}$) [29, 30] because it requires local CSI only. Therefore, our analytical analysis are new and completely different from those earlier reported in [29, 30].

- We derive exact OP expressions for MIMO NCC system with RS strategy $\mathcal{A}$ and $\mathcal{B}$ over i.n.i.d. Rayleigh fading channels.

- The asymptotic outage expressions are further provided to characterize the key performance indicators such as the diversity order and coding gain.

- We further present special cases for our derived analytical expressions to demonstrate that they are generalized versions of those earlier presented in the literature and coincide with them when single-antenna terminals are considered.

- We compare the outage performance of the proposed RS MIMO NCC with two benchmark schemes, namely single-antenna RS NCC [29, 30], and RS MIMO NCC with random antenna selection (RAS) at relays.

- Numerical results are also presented to validate the accuracy of our derivations and quantify the effect of different system parameters on the OP and diversity order.

The remainder of this chapter is organized as follows. In Section 4.1, the system model under consideration is described. In Section 4.2, we derive the OP of single-hop links and discuss the signaling overhead of RS Strategy $\mathcal{A}$ and $\mathcal{B}$. In Section 4.3, the OP and asymptotic expressions of MIMO NCC with RS Strategy $\mathcal{A}$ are derived. Section 4.4 provides the performance of MIMO NCC with RS Strategy $\mathcal{B}$. Analytical

results and Monte-Carlo simulations are compared in Section 4.5. Finally, Section 4.6 concludes this chapter.

4.1   System Model

We consider a MIMO NCC system consisting of N sources $\mathcal{S} = \{S_n\}_{n=1}^{N}$, M relays $\mathcal{R} = \{R_m\}_{m=1}^{M}$, and one destination D. In particular, sources have single antenna, whereas relays and the destination are equipped with $N_r \geq 1$ and $N_d \geq 1$ antennas, respectively. All terminals operate in half-duplex mode. We assume flat fading uncorrelated Rayleigh fading channels, where $\mathbf{h}_{S_n R_m} \in \mathbb{C}^{N_r \times 1}$, $\mathbf{h}_{S_n D} \in \mathbb{C}^{N_d \times 1}$, and $\mathbf{H}_{R_m D} \in \mathbb{C}^{N_d \times N_r}$, respectively denote the channel for $S_n \to R_m$, $S_n \to D$, and $R_m \to D$ links. The $N_d \times 1$ channel vector of the ith transmit antenna for $R_m \to D$ is denoted by $\mathbf{h}_{R_m^{(i)} D}$. We make the practical assumption of i.n.i.d. channels, where the signals transmitted through different links experience different radio environments. In particular, the elements of $\mathbf{h}_{S_n R_m}$, $\mathbf{h}_{S_n D}$, and $\mathbf{H}_{R_m D}$ are modeled as $\mathcal{CN}(0, \lambda_{n,m})$, $\mathcal{CN}(0, \lambda_n)$, and $\mathcal{CN}(0, \lambda_m)$. Furthermore, the noise corresponding to each channel is independent AWGN with $\mathcal{CN}(0, N_0)$.

   In our system, cooperation takes place in two phases, namely the broadcasting and relaying phases. During the broadcasting phase, the sources transmit their symbols to the destination in N non-overlapping time slots. Both the destination and relays employ MRC reception to decode the data symbols received from the sources. During the relaying phase, sources remain silent and the selected relay(s) apply(s) NC in GF and then forward(s) network-coded symbols to the destination using TAS. Finally, the destination decodes encoded symbols received from the relays in the relaying phase by using MRC. We assume a centralized RS method where the RS process, for both Strategy $\mathcal{A}$ and $\mathcal{B}$, is performed by a central unit (e.g., the destination).

4.2 Preliminaries and Discussion

In this section, the OP expressions of single-hop links are derived to facilitate the overall outage analysis of MIMO NCC system. We further discuss the signaling overhead of RS Strategy $\mathcal{A}$ and $\mathcal{B}$.

4.2.1 Outage Probability of Single-Hop Links

In NCC systems, the outage probabilities of the source-to-relay, source-to-destination, and relay-to-destination links are the building blocks of overall OP of the system.

Since relays and the destination employ MRC at the receiver side, the equivalent instantaneous SNR for $S_n \rightarrow R_m$ and $S_n \rightarrow D$ links are respectively given by $\gamma_{n,m} = \bar{\gamma} \|\mathbf{h}_{S_n R_m}\|^2$, and $\gamma_n = \bar{\gamma} \|\mathbf{h}_{S_n D}\|^2$, where $\bar{\gamma}$ is the transmit SNR. Similarly, for the ith transmit antenna at the relay R_m in the relaying phase, the equivalent instantaneous SNR is given by $\gamma_m^{(i)} = \bar{\gamma} \|\mathbf{h}_{R_m^{(i)} D}\|^2$. Furthermore, $\gamma_{n,m}$, γ_n, and $\gamma_m^{(i)}$ are independent Gamma distributed RVs with $\gamma_{n,m} \sim \mathcal{G}(N_r, \bar{\gamma}_{n,m})$, $\gamma_n \sim \mathcal{G}(N_d, \bar{\gamma}_n)$, and $\gamma_m^{(i)} \sim \mathcal{G}(N_d, \bar{\gamma}_m)$, where $\bar{\gamma}_{n,m} = \bar{\gamma}\lambda_{n,m}$, $\bar{\gamma}_n = \bar{\gamma}\lambda_n$, and $\bar{\gamma}_m = \bar{\gamma}\lambda_m$. Replacing $\gamma_{n,m}$, and γ_n in (1.2), the OP of $S_n \rightarrow R_m$ and $S_n \rightarrow D$ links are respectively, given by

$$F_{\gamma_{n,m}}(\gamma_{th}) = 1 - e^{-\frac{\gamma_{th}}{\bar{\gamma}_{n,m}}} \sum_{i=1}^{N_r} \frac{(\gamma_{th}/\bar{\gamma}_{n,m})^{i-1}}{(i-1)!}, \tag{4.1}$$

$$F_{\gamma_n}(\gamma_{th}) = 1 - e^{-\frac{\gamma_{th}}{\bar{\gamma}_n}} \sum_{j=1}^{N_d} \frac{(\gamma_{th}/\bar{\gamma}_n)^{j-1}}{(j-1)!}. \tag{4.2}$$

Furthermore, the OP of the channel between the ith transmit antenna at R_m and D is given by

$$F_{\gamma_m^{(i)}}(\gamma_{th}) = 1 - e^{-\frac{\gamma_{th}}{\bar{\gamma}_m}} \sum_{j=1}^{N_d} \frac{(\gamma_{th}/\bar{\gamma}_m)^{j-1}}{(j-1)!}. \tag{4.3}$$

Note that $\bar{\gamma}_{n,m}$, $\bar{\gamma}_n$, and $\bar{\gamma}_m$ in (4.1), (4.2), and (5.7), respectively denote the average received SNR of $S_n \rightarrow R_m$, $S_n \rightarrow D$, and $R_m \rightarrow D$ links, including path-loss.

4.2.2 Discussion

In RS Strategy $\mathcal{B}$ the destination selects the best relays based on the local CSI of the relay-to-destination links. The RS Strategy $\mathcal{A}$, however, relies on global CSI; i.e.,
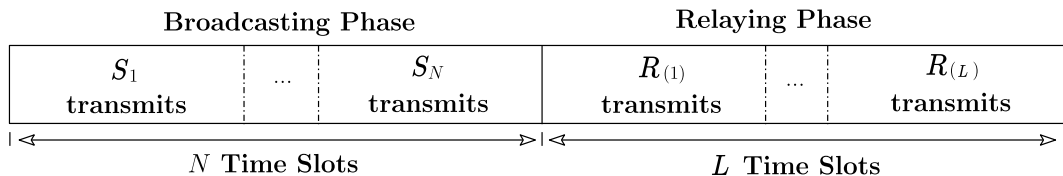
Fig. 4.1: Time-resource allocation for RS Strategy $\mathcal{A}$.

not only the destination requires local CSI of the relay-to-destination links but also it requires CSI of the indirectly connected source-to-relay links. Thus, as opposed to RS Strategy $\mathcal{B}$, in RS Strategy $\mathcal{A}$ the relays need to send the CSI information to the destination. Suppose relay R_m ($\forall m \in \{1, 2, ..., M\}$) obtains CSI of its corresponding source-to-relay links using pilot sequences sent by N sources. Furthermore, assume that real and imaginary parts are quantized with $\mathcal{L}$ bits each, and a rate $\mathcal{C}$ channel code is employed to protect the CSI of source-to-relay channels. The total number of bits needed for CSI acquisition at the destination in Strategy $\mathcal{A}$ is $\mathcal{T}_b^{\mathcal{A}} = \frac{2\mathcal{L}NM}{\mathcal{C}}$, where the factor of two is due to the complex component. On the other hand, the number of required CSI estimations in RS Strategy $\mathcal{A}$ and $\mathcal{B}$ are, respectively, equal to $\mathcal{N}_{\mathcal{A}} = M(N+1)$ and $\mathcal{N}_{\mathcal{B}} = M$. It can be seen that the additional signaling overhead imposed by RS Strategy $\mathcal{A}$ is scaled by the product of the number of sources N and number of relays M. Such high signaling overhead is even more crucial in a network with a large number of branches (i.e., $N \gg 1$, $M \gg 1$). This additional signaling overhead clearly demonstrates the superiority of RS Strategy $\mathcal{B}$ over RS Strategy $\mathcal{A}$.

In the next two sections, we explain RS Strategy $\mathcal{A}$, $\mathcal{B}$ in detail and derive their outage probabilities.

4.3 RS Strategy $\mathcal{A}$

In RS under Strategy $\mathcal{A}$, L relays (out of M cooperative relays) based on "*max-min*" criterion are selected to maximize the worst E2E SNR. According to "*max-min*" criterion, the E2E performance is dominated by the worst link between $S_n \rightarrow R_m$, ($n = 1, 2, ..., N$) and $R_m \rightarrow D$ links. In other words, amongst the links corresponding to relay R_m, the link whose instantaneous SNR is less than that of others determines

the bottleneck link. Let γ_m^b denote the SNR of the bottleneck link for relay R_m. Accordingly, based on "*max-min*" criterion, relays $R_{(1)}, R_{(2)}, \cdots, R_{(L)}$ are selected, where $(v) = \text{argmax}_{m=1,2,\cdots,M}^{v\text{th}}\{\gamma_m^b\}$. During the relaying phase, these L best relays participate in a round-robin fashion. In particular, in the first relaying time-slot, the best relay $R_{(1)}$ transmits; then, in the second relaying time-slot, the second best relay $R_{(2)}$ transmits; and this procedure continues until relay $R_{(L)}$ transmits.

4.3.1 Outage Probability

In this section, we derive closed-form outage expression for MIMO NCC systems with RS Strategy $\mathcal{A}$. The high-SNR approximation of the OP is also provided to obtain valuable insights into the system-design parameters such as the diversity order and coding gain.

Since, MRC is employed at the relay R_m and a single best antenna $\hat{i}$ at this relay is selected to transmit encoded symbols in the relaying phase, the SNR of the bottleneck link for relay R_m can be written as

$$\gamma_m^b = \min\left\{\gamma_{1,m},\ \gamma_{2,m},\ ...,\gamma_{N,m},\ \gamma_m^{(\hat{i})}\right\}, \tag{4.4}$$

where $\gamma_m^{(\hat{i})} = \max_{i=1,\,2,\,...,N_r} \bar{\gamma}_m\|\mathbf{h}_{R_m^{(i)}D}\|^2$ is the maximum SNR value among all the output instantaneous SNRs of the MRC at the destination.

Using (4.4), the OP of relay R_m can be then expressed as

$$F_{\gamma_m^b}(\gamma_{th}) = 1 - \Pr\left\{\gamma_m^b > \gamma_{th}\right\}. \tag{4.5}$$

Noting that the SNRs in (4.4) are mutually independent RVs, and using the theory of order statistics, (4.5) can be written as

$$F_{\gamma_m^b}(\gamma_{th}) = 1 - \prod_{n=1}^{N}\left[1 - F_{\gamma_{n,m}}(\gamma_{th})\right]\left[1 - F_{\gamma_m^{(\hat{i})}}(\gamma_{th})\right]. \tag{4.6}$$

Applying the multinomial expansion, we obtain

$$\prod_{n=1}^{N}\left[1 - F_{\gamma_{n,m}}(\gamma_{th})\right] = 1 + \sum_{k=1}^{N}(-1)^k \sum_{\substack{i_1=1,\cdots,i_k=1 \\ i_1<\cdots<i_k}}^{N} \prod_{n=i_1}^{i_k} F_{\gamma_{n,m}}(\gamma_{th}), \tag{4.7}$$

where $i_1, i_2, \cdots, i_N \in \{1, 2, \cdots, N\}$.

On the other hand, $F_{\gamma_m^{(i)}}(\gamma_{th})$ in (4.6) is given by

$$F_{\gamma_m^{(i)}}(\gamma_{th}) = \left(1 - e^{-\frac{\gamma_{th}}{\bar{\gamma}_m}} \sum_{j=1}^{N_d} \frac{(\gamma_{th}/\bar{\gamma}_m)^{j-1}}{(j-1)!}\right)^{N_r}. \tag{4.8}$$

Let $\gamma_{(1)}^b \geq \gamma_{(2)}^b \geq \cdots \geq \gamma_{(M)}^b$ denote the order statistics of bottleneck SNRs of the relays in a decreasing order of magnitude, where $\gamma_{(v)}^b = \max_{m=1,2,\cdots,M}^{v\text{th}}\{\gamma_m^b\}$ is the vth largest SNR. Then, we can write

$$\Pr\{\gamma_{(v)}^b < \gamma, \ \gamma_{(v-1)}^b > \gamma\} = \Pr\Big\{(v - 1 \ \text{of} \ \gamma_m^b\text{'s} > \gamma)$$
$$\bigcap (M - v + 1 \ \text{of} \ \gamma_m^b\text{'s} < \gamma)\Big\}. \tag{4.9}$$

Since γ_m^b's are mutually independent RVs, (4.9) can be expresses as

$$F_{\gamma_{(v)}^b}(\gamma) = \sum_{i_1,\cdots,i_M}^{M} \prod_{m=i_1}^{i_{v-1}} \left[1 - F_{\gamma_m^b}(\gamma)\right] \prod_{m'=i_v}^{i_M} F_{\gamma_{m'}^b}(\gamma), \tag{4.10}$$

where $i_1, i_2, \cdots, i_M \in \{1, 2, \cdots, M\}$, $i_1 \neq i_2 \neq \cdots \neq i_M$, $i_1 < i_2 < \cdots < i_{v-1}$, and $i_v < i_2 < \cdots < i_M$.

We can write (4.10) in a simple-form expression as

$$F_{\gamma_{(v)}^b}(\gamma) = \sum_{k=1}^{v} \mathcal{C}_{M-v+1}^{M-v+k}(-1)^{k-1} \sum_{i_1,i_2,\cdots,i_{M-v+k}} \prod_{m=i_1}^{i_{M-v+k}} F_{\gamma_m^b}(\gamma). \tag{4.11}$$

Furthermore, the probability that τ sources be operational (i.e., not in outage) and the remaining $N - \tau$ sources be in outage in the broadcasting phase is given by

$$\Phi(\tau) = \sum_{k=1}^{\tau+1} \mathcal{C}_{N-\tau}^{N+k-\tau-1}(-1)^{k-1} \sum_{i_1,i_2,\cdots,i_{N+k-\tau-1}} \prod_{n=i_1}^{i_{N+k-\tau-1}} F_{\gamma_n}(\gamma_{th}). \tag{4.12}$$

In (4.12), $i_1, i_2, \cdots, i_N \in \{1, 2, \cdots, N\}$, $i_1 < i_2 < \cdots < i_N$, and $F_{\gamma_n}(\gamma_{th})$ is given by (4.2). Furthermore, for the case of i_0 we have one.

In RS Strategy $\mathcal{A}$, the destination receives potentially $N + L$ packets; N original packets from direct transmissions and L network-coded packets from selected relays. An outage occurs if fewer than N packets are received. Let $N_{\text{op}} \leq N$, and $L_{\text{op}}^{\mathcal{A}} \leq L$ denote the number of operational sources and relays, respectively. Therefore, we have

$$\mathcal{O}_{\mathcal{A}} = \mathcal{O}_{\mathcal{A}}^{(1)} \bigcup \mathcal{O}_{\mathcal{A}}^{(2)}, \tag{4.13}$$

where

1. $\mathcal{O}_{\mathcal{A}}^{(1)}$ denotes the outage events when $N_{\mathrm{op}} + L < N$, implying that there are not enough operational $S \to D$ links, N_{op}, such that even if all L selected relays be operational i.e., $L_{\mathrm{op}} = L$, the system is still in outage. Note that $\mathcal{O}_{\mathcal{A}}^{(1)}$ only occurs when $N > L$.

2. $\mathcal{O}_{\mathcal{A}}^{(2)}$ represents the outage events when $N_{\mathrm{op}} + L \geq N$ but $N_{\mathrm{op}} + L_{\mathrm{op}}^{\mathcal{A}} < N$.

From (4.13), the overall OP can be expressed as

$$\mathsf{Pr}\{\mathcal{O}_{\mathcal{A}}\} = \mathsf{Pr}\{\mathcal{O}_{\mathcal{A}}^{(1)}\} + \mathsf{Pr}\{\mathcal{O}_{\mathcal{A}}^{(2)}\}. \tag{4.14}$$

Considering all outage events, the exact closed-form expressions for OP of MIMO NCC system with RS Strategy $\mathcal{A}$ when $N > L$ can be derived as (4.15), where $F_{\gamma_{(v)}^{b}}(\gamma)$ and $\Phi(\tau)$ are already given by (4.11) and (4.12), respectively.

$$\mathcal{P}_{\mathrm{out}_1}^{\mathcal{A}} = \underbrace{\sum_{\tau=0}^{N-L-1} \Phi(\tau)}_{\mathsf{Pr}\{\mathcal{O}_{\mathcal{A}}^{(1)}\}} + \underbrace{\sum_{\tau=1}^{L} \left(\Phi(N-\tau) \sum_{v=1}^{\tau} F_{\gamma_{(v)}^{b}}(\gamma_{th}) \right)}_{\mathsf{Pr}\{\mathcal{O}_{\mathcal{A}}^{(2)}\}}. \tag{4.15}$$

On the other hand, the OP of the system when $N \leq L$ can be formulated as

$$\mathcal{P}_{\mathrm{out}_2}^{\mathcal{A}} = \underbrace{\sum_{\tau=1}^{N} \left(\Phi(N-\tau) \sum_{v=1}^{\tau} F_{\gamma_{(v)}^{b}}(\gamma_{th}) \right)}_{\mathsf{Pr}\{\mathcal{O}_{\mathcal{A}}^{(2)}\}}. \tag{4.16}$$

Although the derived OP expressions given by (4.15) and (4.16) are exact and valid for any arbitrary SNR values, direct insights into the effect of different system parameters on the outage performance are desirable. Motivated by this, we turn our attention to obtain the asymptotic outage expressions in the high-SNR regime which easily enable us to obtain the diversity order and coding gain.

4.3.2 Asymptotic Analysis

For asymptotically high-SNR values, we express exponential function in terms of its Taylor series expansions given by $e^{-x} = \sum_{k=0}^{\infty} \frac{(-x)^k}{k!}$ to approximate (4.2) in high-SNR

regime. This is given by

$$\lim_{\bar{\gamma} \to \infty} F_{\gamma_n}(\gamma_{th}) = F_{\gamma_n}^{\infty}(\gamma_{th}) = \frac{\beta_n^{N_d}}{N_d!}, \tag{4.17}$$

where $\beta_n = \gamma_{th}/\bar{\gamma}_n$.

Substituting (4.17) into (4.12) and then ignoring higher order terms, we find

$$\Phi^{\infty}(\tau) = \sum_{i_1,i_2,\cdots,i_{N-\tau}}^{N} \prod_{n=i_1}^{i_{N-\tau}} \frac{\beta_n^{N_d}}{N_d!}. \tag{4.18}$$

Furthermore, we approximate $F_{\gamma_m^b}(\gamma_{th})$ in (4.6) as follows

$$F_{\gamma_m^b}^{\infty}(\gamma_{th}) = \eta + \sum_{i_1=1}^{N} \frac{\beta_{i_1,m}^{N_r}}{N_r!}. \tag{4.19}$$

In (4.19), $\beta_{n,m} = \gamma_{th}/\bar{\gamma}_{n,m}$. Also, $\eta = 0$ if $N_d \neq 1$ and $\eta = \beta_m^{N_r}$ if $N_d = 1$, where $\beta_m = \gamma_{th}/\bar{\gamma}_m$.

Plugging (4.19) into (4.11) and then keeping the dominant terms, we obtain

$$F_{\gamma_{(v)}^b}^{\infty}(\gamma_{th}) = \sum_{i_1,i_2,\cdots,i_{M-v+1}}^{M} \prod_{m=i_1}^{i_{M-v+1}} \left(\eta + \sum_{i_1=1}^{N} \frac{\beta_{i_1,m}^{N_r}}{N_r!} \right). \tag{4.20}$$

Substituting (4.18) and (4.20) in (4.15), we have

$$\mathcal{P}_{\text{out}_1^{\infty}}^{\mathcal{A}} = \sum_{\tau=0}^{N-L-1} \Phi^{\infty}(\tau) + \sum_{\tau=1}^{L} \left(\Phi^{\infty}(N-\tau) \sum_{v=1}^{\tau} F_{\gamma_{(v)}}^{\infty}(\gamma_{th}) \right). \tag{4.21}$$

Keeping the dominant terms in (4.21) i.e., when $\tau = N - L - 1$ in the first summation and $v = \tau = 1$ in the second and third summations, (4.15) can be further approximated as

$$\mathcal{P}_{\text{out}_1^{\infty}}^{\mathcal{A}} = \Phi^{\infty}(N-L-1) + \Phi^{\infty}(N-1)F_{\gamma_{(1)}}^{\infty}(\gamma_{th}). \tag{4.22}$$

The asymptotic outage expression depends on the system parameters. In particular, we have the following three cases:

- **Case 1:** $MN_r > LN_d$. In this case, $\mathcal{P}_{\text{out}_1^{\infty}}^{\mathcal{A}}$ is determined by the first term in (4.22) as $\mathcal{P}_{\text{out}_1^{\infty}}^{\mathcal{A}} = \Phi^{\infty}(N-L-1)$ and is given by

$$\mathcal{P}_{\text{out}_1^{\infty}}^{\mathcal{A}} = \Xi_1^{\mathcal{A}} \left(\frac{\gamma_{th}}{\bar{\gamma}} \right)^{(L+1)N_d}, \tag{4.23}$$

where the system-dependent parameter, $\Xi_1^{\mathcal{A}}$, is

$$\Xi_1^{\mathcal{A}} = \sum_{i_1, i_2, \cdots, i_{L+1}}^{N} \prod_{n=i_1}^{i_{L+1}} \frac{\lambda_n^{-N_d}}{N_d!}. \tag{4.24}$$

- **Case 2:** $MN_r < LN_d$. In this case, $\mathcal{P}_{\text{out}_1^{\infty}}^{\mathcal{A}}$ is determined by the second term in (4.22) as $\mathcal{P}_{\text{out}_1^{\infty}}^{\mathcal{A}} = \Phi^{\infty}(N-1)F_{\gamma_{(1)}}^{\infty}(\gamma_{th})$. This can be written as

$$\mathcal{P}_{\text{out}_1^{\infty}}^{\mathcal{A}} = \Xi_{1'}^{\mathcal{A}} \left(\frac{\gamma_{th}}{\bar{\gamma}} \right)^{MN_r + N_d}, \tag{4.25}$$

  where

$$\Xi_{1'}^{\mathcal{A}} = \sum_{i_1=1}^{N} \frac{\lambda_{i_1}^{-N_d}}{N_d!} \prod_{m=i_1}^{i_M} \left(\sum_{i_1=1}^{N} \frac{\lambda_{i_1,m}^{-N_r}}{N_r!} \right). \tag{4.26}$$

- **Case 3:** $MN_r = LN_d$. In this case, both the first and the second terms in (4.22) determine the asymptotic outage given by $\mathcal{P}_{\text{out}_1^{\infty}}^{\mathcal{A}} = \Phi^{\infty}(N-L-1) + \Phi^{\infty}(N-1)F_{\gamma_{(1)}}^{\infty}(\gamma_{th})$, where $\Phi^{\infty}(N-L-1)$, and $\Phi^{\infty}(N-1)F_{\gamma_{(1)}}^{\infty}(\gamma_{th})$ are derived in (4.23) and (4.25), respectively.

Now, we proceed to obtain the asymptotic outage expression for $N \leq L$. Substituting (4.18) and (4.20) into (4.16), we have

$$\mathcal{P}_{\text{out}_2^{\infty}}^{\mathcal{A}} = \sum_{\tau=1}^{N} \left(\Phi^{\infty}(N-\tau) \sum_{\upsilon=1}^{\tau} F_{\gamma_{(\upsilon)}^b}^{\infty}(\gamma_{th}) \right). \tag{4.27}$$

Based on the relationship between N_d and N_r, (4.16) in high SNRs is derived in the following three cases:

- **Case 1:** $N_d > N_r$. In this case, the dominant terms of (4.27) can be obtained when $\upsilon = \tau = 1$ i.e., $\mathcal{P}_{\text{out}_2^{\infty}}^{\mathcal{A}} = \Phi^{\infty}(N-1)F_{\gamma_{(1)}}^{\infty}(\gamma_{th})$. This means

$$\mathcal{P}_{\text{out}_2^{\infty}}^{\mathcal{A}} = \Xi_2^{\mathcal{A}} \left(\frac{\gamma_{th}}{\bar{\gamma}} \right)^{MN_r + N_d}, \tag{4.28}$$

  where

$$\Xi_2^{\mathcal{A}} = \sum_{i_1=1}^{N} \frac{\lambda_{i_1}^{-N_d}}{N_d!} \prod_{m=i_1}^{i_M} \left(\sum_{i_1=1}^{N} \frac{\lambda_{i_1,m}^{-N_r}}{N_r!} \right). \tag{4.29}$$

67

- **Case 2:** $N_d < N_r$. In this case, the dominant terms of (4.27) can be obtained when $\tau = \upsilon = N$ i.e., $\mathcal{P}^{\mathcal{A}}_{\text{out}_2^\infty} = \Phi^\infty(0)F^\infty_{\gamma_{(N)}}(\gamma_{th})$. This can be expressed as

$$\mathcal{P}^{\mathcal{A}}_{\text{out}_2^\infty} = \Xi^{\mathcal{A}}_{2'} \left(\frac{\gamma_{th}}{\bar{\gamma}} \right)^{(M-N+1)N_r+NN_d}, \tag{4.30}$$

where

$$\Xi^{\mathcal{A}}_{2'} = \prod_{n=i_1}^{i_N} \frac{\lambda_n^{-N_d}}{N_d!} \sum_{i_1,i_2,\cdots,i_{M-N+1}} \prod_{m=i_1}^{i_{M-N+1}} \left(\eta' + \sum_{i_1=1}^{N} \frac{\lambda_{i_1,m}^{-N_r}}{N_r!} \right), \tag{4.31}$$

and $\eta' = 0$ if $N_d \neq 1$ and $\eta' = \lambda_m^{-N_r}$ if $N_d = 1$.

- **Case 3:** $N_d = N_r = \tilde{N}$. In this case, the dominant terms can be obtained when $\upsilon = \tau$ in (4.27) i.e., $\mathcal{P}^{\mathcal{A}}_{\text{out}_2^\infty} = \sum_{\tau=1}^{N} \left(\Phi^\infty(N-\tau)F^\infty_{\gamma_{(\tau)}}(\gamma_{th}) \right)$ and is given by

$$\mathcal{P}^{\mathcal{A}}_{\text{out}_2^\infty} = \Xi^{\mathcal{A}}_{2''} \left(\frac{\gamma_{th}}{\bar{\gamma}} \right)^{(M+1)\tilde{N}}, \tag{4.32}$$

where

$$\Xi^{\mathcal{A}}_{2''} = \sum_{\tau=1}^{N} \left(\sum_{i_1,i_2,\cdots,i_\tau} \left(\prod_{n=i_1}^{i_\tau} \frac{\lambda_n^{-\tilde{N}}}{\tilde{N}!} \right) \sum_{i_1,i_2,\cdots,i_{M-\tau+1}} \prod_{m=i_1}^{i_{M-\tau+1}} \left(\sum_{i_1=1}^{N} \frac{\lambda_{i_1,m}^{-\tilde{N}}}{\tilde{N}!} \right) \right). \tag{4.33}$$

Therefore, the diversity order and the coding gain of MIMO NCC system with RS Strategy $\mathcal{A}$ when $N > L$ and $N \leq L$ are respectively given by

$$G^{\mathcal{A}}_{d_1} = \min\{MN_r, LN_d\} + N_d, \tag{4.34}$$

$$G^{\mathcal{A}}_{c_1} = \begin{cases} \dfrac{\Xi^{\mathcal{A}-\frac{1}{(L+1)N_d}}_1}{\gamma_{th}}, & MN_r > LN_d \\[2ex] \dfrac{\Xi^{\mathcal{A}-\frac{1}{MN_r+N_d}}_{1'}}{\gamma_{th}}, & MN_r < LN_d \\[2ex] \dfrac{\left(\Xi^{\mathcal{A}}_1 + \Xi^{\mathcal{A}}_{1'} \right)^{-\frac{1}{(L+1)N_d}}}{\gamma_{th}}, & MN_r = LN_d \end{cases} \tag{4.35}$$

$$G^{\mathcal{A}}_{d_2} = (M+1)N_r + \min\{N_d - N_r, N(N_d - N_r)\}, \tag{4.36}$$

$$G^{\mathcal{A}}_{c_2} = \begin{cases} \dfrac{\Xi^{\mathcal{A}-\frac{1}{MN_r+N_d}}_2}{\gamma_{th}}, & N_d > N_r \\[2ex] \dfrac{\Xi^{\mathcal{A}-\frac{1}{(M-N+1)N_r+NN_d}}_{2'}}{\gamma_{th}}, & N_d < N_r \\[2ex] \dfrac{\Xi^{\mathcal{A}-\frac{1}{(M+1)\tilde{N}}}_{2''}}{\gamma_{th}}, & \tilde{N} = N_d = N_r \end{cases} \tag{4.37}$$

Table 4.1: **Diversity Order of RS Strategy $\mathcal{A}$**

Diversity Order for $N > L$ (4.34)		
$N_d = N_r = \tilde{N}$	$N_r > N_d$ or $(N_d > N_r, \frac{M}{L} > \frac{N_d}{N_r})$	$N_d > N_r, \frac{M}{L} < \frac{N_d}{N_r}$
$(L+1)\tilde{N}$	$(L+1)N_d$	$MN_r + N_d$
Diversity Order for $N \leq L$ (4.36)		
$N_d = N_r = \tilde{N}$	$N_r > N_d$	$N_r < N_d$
$(M+1)\tilde{N}$	$(M-N+1)N_r + NN_d$	$MN_r + N_d$

Special Case 4.1. *Single best RS is a special case of $N > L$ when $L = 1$. Furthermore, when $\tilde{N} = N_d = N_r = 1$, the diversity orders given by (4.34) and (4.36) reduce to $L+1$, and $M+1$ for $N > L$, and $N \leq L$, respectively. Therefore, our diversity order analysis is a generalized version of those earlier presented in [29, 30] and coincide with them when single-antenna terminals are considered.*

To have further insights and guidelines for practical implementation obtained through our diversity analyses, the diversity orders i.e., (4.34) and (4.36) for different values of system parameters N_d, N_r, N, M, and L are provided in Table 4.1. These insights and guidelines may be useful in designing practical MIMO NCC systems with RS protocols. In the following we provide some remarks.

Remark 4.1. *The diversity order is equal to $Mn_r + N_d$ for both $N > L$, $(N_d > N_r, \frac{M}{L} < \frac{N_d}{N_r})$ and $N \leq L$ when $N_r < N_d$.*

Remark 4.2. *The diversity is always independent of selected relays, L, when $N \leq L$. Thus, increasing number of selected relays not only does not provide any performance gain but also decreases the system throughput.*

Remark 4.3. *Interestingly, but counter-intuitively, for $N \leq L$ $(N_r > N_d)$, the diversity order is a function of N. This is the only case that increasing the number of sources (while keeping M, N_r, and N_d fixed) leads to the diversity loss.*

Remark 4.4. *It can be seen from Table 4.1 that the achievable diversity order for SRS (i.e., when $L = 1$) depends on the number of relays M when $\frac{N_d}{N_r} > M$ i.e., $MN_r + N_d$.*

However, for single-antenna NCC system the diversity order is always two irrespective of the number of relays [29, 30].

Remark 4.5. *If a single-antenna destination is used i.e., $N_d = 1$, the diversity order for the case of $N > L$ reduces to $L + 1$. Therefore, increasing M or N_r does not improve the diversity order. However, for $N \leq L$, adding relays and the antennas at relays increases diversity order. This reveals that in order to take benefit from relays and the antennas at relays when $N > L$, the destination should be equipped with multiple antennas such that it satisfies the condition $\frac{N_d}{N_r} > \frac{M}{L}$.*

4.4 RS Strategy $\mathcal{B}$

We have just derived the OP, diversity order, and coding gain of RS Strategy $\mathcal{A}$. However, as mentioned before, this RS strategy may not be always practical and feasible for a network with a large number of branches. It requires large signaling overheads due to the need of global CSI of all source-relay and relay-destination links (4.4) for RS process. We thus propose a new RS strategy for NCC system based on local CSI of the relay-to-destination channels, and it can be described as follows:

In Strategy $\mathcal{B}$, after the end of the first phase, the relays that have correctly decoded all the packets from N sources form a decoding set $\mathcal{D}$. Mathematically, this set can be written as $\mathcal{D} \triangleq \{m : \gamma_{n,m} > \gamma_{th}, \forall n\}$. Let $\mathcal{D}_l$ be a decoding set with l relays. In RS Strategy $\mathcal{B}$, L out of l relays in $\mathcal{D}_l$ are selected to transmit their encoded sources' packets to the destination. In particular, the υth best relay $R^*_{(\upsilon)}$ ($\upsilon = 1, 2, \cdots, L$) is selected according to the following policy:

$$(\upsilon) = \text{argmax}^{\upsilon \text{th}}_{m \in \mathcal{D}_l} \{\gamma_m^{(\hat{i})}\}, \tag{4.38}$$

which implies that L best relays belonging to $\mathcal{D}_l$ with the highest instantaneous SNR of the relay-to-destination channels are chosen to cooperate.[2] The destination will thus receive some network-coded packets as well as original packets directly from the sources. If it receives less than N correct packets, an outage occurs.

[2]Unlike RS Strategy $\mathcal{A}$, in RS Strategy $\mathcal{B}$, the relays that decode incorrectly are not allowed to take part in cooperation. Hence, no error propagation occurs.

Broadcasting Phase

S_1 transmits	...	S_N transmits

N Time Slots

(a)

Broadcasting Phase   Relaying Phase

S_1 transmits	...	S_N transmits	$R^*_{(1)} \in \mathcal{D}$ transmits	...	$R^*_{(L)} \in \mathcal{D}$ transmits

N Time Slots L Time Slots

(b)
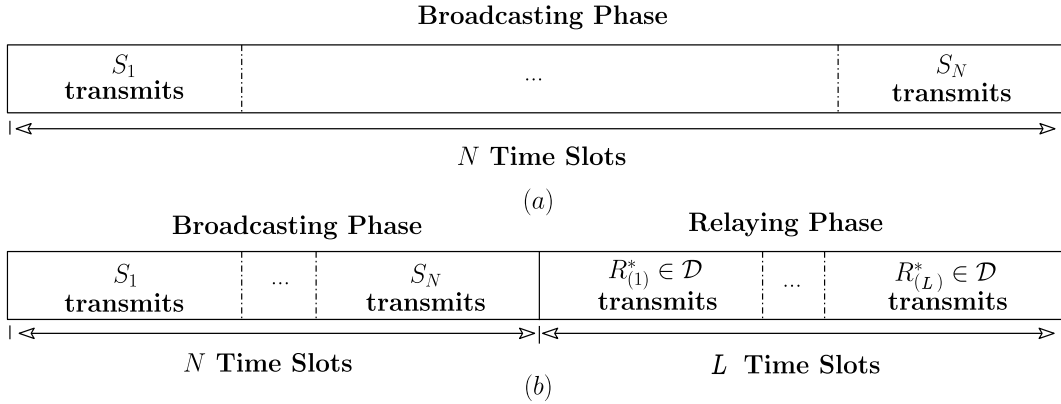
Fig. 4.2: Time-resource allocation for RS Strategy $\mathcal{B}_1$ (a) $0 \leq l < L$, (b) $L \leq l \leq M$.

The RS policy under Strategy $\mathcal{B}$ (4.38) depends on $\mathcal{D}_l$. Since the number of selected relays, L, is a priory fixed number and the size of $\mathcal{D}_l$, l, is randomly varying with fluctuation of channels (i.e., $0 \leq l \leq M$), it is possible that $l < L$.[3] Two strategies can be made when $l < L$. In this section, we investigate the performance of these two strategies namely, Strategy $\mathcal{B}_1$ and Strategy $\mathcal{B}_2$.

4.4.1 RS Strategy $\mathcal{B}_1$

For RS under Strategy $\mathcal{B}_1$, if the number of relays in $\mathcal{D}_l$ is less than L, the RS process is not performed and all the relays belonging to $\mathcal{D}_l$ keep silent until the next round of cooperation begins. On the other hand, if the size of $\mathcal{D}_l$ is greater than or equal to L, then L best relays out of l relays in $\mathcal{D}_l$ are selected to transmit during the relaying phase. Fig. 4.2 depicts the time-resource allocation for RS Strategy $\mathcal{B}_1$.

4.4.1.1 Outage Probability

In this section, we derive closed-form expressions of the OP for MIMO NCC systems with RS under strategy $\mathcal{B}_1$. The asymptotic outage expressions are also derived to obtain the achievable diversity order and coding gain.

---

[3]The decoding set $\mathcal{D}_l$, is the set of relays that have been successful in decoding all sources' packets. Hence, the size of $\mathcal{D}_l$, l, is not controllable and is determined by channel fading, which is random. Therefore, it is impossible to control l to be always greater than number of selected relays.

The overall OP of the system under Strategy $\mathcal{B}_i$ ($i = 1, 2$) can be expressed as

$$\mathcal{P}_{\text{out}}^{\mathcal{B}_i} = \sum_{l=0}^{M} \sum_{\mathcal{D}_l} \Pr\{\mathcal{O}_{\mathcal{B}_i} | \mathcal{D}_l\} \Psi(l), \tag{4.39}$$

where $\Pr\{\mathcal{O}_{\mathcal{B}_i} | \mathcal{D}_l\}$ represents the OP conditioned on $\mathcal{D}_l$ and $\Psi(l) = \Pr\{\mathcal{D}_l\}$. In the following, we proceed to obtain the OP of Strategy $\mathcal{B}_1$ by deriving $\Psi(l)$ and $\Pr\{\mathcal{O}_{\mathcal{B}_1} | \mathcal{D}_l\}$.

In (4.39), $\Psi(l)$ can be written as

$$\Psi(l) = \prod_{m' \in \mathcal{D}_l} \mathsf{P}\{\mathcal{S}_{m'}\} \prod_{m \notin \mathcal{D}_l} \left(1 - \mathsf{P}\{\mathcal{S}_m\}\right), \tag{4.40}$$

which can be rewritten as

$$\Psi(l) = \sum_{k=0}^{l} (-1)^k \sum_{i_1, \cdots, i_k \in \mathcal{D}_l} \prod_{m'=i_1}^{i_k} \mathsf{P}'\{\mathcal{S}_{m'}\} \prod_{m \notin \mathcal{D}_l} \mathsf{P}'\{\mathcal{S}_m\}, \tag{4.41}$$

where $\mathsf{P}'\{\mathcal{S}_m\} = 1 - \mathsf{P}\{\mathcal{S}_m\}$ and $\mathsf{P}\{\mathcal{S}_m\}$ is the probability that relay R_m successfully decodes all N sources' packets. This can be written as

$$\mathsf{P}\{\mathcal{S}_m\} = 1 + \sum_{k=1}^{N} (-1)^k \sum_{\substack{i_1, i_2, \cdots, i_k \\ i_1 < i_2 < \cdots < i_k}}^{N} \prod_{n=i_1}^{i_k} F_{\gamma_{n,m}}(\gamma_{th}). \tag{4.42}$$

Let $\gamma_{(v)} = \max_{m \in \mathcal{D}_l}^{v\text{th}} \{\gamma_m^{(\hat{i})}\}$ denote the SNR of relay $R_{(v)}^*$. Then, we have

$$\Pr\{\gamma_{(v)|\mathcal{D}_l} < \gamma, \; \gamma_{(v-1)|\mathcal{D}_l} > \gamma\} =$$
$$\Pr\left\{\left(v - 1 \text{ of } \gamma_m^{(\hat{i})}\text{'s} > \gamma\right) \bigcap \left(l - v + 1 \text{ of } \gamma_m^{(\hat{i})}\text{'s} < \gamma\right)\right\}. \tag{4.43}$$

Since SNRs of the relays are independent RVs, (4.43) can be derived as

$$F_{\gamma_{(v)|l}}(\gamma) = \sum_{k=1}^{v} C_{l-v+1}^{l-v+k} (-1)^{k-1} \sum_{i_1, i_2, \cdots, i_{l-v+k} \in \mathcal{D}_l} \prod_{m=i_1}^{i_{l-v+k}} F_{\gamma_m^{(\hat{i})}}(\gamma). \tag{4.44}$$

Under RS Strategy $\mathcal{B}_1$, the destination potentially receives (i) N packets if $0 \le l < L$ and (ii) $N + L$ packets if $L \le l \le M$. In both cases an outage occurs if less than N packets are decoded correctly by the destination. Let $L_{\text{op}}^{\mathcal{B}} \le L$ denote the number of selected relays whose relay-to-destination channels are not in outage. Now, depending on l, we have the following events which lead to th outage of the system:

1. $0 \leq l < L$: When the number of available relays in $\mathcal{D}_l$ is less than L, all l relays in $\mathcal{D}_l$ remain silent. Therefore, the destination receives only N packets from direct transmissions through the source-to-destination channels. An outage occurs if at most $N-1$ links from N source-to-destination links be operational i.e., $N_{\text{op}} < N$. We denote this event by $\mathcal{O}_{\mathcal{B}_1}^{(1)}$.

2. $L \leq l \leq M$: If the number of available relays in $\mathcal{D}_l$ is equal or more than L, then RS is performed. In this case, we have the following two outage events:

   - $\mathcal{O}_{\mathcal{B}_1}^{(2)}|\mathcal{D}_l$ represents the outage events when $N_{\text{op}} + L < N$.

   - $\mathcal{O}_{\mathcal{B}_1}^{(2')}|\mathcal{D}_l$ corresponds to the outage events when $N_{\text{op}} + L \geq N$ but $N_{\text{op}} + L_{\text{op}}^{\mathcal{B}} < N$.

Thus, the overall outage event in (4.39) can be calculated as

$$\mathcal{O}_{\mathcal{B}_1}|\mathcal{D}_l = \mathcal{O}_{\mathcal{B}_1}^{(1)} \bigcup \mathcal{O}_{\mathcal{B}_1}^{(2)}|\mathcal{D}_l \bigcup \mathcal{O}_{\mathcal{B}_1}^{(2')}|\mathcal{D}_l. \tag{4.45}$$

Using (4.45), the OP of the system conditioned on $\mathcal{D}_l$ is given by

$$\Pr\{\mathcal{O}_{\mathcal{B}_1}|\mathcal{D}_l\} = \Pr\{\mathcal{O}_{\mathcal{B}_1}^{(1)}\} + \Pr\{\mathcal{O}_{\mathcal{B}_1}^{(2)}|\mathcal{D}_l\} + \Pr\{\mathcal{O}_{\mathcal{B}_1}^{(2')}|\mathcal{D}_l\}. \tag{4.46}$$

The term $\Pr\{\mathcal{O}_{\mathcal{B}_1}^{(1)}\}$ can be obtained as

$$\Pr\{\mathcal{O}_{\mathcal{B}_1}^{(1)}\} = \sum_{\tau=0}^{N-1} \Phi(\tau), \quad 0 \leq l < L, \tag{4.47}$$

where $\Phi(\tau)$ is given by (4.12).

Furthermore, $\Pr\{\mathcal{O}_{\mathcal{B}_1}^{(2)}|\mathcal{D}_l\} + \Pr\{\mathcal{O}_{\mathcal{B}_1}^{(2')}|\mathcal{D}_l\}$ when $N > L$ can be formulated as

$$\Pr\{\mathcal{O}_{\mathcal{B}_1}^{(2)}|\mathcal{D}_l\} + \Pr\{\mathcal{O}_{\mathcal{B}_1}^{(2')}|\mathcal{D}_l\} = \sum_{\tau=0}^{N-L-1} \Phi(\tau)$$
$$+ \sum_{\tau=1}^{L} \left(\Phi(N-\tau) \sum_{v=1}^{\tau} F_{\gamma_{(v)|l}}(\gamma_{th}) \right), \quad L \leq l \leq M, \tag{4.48}$$

where $F_{\gamma_{(v)|l}}(\gamma)$ is given by (4.44).

Finally, substituting (4.47), (4.48), and (4.41) into (4.39), one can obtain the exact OP of RS Strategy $\mathcal{B}_1$ when $N > L$. This can be expressed in the closed-form expression

given by (4.49). Similarly, the OP of the system when $N \leq L$ is derived as (4.50).

$$
\mathcal{P}_{\text{out}_1}^{\mathcal{B}_1} = \underbrace{\sum_{l=0}^{L-1} \sum_{\mathcal{D}_l} \left(\sum_{\tau=0}^{N-1} \Phi(\tau) \right) \Psi(l)}_{\Pr\{\mathcal{O}_{\mathcal{B}_1}^{(1)}\}} + \underbrace{\sum_{l=L}^{M} \sum_{\mathcal{D}_l} \left(\sum_{\tau=0}^{N-L-1} \Phi(\tau) \right) \Psi(l)}_{\Pr\{\mathcal{O}_{\mathcal{B}_1}^{(2)}\}}
$$

$$
+ \underbrace{\sum_{l=L}^{M} \sum_{\mathcal{D}_l} \left(\sum_{\tau=1}^{L} \Phi(N-\tau) \sum_{v=1}^{\tau} F_{\gamma_{(v)|l}}(\gamma_{th}) \right) \Psi(l)}_{\Pr\{\mathcal{O}_{\mathcal{B}_1}^{(2')}\}}. \tag{4.49}
$$

$$
\mathcal{P}_{\text{out}_2}^{\mathcal{B}_1} = \underbrace{\sum_{l=0}^{L-1} \sum_{\mathcal{D}_l} \left(\sum_{\tau=0}^{N-1} \Phi(\tau) \right) \Psi(l)}_{\Pr\{\mathcal{O}_{\mathcal{B}_1}^{(1)}\}} + \underbrace{\sum_{l=L}^{M} \sum_{\mathcal{D}_l} \left(\sum_{\tau=1}^{N} \Phi(N-\tau) \sum_{v=1}^{\tau} F_{\gamma_{(v)|l}}(\gamma_{th}) \right) \Psi(l)}_{\Pr\{\mathcal{O}_{\mathcal{B}_1}^{(2')}\}}.
$$

$$\tag{4.50}$$

4.4.1.2 Asymptotic Analysis

$\mathsf{P}'\{\mathcal{S}_m\}$ for high SNRs is approximated as $\mathsf{P}'^{\infty}\{\mathcal{S}_m\} = \sum_{i_1=1}^{N} \left(\frac{\beta_{i_1,m}^{N_r}}{N_r!} \right)$. Substituting this expression into (4.41) and discarding higher order terms, $\Psi(l)$ can be approximated as

$$
\Psi^{\infty}(l) = \prod_{\substack{m=i_1 \\ m \notin \mathcal{D}_l}}^{i_{M-l}} \left(\sum_{i_1=1}^{N} \frac{\beta_{i_1,m}^{N_r}}{N_r!} \right). \tag{4.51}
$$

Furthermore, we obtain (4.44) in high SNRs as

$$
F_{\gamma_{(v)|l}}^{\infty}(\gamma_{th}) = \sum_{i_1, i_2, \cdots, i_{l-v+1} \in \mathcal{D}_l} \prod_{m=i_1}^{i_{l-v+1}} \left(\frac{\beta_m^{N_d}}{N_d!} \right)^{N_r}. \tag{4.52}
$$

Plugging (4.51), (4.52), and (4.18) into (4.49) and then retaining the dominant terms, we have

$$
\mathcal{P}_{\text{out}_1^{\infty}}^{\mathcal{B}_1} = \sum_{\mathcal{D}_{L-1}} \Phi^{\infty}(N-1) \Psi^{\infty}(L-1) + \Phi^{\infty}(N-L-1) \Psi^{\infty}(M). \tag{4.53}
$$

Based on the relationship between $(M-L+1)N_r$ and LN_d, (4.49) in high SNRs can be derived as follows:

- **Case 1:** $(M-L+1)N_r < LN_d$. In this case, $\mathcal{P}_{\text{out}_1^{\infty}}^{\mathcal{B}_1}$ is determined by the first term in (4.53) as $\mathcal{P}_{\text{out}_1^{\infty}}^{\mathcal{B}_1} = \sum_{\mathcal{D}_{L-1}} \Phi^{\infty}(N-1) \Psi^{\infty}(L-1)$. This is given by

$$
\mathcal{P}_{\text{out}_1^{\infty}}^{\mathcal{B}_1} = \Xi_1^{\mathcal{B}_1} \left(\frac{\gamma_{th}}{\bar{\gamma}} \right)^{(M-L+1)N_r+N_d}, \tag{4.54}
$$

where

$$\Xi_1^{\mathcal{B}_1} = \sum_{\mathcal{D}_{L-1}} \left(\sum_{i_1=1}^{N} \frac{\lambda_{i_1}^{-N_d}}{N_d!} \prod_{m=i_1}^{i_{M-L+1}} \left(\sum_{i_1=1}^{N} \frac{\lambda_{i_1,m}^{-N_r}}{N_r!} \right) \right). \tag{4.55}$$

- **Case 2:** $(M-L+1)N_r > LN_d$. In this case, $\mathcal{P}_{\text{out}_1^\infty}^{\mathcal{B}_1}$ is determined by the second term in (4.53) i.e., $\mathcal{P}_{\text{out}_1^\infty}^{\mathcal{B}_1} = \Phi^\infty(N-L-1)\Psi^\infty(M)$. This can be written as

$$\mathcal{P}_{\text{out}_1^\infty}^{\mathcal{B}_1} = \Xi_{1'}^{\mathcal{B}_1} \left(\frac{\gamma_{th}}{\bar{\gamma}} \right)^{(L+1)N_d}, \tag{4.56}$$

where

$$\Xi_{1'}^{\mathcal{B}_1} = \sum_{i_1,i_2,\cdots,i_{L+1}}^{N} \left(\prod_{n=i_1}^{i_{L+1}} \frac{\lambda_n^{-N_d}}{N_d!} \right). \tag{4.57}$$

- **Case 3:** $(M-L+1)N_r = LN_d$. In this case, $\mathcal{P}_{\text{out}_1^\infty}^{\mathcal{B}_1}$ is determined by both the first and second terms in (4.53) as $\mathcal{P}_{\text{out}_1^\infty}^{\mathcal{B}_1} = \sum_{\mathcal{D}_{L-1}} \Phi^\infty(N-1)\Psi^\infty(L-1) + \Phi^\infty(N-L-1)\Psi^\infty(M)$.

Now, we proceed to obtain the asymptotic outage expression when $N \leq L$. Substituting (4.51), (4.52), and (4.18) into (4.50), and then keeping the dominant terms, it can be checked that the asymptotic outage is independent of the relationship between system parameters and is always equal to $\mathcal{P}_{\text{out}_2^\infty}^{\mathcal{B}_1} = \sum_{\mathcal{D}_{L-1}} \Phi^\infty(N-1)\Psi^\infty(L-1)$. This can be expressed as

$$\mathcal{P}_{\text{out}_2^\infty}^{\mathcal{B}_1} = \Xi_2^{\mathcal{B}_1} \left(\frac{\gamma_{th}}{\bar{\gamma}} \right)^{(M-L+1)N_r+N_d}, \tag{4.58}$$

where

$$\Xi_2^{\mathcal{B}_1} = \sum_{\mathcal{D}_{L-1}} \left(\sum_{i_1=1}^{N} \frac{\lambda_{i_1}^{-N_d}}{N_d!} \prod_{m=i_1}^{i_{M-L+1}} \left(\sum_{i_1=1}^{N} \frac{\lambda_{i_1,m}^{-N_r}}{N_r!} \right) \right). \tag{4.59}$$

Thus, the diversity order and the coding gain of MIMO NCC system with RS Strategy $\mathcal{B}_1$ for $N > L$ and $N \leq L$ are respectively given by

$$G_{d_1}^{\mathcal{B}_1} = \min\{(M-L+1)N_r, LN_d\} + N_d, \tag{4.60}$$

Table 4.2: **Diversity Order of RS Strategy $\mathcal{B}_1$**

Diversity Order for $N > L$ (4.60)	
$L \leq \frac{(M+1)N_r}{N_r+N_d}$	$L > \frac{(M+1)N_r}{N_r+N_d}$
$(L+1)N_d$	$(M-L+1)N_r + N_d$
Diversity Order for $N \leq L$ (4.62)	
$(M-L+1)N_r + N_d$	

$$G_{c_1}^{\mathcal{B}_1} = \begin{cases} \dfrac{\Xi_1^{\mathcal{B}_1 - \frac{1}{(M-L+1)N_r+N_d}}}{\gamma_{th}}, \\ \qquad\qquad (M-L+1)N_r < LN_d \\[2mm] \dfrac{\Xi_{1'}^{\mathcal{B}_1 - \frac{1}{(L+1)N_d}}}{\gamma_{th}}, \\ \qquad\qquad (M-L+1)N_r > LN_d \\[2mm] \dfrac{\left(\Xi_1^{\mathcal{B}_1} + \Xi_{1'}^{\mathcal{B}_1}\right)^{-\frac{1}{(L+1)N_d}}}{\gamma_{th}}, \\ \qquad\qquad (M-L+1)N_r = LN_d \end{cases} \tag{4.61}$$

$$G_{d_2}^{\mathcal{B}_1} = (M-L+1)N_r + N_d, \tag{4.62}$$

$$G_{c_2}^{\mathcal{B}_1} = \frac{\Xi_2^{\mathcal{B}_1 - \frac{1}{(M-L+1)N_r+N_d}}}{\gamma_{th}}. \tag{4.63}$$

Comparing (4.60) and (4.62) with (4.34) and (4.36), one can realize that the achievable diversity order of RS Strategy $\mathcal{B}_1$ is always equal or less than that of Strategy $\mathcal{A}$.

The diversity orders of Strategy $\mathcal{B}_1$ i.e., (4.60) and (4.62) for different values of N_d, N_r, M, and L are provided in Table 4.2. Based on Table 4.2, the following insights are highlighted:

Remark 4.6. *The diversity order is a function of all system parameters except for the number of sources N. Accordingly, increasing or decreasing the number of sources does not change the diversity.*

Remark 4.7. *For the case of $L < \frac{(M+1)N_r}{N_r+N_d}$, the diversity order and the coding gain are exactly the same to that of Strategy $\mathcal{A}$ when $N > L$ and $MN_r > LN_d$.*
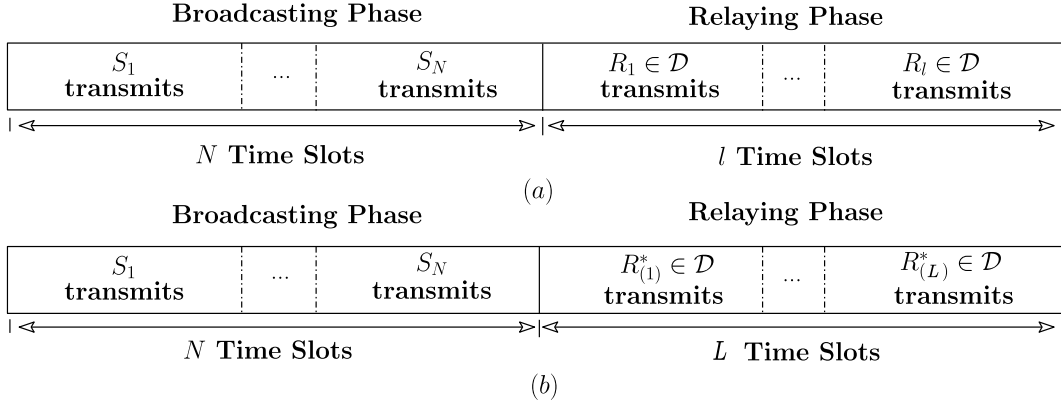
Fig. 4.3: Time-resource allocation for RS Strategy $\mathcal{B}_2$ (a) $0 \leq l \leq L$, (b) $L < l \leq M$.

Remark 4.8. *Interestingly, but counter-intuitively, an increase in the number of selected relays has negative impact on the diversity when $L > \frac{(M+1)N_r}{N_r+N_d}$, $(N > L)$ or $N \leq L$. This contradicts our expectation that selecting more relays improves the system performance.*

Remark 4.9. *The diversity order is independent of M and N_r when $L \leq \frac{(M+1)N_r}{N_r+N_d}$. Thus, adding relays or the antennas at relays does not improve the performance.*

4.4.2 RS Strategy $\mathcal{B}_2$

The RS Strategy $\mathcal{B}_1$ is not capable of achieving the diversity orders similar to Strategy $\mathcal{A}$. The assumption that the relays in $\mathcal{D}_l$ have to be silent when $0 \leq l < L$ may be too restrictive for such scheme. In this section, we relax this assumption and assume that the relays in $\mathcal{D}_l$ will cooperate without RS when $0 \leq l \leq L$, while RS is carried out when $L < l \leq M$. Fig. 4.3 depicts time-resource allocation for RS Strategy $\mathcal{B}_2$.

4.4.2.1 Outage Probability

Recall that the OP of Strategy $\mathcal{B}_2$ is given by (4.39), where $\Psi(l)$ has been derived in the previous section (4.41). In the following, we proceed to obtain $\Pr\{\mathcal{O}_{\mathcal{B}_2}|\mathcal{D}_l\}$.

In RS Strategy $\mathcal{B}_2$, the destination potentially receives (i) $N+l$ packets if $0 \leq l \leq L$ and (ii) $N + L$ packets if $L < l \leq M$. An outage occurs if fewer than N packets are decoded by the destination. Let $l_{\mathrm{op}} \leq l$ denote the number of relays in $\mathcal{D}_l$ whose

relay-to-destination channels are not in outage. Depending on l, we have the following outage events:

1. $0 \leq l \leq L$: When the number of available relays in $\mathcal{D}_l$ is less than or equal to L, all l relays transmit without selection. In this case, an outage occurs if at most $N-1$ links from N source-to-destination links and l relay-to-destination links be operational i.e., $N_{op} + l_{op} < N$. This event is denoted as $\mathcal{O}_{\mathcal{B}_2}^{(1)}|\mathcal{D}_l$.

2. $L < l \leq M$: If the number of available relays in $\mathcal{D}_l$ is more than L, then RS is performed. Therefore, two outage events happen:

   - $\mathcal{O}_{\mathcal{B}_2}^{(2)}|\mathcal{D}_l$ represents the outage events when $N_{op} < N - L$.

   - $\mathcal{O}_{\mathcal{B}_2}^{(2')}|\mathcal{D}_l$ corresponds to the outage events when $N_{op} \geq N-L$ but $N_{op}+L_{op}^{\mathcal{B}} < N$.

The overall OP conditioned on $\mathcal{D}_l$ in (4.39) can be then written as

$$\Pr\{\mathcal{O}_{\mathcal{B}_2}|\mathcal{D}_l\} = \Pr\{\mathcal{O}_{\mathcal{B}_2}^{(1)}|\mathcal{D}_l\} + \Pr\{\mathcal{O}_{\mathcal{B}_2}^{(2)}|\mathcal{D}_l\} + \Pr\{\mathcal{O}_{\mathcal{B}_2}^{(2')}|\mathcal{D}_l\}. \tag{4.64}$$

In (4.64), $\Pr\{\mathcal{O}_{\mathcal{B}_2}^{(1)}|\mathcal{D}_l\}$ can be formulated as

$$\Pr\{\mathcal{O}_{\mathcal{B}_2}^{(1)}|\mathcal{D}_l\} = \sum_{m=0}^{l} \Theta(m|l) \sum_{\tau=0}^{N-1-m} \Phi(\tau), \ 0 \leq l \leq L, \tag{4.65}$$

where $\Theta(m|l)$ is the probability that m relays out of l relays be operational and can be written as

$$\Theta(m|l) = \sum_{k=1}^{m+1} \mathcal{C}_{l-m}^{l+k-m-1}(-1)^{k-1} \sum_{i_1,i_2,\cdots,i_{l+k-m-1}\in\mathcal{D}_l} \prod_{m=i_1}^{i_{l+k-m-1}} F_{\gamma_m^{(i)}}(\gamma_{th}). \tag{4.66}$$

On the other hand, $\Pr\{\mathcal{O}_{\mathcal{B}_2}^{(2)}|\mathcal{D}_l\} + \Pr\{\mathcal{O}_{\mathcal{B}_2}^{(2')}|\mathcal{D}_l\}$ for $N > L$ can be derived as

$$\Pr\{\mathcal{O}_{\mathcal{B}_2}^{(2)}|\mathcal{D}_l\} + \Pr\{\mathcal{O}_{\mathcal{B}_2}^{(2')}|\mathcal{D}_l\} = \sum_{\tau=0}^{N-L-1} \Phi(\tau)$$
$$+ \sum_{\tau=1}^{L} \left(\Phi(N-\tau) \sum_{v=1}^{\tau} F_{\gamma_{(v)|l}}(\gamma_{th}) \right), \quad L < l \leq M. \tag{4.67}$$

By plugging (4.65), (4.67), and (4.41) into (4.39), the exact OP for $N > L$ under Strategy $\mathcal{B}_2$ can be derived as (4.68). With similar arguments used above, we obtain

the OP of the system when $N \leq L$ as (4.69).

$$\mathcal{P}_{\text{out}_1}^{\mathcal{B}_2} = \underbrace{\sum_{l=0}^{L} \sum_{\mathcal{D}_l} \left(\sum_{m=0}^{l} \Theta(m|l) \sum_{\tau=0}^{N-1-m} \Phi(\tau) \right) \Psi(l)}_{\Pr\{\mathcal{O}_{\mathcal{B}_2}^{(1)}\}} + \underbrace{\sum_{l=L+1}^{M} \sum_{\mathcal{D}_l} \left(\sum_{\tau=0}^{N-L-1} \Phi(\tau) \right) \Psi(l)}_{\Pr\{\mathcal{O}_{\mathcal{B}_2}^{(2)}\}}$$

$$+ \underbrace{\sum_{l=L+1}^{M} \sum_{\mathcal{D}_l} \left(\sum_{\tau=1}^{L} \Phi(N-\tau) \sum_{\upsilon=1}^{\tau} F_{\gamma_{(\upsilon)|l}}(\gamma_{th}) \right) \Psi(l)}_{\Pr\{\mathcal{O}_{\mathcal{B}_2}^{(2')}\}}. \tag{4.68}$$

$$\mathcal{P}_{\text{out}_2}^{\mathcal{B}_2} = \underbrace{\sum_{l=0}^{N-1} \sum_{\mathcal{D}_l} \left(\sum_{m=0}^{l} \Theta(m|l) \sum_{\tau=0}^{N-1-m} \Phi(\tau) \right) \Psi(l)}_{\Pr\{\mathcal{O}_{\mathcal{B}_2}^{(1)}\}} + \underbrace{\sum_{l=N}^{L} \sum_{\mathcal{D}_l} \left(\sum_{m=0}^{N-1} \Theta(m|l) \sum_{\tau=0}^{N-1-m} \Phi(\tau) \right) \Psi(l)}_{\Pr\{\mathcal{O}_{\mathcal{B}_2}^{(1)}\}}$$

$$+ \underbrace{\sum_{l=L+1}^{M} \sum_{\mathcal{D}_l} \left(\sum_{\tau=1}^{N} \Phi(N-\tau) \sum_{\upsilon=1}^{\tau} F_{\gamma_{(\upsilon)|l}}(\gamma_{th}) \right) \Psi(l)}_{\Pr\{\mathcal{O}_{\mathcal{B}_2}^{(2')}\}}. \tag{4.69}$$

4.4.2.2 Asymptotic Analysis

$\Theta(m|l)$ in high SNRs can be approximated as

$$\Theta^{\infty}(m|l) = \sum_{i_1, i_2, \cdots, i_{l-m} \in \mathcal{D}_l} \prod_{m=i_1}^{i_{l-m}} \left(\frac{\beta_m^{N_d}}{N_d!} \right)^{N_r}. \tag{4.70}$$

Substituting (4.18), (4.51), (4.52) and (4.70) in (4.68) and ignoring higher order terms, we have

$$\mathcal{P}_{\text{out}_1^{\infty}}^{\mathcal{B}_2} = \Psi^{\infty}(0)\Phi^{\infty}(N-1) + \Phi^{\infty}(N-L-1)\Psi^{\infty}(M). \tag{4.71}$$

The asymptotic outage depends on the system parameters. In particular, (4.68) in high SNRs is derived in the following three cases:

- **Case 1:** $MN_r > LN_d$. In this case, $\mathcal{P}_{\text{out}_1^{\infty}}^{\mathcal{B}_2}$ is determined by the second term in (4.71) as $\mathcal{P}_{\text{out}_1^{\infty}}^{\mathcal{B}_2} = \Phi^{\infty}(N-L-1)\Psi^{\infty}(M)$. This is expressed as

$$\mathcal{P}_{\text{out}_1^{\infty}}^{\mathcal{B}_2} = \Xi_1^{\mathcal{B}_2} \left(\frac{\gamma_{th}}{\bar{\gamma}} \right)^{(L+1)N_d}, \tag{4.72}$$

  where

$$\Xi_1^{\mathcal{B}_2} = \sum_{i_1, i_2, \cdots, i_{L+1}}^{N} \left(\prod_{n=i_1}^{i_{L+1}} \frac{\lambda_n^{-N_d}}{N_d!} \right). \tag{4.73}$$

79

- **Case 2:** $MN_r < LN_d$. In this case, $\mathcal{P}^{\mathcal{B}_2}_{\text{out}_1 \infty}$ is determined by the first term in (4.71) as $\mathcal{P}^{\mathcal{B}_2}_{\text{out}_1 \infty} = \Psi^\infty(0)\Phi^\infty(N-1)$. This can be written as

$$\mathcal{P}^{\mathcal{B}_2}_{\text{out}_1 \infty} = \Xi^{\mathcal{B}_2}_{1'} \left(\frac{\gamma_{th}}{\bar{\gamma}}\right)^{MN_r + N_d}, \qquad (4.74)$$

where

$$\Xi^{\mathcal{B}_2}_{1'} = \sum_{i_1=1}^{N} \frac{\lambda_{i_1}^{-N_d}}{N_d!} \prod_{m=i_1}^{i_M} \left(\sum_{i_1=1}^{N} \frac{\lambda_{i_1,m}^{-N_r}}{N_r!}\right). \qquad (4.75)$$

- **Case 3:** $MN_r = LN_d$. In this case, $\mathcal{P}^{\mathcal{B}_2}_{\text{out}_1 \infty}$ is determined by the first and the second terms in (4.71), where $\Phi^\infty(N-L-1)\Psi^\infty(M)$ and $\Psi^\infty(0)\Phi^\infty(N-1)$ are derived in (4.72) and (4.74), respectively.

The OP for $N \leq L$ (4.69) in high SNRs is derived in the following four cases according to the relationship between N_d and N_r.

- **Case 1:** $N_d > N_r$. In this case, we have

$$\mathcal{P}^{\mathcal{B}_2}_{\text{out}_2 \infty} = \Xi^{\mathcal{B}_2}_{2} \left(\frac{\gamma_{th}}{\bar{\gamma}}\right)^{MN_r + N_d}, \qquad (4.76)$$

where

$$\Xi^{\mathcal{B}_2}_{2} = \sum_{i_1=1}^{N} \frac{\lambda_{i_1}^{-N_d}}{N_d!} \prod_{m=i_1}^{i_M} \left(\sum_{i_1=1}^{N} \frac{\lambda_{i_1,m}^{-N_r}}{N_r!}\right). \qquad (4.77)$$

- **Case 2:** $N_d < N_r, N_d = 1$. In this case, we have

$$\mathcal{P}^{\mathcal{B}_2}_{\text{out}_2 \infty} = \Xi^{\mathcal{B}_2}_{2'} \left(\frac{\gamma_{th}}{\bar{\gamma}}\right)^{(M-N+1)N_r + N}, \qquad (4.78)$$

where $\Xi^{\mathcal{B}_2}_{2'}$ is given by (4.79).

$$
\begin{aligned}
\Xi^{\mathcal{B}_2}_{2'} = &\sum_{\mathcal{D}_{N-1}} \left(\prod_{n=i_1}^{i_N} \lambda_n^{-1} \prod_{m=i_1}^{i_{M-N+1}} \left(\sum_{i_1=1}^{N} \frac{\lambda_{i_1,m}^{-N_r}}{N_r!}\right)\right) \\
&+ \sum_{l=N}^{L} \sum_{\mathcal{D}_l} \left(\sum_{i_1,i_2,\cdots,i_{l-N+1}\in\mathcal{D}_l} \prod_{m=i_1}^{i_{l-N+1}} \lambda_m^{-N_r} \prod_{n=i_1}^{i_N} \lambda_n^{-1} \prod_{m=i_1}^{i_{M-l}} \left(\sum_{i_1=1}^{N} \frac{\lambda_{i_1,m}^{-N_r}}{N_r!}\right)\right) \\
&+ \sum_{l=L+1}^{M} \sum_{\mathcal{D}_l} \left(\prod_{n=i_1}^{i_N} \lambda_n^{-1} \sum_{i_1,i_2,\cdots,i_{l-N+1}\in\mathcal{D}_l} \prod_{m=i_1}^{i_{l-N+1}} \lambda_m^{-N_r} \prod_{m=i_1}^{i_{M-l}} \left(\sum_{i_1=1}^{N} \frac{\lambda_{i_1,m}^{-N_r}}{N_r!}\right)\right). \quad (4.79)
\end{aligned}
$$

80

- **Case 3:** $N_d < N_r, N_d \neq 1$. In this case,

$$\mathcal{P}^{\mathcal{B}_2}_{\text{out}_2^\infty} = \Xi^{\mathcal{B}_2}_{2''} \left(\frac{\gamma_{th}}{\bar{\gamma}}\right)^{(M-N+1)N_r+NN_d}, \tag{4.80}$$

where

$$\Xi^{\mathcal{B}_2}_{2''} = \sum_{\mathcal{D}_{N-1}} \left(\prod_{n=i_1}^{i_N} \frac{\lambda_n^{-N_d}}{N_d!} \prod_{m=i_1}^{i_{M-N+1}} \left(\sum_{i_1=1}^{N} \frac{\lambda_{i_1,m}^{-N_r}}{N_r!} \right) \right). \tag{4.81}$$

- **Case 4:** $N_d = N_r = \tilde{N}$. For this case, $\mathcal{P}^{\mathcal{B}_2}_{\text{out}_2^\infty}$ can be obtained as

$$\mathcal{P}^{\mathcal{B}_2}_{\text{out}_2^\infty} = \Xi^{\mathcal{B}_2}_{2'''} \left(\frac{\gamma_{th}}{\bar{\gamma}}\right)^{(M+1)\tilde{N}}, \tag{4.82}$$

where

$$\Xi^{\mathcal{B}_2}_{2'''} = \sum_{l=0}^{N-1} \sum_{\mathcal{D}_l} \left(\sum_{i_1,i_2,\cdots,i_{l+1}} \prod_{n=i_1}^{i_{l+1}} \frac{\lambda_n^{-\tilde{N}}}{\tilde{N}!} \prod_{m=i_1}^{i_{M-l}} \left(\sum_{i_1=1}^{N} \frac{\lambda_{i_1,m}^{-\tilde{N}}}{\tilde{N}!} \right) \right). \tag{4.83}$$

The diversity order and the coding gain of MIMO NCC system with RS under strategy $\mathcal{B}_2$ for $N > L$ and $N \leq L$ are given, respectively, by

$$G^{\mathcal{B}_2}_{d_1} = \min\{MN_r, LN_d\} + N_d. \tag{4.84}$$

$$G^{\mathcal{B}_2}_{c_1} = \begin{cases} \dfrac{\Xi_1^{\mathcal{B}_2 - \frac{1}{(L+1)N_d}}}{\gamma_{th}}, & MN_r > LN_d \\[3mm] \dfrac{\Xi_{1'}^{\mathcal{B}_2 - \frac{1}{MN_r+N_d}}}{\gamma_{th}}, & MN_r < LN_d \\[3mm] \dfrac{\left(\Xi_1^{\mathcal{B}_2} + \Xi_{1'}^{\mathcal{B}_2}\right)^{-\frac{1}{(L+1)N_d}}}{\gamma_{th}}, & MN_r = LN_d \end{cases} \tag{4.85}$$

$$G^{\mathcal{B}_2}_{d_2} = (M+1)N_r + \min\{N_d - N_r, N(N_d - N_r)\}. \tag{4.86}$$

$$G^{\mathcal{B}_2}_{c_2} = \begin{cases} \dfrac{\Xi_2^{\mathcal{B}_2 - \frac{1}{MN_r+N_d}}}{\gamma_{th}}, & N_d > N_r \\[3mm] \dfrac{\Xi_{2'}^{\mathcal{B}_2 - \frac{1}{(M-N+1)N_r+N}}}{\gamma_{th}}, & N_d < N_r, N_d = 1 \\[3mm] \dfrac{\Xi_{2''}^{\mathcal{B}_2 - \frac{1}{(M-N+1)N_r+NN_d}}}{\gamma_{th}}, & N_d < N_r, N_d \neq 1 \\[3mm] \dfrac{\Xi_{2'''}^{\mathcal{B}_2 - \frac{1}{(M+1)\tilde{N}}}}{\gamma_{th}}, & \tilde{N} = N_d = N_r \end{cases} \tag{4.87}$$

As can be seen form (4.84) and (4.86), RS Strategy $\mathcal{B}_2$ is capable of achieving diversity orders similar to Strategy $\mathcal{A}$ given by (4.34) and (4.36). Furthermore, although the derived outage expressions in (4.68) and (4.69) are completely different from (4.15) and (4.16), there are *exactly the same* for all SNR values. Therefore, the proposed RS strategy has the outage performance similar to Strategy $\mathcal{A}$, while it significantly reduces signaling overhead.

Special Case 4.2. *The derived analytical expressions are the generalized versions of i.i.d Rayleigh fading channels when $\bar{\gamma}_n = \bar{\gamma}_{n,m} = \bar{\gamma}_m$, $(\forall n, m)$ [67].*

4.5   Numerical Results and Discussions

Herein, we present numerical results to illustrate the outage performance of RS Strategy $\mathcal{A}$ and Strategy $\mathcal{B}$. Insightful discussions related to the impact of different system parameters on the system performance will be presented. Monte-Carlo simulation results are further provided to support our analytical results.

4.5.1   i.i.d. Fading Channels

4.5.1.1   Outage Performance of RS Strategy $\mathcal{A}$ and $\mathcal{B}$

Here, we investigate the OP and diversity order of RS Strategy $\mathcal{A}$ and $\mathcal{B}$.

Fig. 4.4 illustrates the OP of RS Strategy $\mathcal{B}_1$ when $N = 4$, $M = 5$, $N_r = 2$, $N_d = 2$ and $L = 1, 2, 3, 4$. The exact OP expressions are plotted along with the Monte-Carlo simulations. The analytical curves (4.49), (4.50) are in excellent agreement with Monte-Carlo simulations, confirming the accuracy of our derivations. Furthermore, the asymptotic lines perfectly predict the diversity orders and coding gains. It is observed that $L = 1, 2$ achieve the diversity order of 4 and 6, respectively, indicating that the diversity order is determined by $(L + 1)N_d$ (4.60), when $L < \frac{(M+1)N_r}{N_r+N_d} = 3$. We also observe that the maximum diversity order of $(L + 1)N_d = 8$ is achieved when $L = \frac{(M+1)N_r}{N_r+N_d} = 3$. However, as L increases form 3 to 4 the diversity decreases from 8 to $(M - L + 1)N_r + N_d = 6$ (4.62). Furthermore, although $L = 4$ and $L = 2$ both achieve
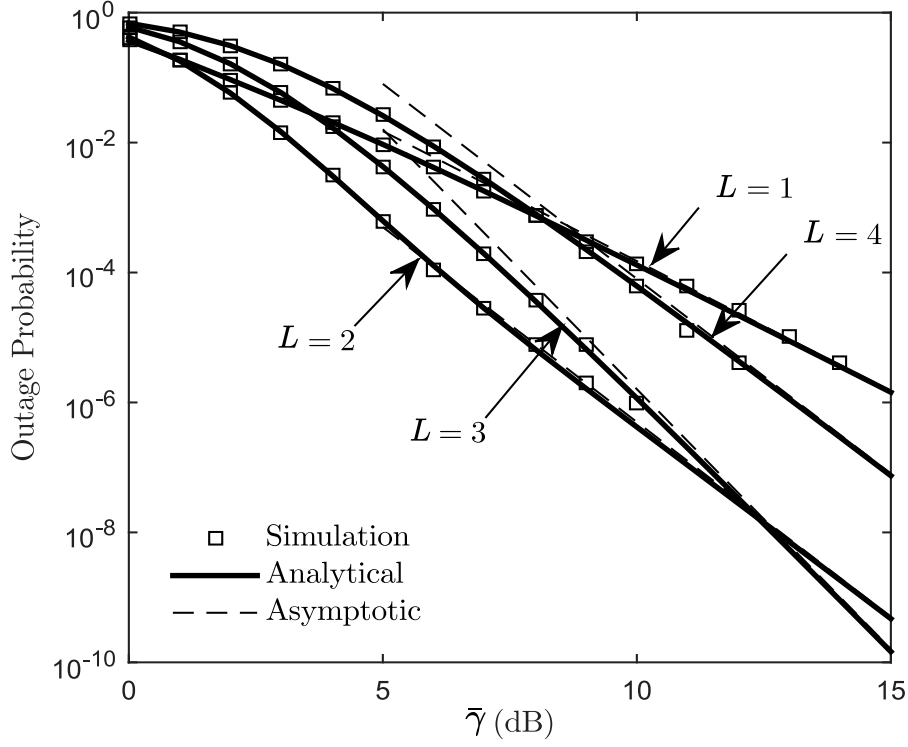
Fig. 4.4: OP versus $\bar{\gamma}$ for Strategy $\mathcal{B}_1$ when $N = 4$, $M = 5$, $N_r = 2$, $N_d = 2$, and $L = 1$, 2, 3, 4.

the diversity order of 6, $L = 2$ outperforms $L = 4$ for all SNR values. In conclusion, the performance improvement corresponding to the number of selected relays can only be obtained when the condition of $L \leq \frac{(M+1)N_r}{N_r+N_d}$ is satisfied. Otherwise, increasing L significantly reduces the diversity order and coding gain.

In Fig. 4.5, we plot the OP of Strategy $\mathcal{A}$ and that of Strategy $\mathcal{B}_2$. We consider $N = 4$, $M = 6$, $L = 2$, $N_r = 1, 2, 5$ and $N_d = 1, 2, 5$. This assumption satisfies the condition $N > L$. We observe that the outage performances of both strategies are exactly the same for the entire SNR regime. Furthermore, it can be seen that adding more antennas at relays does not improve outage performance in all SNRs. For example, for the case of $N_r > N_d$, the diversity order is always equal to $(L+1)N_d$. More precisely, the outage performance for $(N_r, N_d) = (5, 1)$ is slightly better than that of $(N_r, N_d) = (2, 1)$ in very low SNR regime. However, both curves have the same outage performance in medium to high-SNR regime and their corresponding asymptotic slopes

are identical and equal to $(L+1)N_d = 3$. It can also be seen that when $(N_r, N_d) = (1, 2)$, the outage performance gets better but still the slope of the curve at high-SNR regime is determined by $(L + 1)N_d$ and is equal to 6. However, when $(N_r, N_d) = (1, 5)$, the asymptotic slope of the curve is equal to $MN_r + N_d = 11$. This indicates that asymptotic diversity of the system is determined by $(L + 1)N_d$ and $MN_r + N_d$ for the case of $\frac{M}{L} > \frac{N_d}{N_r}$ and $\frac{M}{L} < \frac{N_d}{N_r}$, respectively (cf. Table 4.1). Thus, the diversity improvement associated with the number of relays M and the number of antennas at relays N_r can only be obtained when the conditions $N_d > N_r$ and $\frac{M}{L} < \frac{N_d}{N_r}$ are satisfied. Otherwise, the gains corresponding to M or N_r are either negligible or even non-existent.
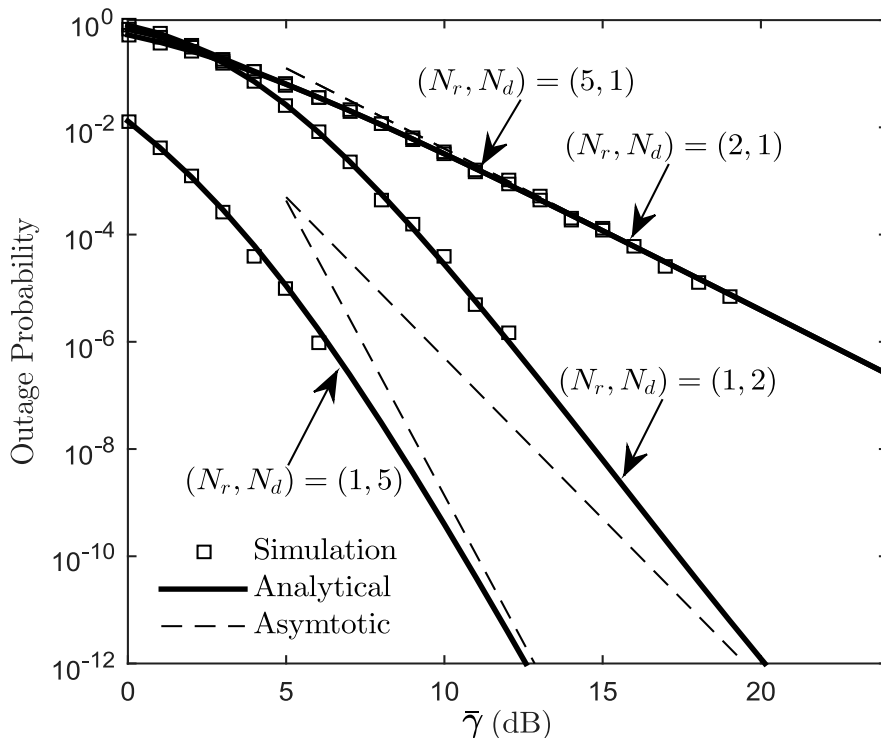
Fig. 4.5: OP versus $\bar{\gamma}$ for RS Strategy $\mathcal{A}$ $(\mathcal{B}_2)$ when $N = 4$, $M = 6$, $L = 2$, $N_r = 1, 2,$ 5 and $N_d = 1, 2, 5$ $(N > L)$.

Fig. 4.6 depicts the OP of RS Strategy $\mathcal{A}$ $(\mathcal{B}_2)$ for $N = 2, 3$, $M = 4$, $L = 3$, $N_r = 2,$ 4 and $N_d = 2, 4$. These assumptions satisfy the condition $N \leq L$. As expected, by increasing N the system is more likely to undergo outage which results in higher outage

values. It is also observed that when $N_r > N_d$, adding more sources also reduces the diversity order of the system from 16 to 14 as the diversity order is determined by $(M - N + 1)N_r + NN_d$ (cf. Table 4.1). While, for the case of $N_r < N_d$ the slope of the curves remain fix and is equal to $MN_r + N_d = 12$.
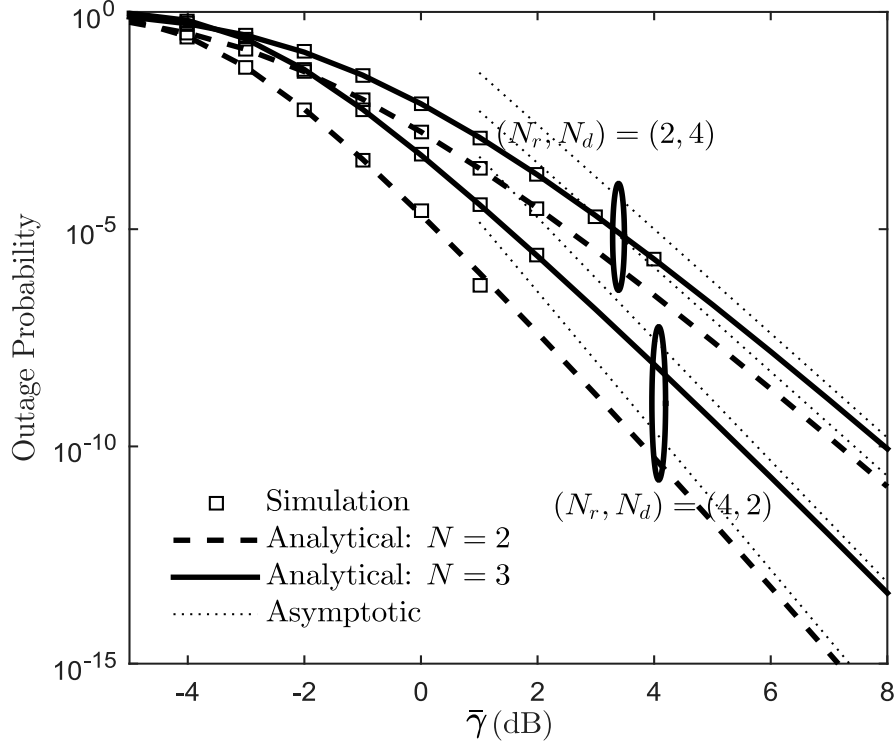
Fig. 4.6: OP versus $\bar{\gamma}$ for RS Strategy $\mathcal{A}$ ($\mathcal{B}_2$) for $N = 2, 3$, $M = 4$, $L = 3$, $N_r = 2, 4$ and $N_d = 2, 4$ ($N \leq L$).

Fig. 4.7 compares the outage performance between Strategy $\mathcal{A}$ ($\mathcal{B}_2$) and Strategy $\mathcal{B}_1$ when $N = 3$, $M = 6$, $L = 2, 3$, $N_r = 2$, and $N_d = 2$. We observe that for $L = 2$ ($N > L$) Strategy $\mathcal{A}$ ($\mathcal{B}_2$) performs slightly better than Strategy $\mathcal{B}_1$ at low SNR values, while as SNR increases both have similar outage performances. This indicates that both strategies achieve the same diversity order and coding gain in high SNRs. However, for the case of $L = 3$, ($N \leq L$), Strategy $\mathcal{A}$ ($\mathcal{B}_2$) achieves higher diversity order and thus significantly outperforms Strategy $\mathcal{B}_1$ in all SNRs. Specifically, to achieve a target outage rate of 10^{-6}, SNR=5 dB is required for Strategy $\mathcal{A}$ ($\mathcal{B}_2$), while this increases to 8 dB for Strategy $\mathcal{B}_1$, indicating an SNR gain of 3 dB. Thus, the achievable diversity

order and coding gain of RS Strategy $\mathcal{B}_1$ are always equal or less than that of Strategy $\mathcal{A}$ or Strategy $\mathcal{B}_2$. Therefore, RS Strategy $\mathcal{B}_1$ does not provide any performance gain.

4.5.1.2 Performance Comparison With Two Benchmark Schemes

Here, we compare the outage performance of our proposed RS MIMO NCC with two benchmark schemes, namely single-antenna RS NCC [29, 30], and RS MIMO NCC with RAS at relays.
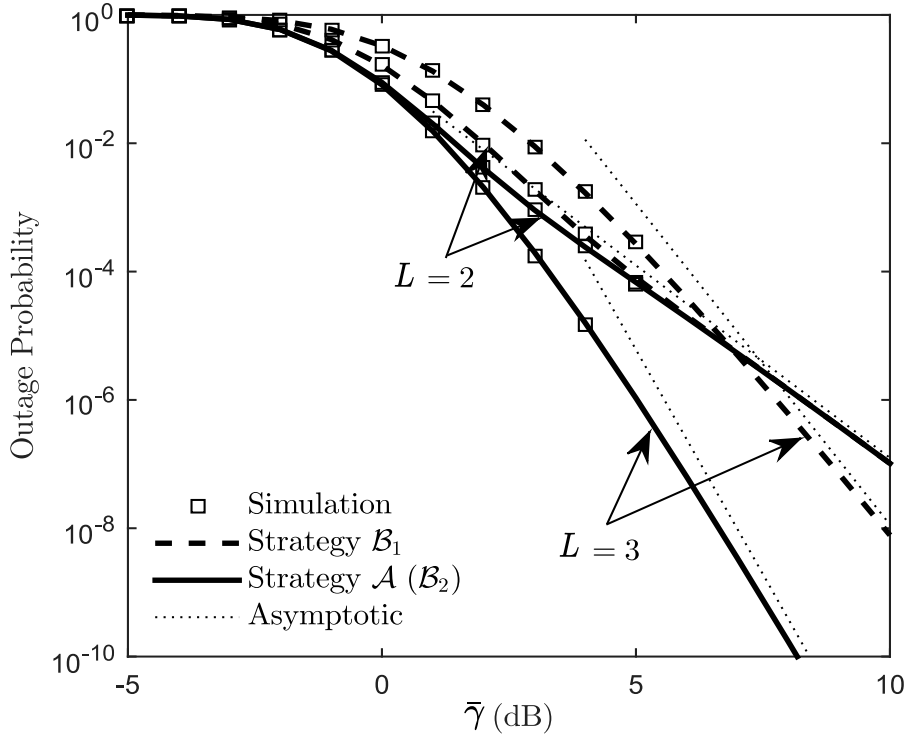
Fig. 4.7: Comparison between Strategy $\mathcal{A}$ ($\mathcal{B}_2$) and Strategy $\mathcal{B}_1$ when $N = 3$, $M = 6$, $L = 2, 3$, $N_r = 2$, and $N_d = 2$.

Fig. 4.8 plots the outage performance of single-antenna RS NCC [29, 30] and that of RS Strategy $\mathcal{A}$ ($\mathcal{B}_2$) when $N = 3$, $M = 5$, $N_r = 2$, $N_d = 2$, and $L = 1, 2, 3$. As can be seen, RS MIMO NCC achieves impressive performance gains. For example, the required SNR to achieve a target outage of 10^{-3} for single-antenna RS NCC is 17, 11, 10.5 dB for $L = 1, 2, 3$, respectively. This reduces to 7 and 3 dB for RS MIMO NCC with $L = 1, 2$. It further reduces to 2.5 dB for $L = 3$. In addition, the asymptotic

lines reveal that the diversity order of single-antenna RS NCC for $L = 1$, 2, and 3 are respectively equal to 2 and 3, and 6. On the other hand, RS MIMO NCC achieves the diversity order of 4, 6, and 12 for $L = 1$, 2, 3 (cf. Table 4.1).
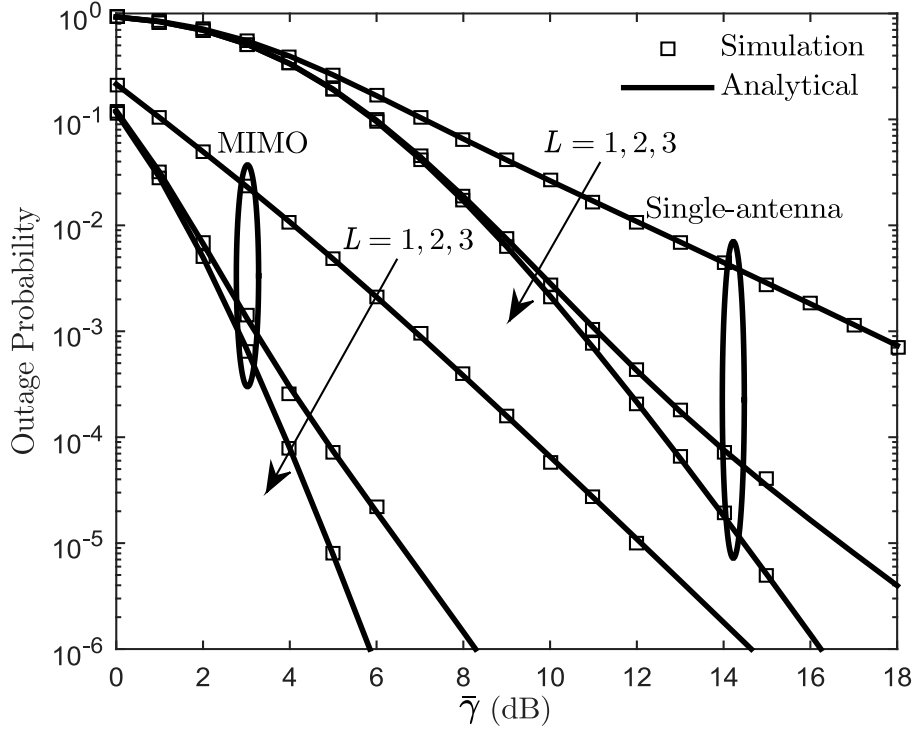
Fig. 4.8: Comparison between single-antenna RS NCC and RS Strategy $\mathcal{A}$ ($\mathcal{B}_2$) when $N = 3$, $M = 5$, $N_r = 2$, $N_d = 2$, and $L = 1$, 2, 3.

Fig. 4.9 compares the outage performance between the proposed RS MIMO NCC with TAS and RAS at relays. We assume $N = 2$, $M = 4$, $N_r = 2$, 3, $N_d = 2$, 3 and $L = 1$, 2. It is observed that when $L = 1$ or $L = 2$ and $N_d > N_r$ TAS has slightly better outage performance in finite SNR regime. However, as SNR tends to infinity, the diversity order and coding gain for both schemes becomes identical, leading to the same outage performance. On the other hand, when $L = 2$ and $N_d < N_r$, TAS achieves higher diversity order and thus significantly outperforms RAS in both finite and asymptotic SNRs. This indicates that the diversity gains of TAS can only be obtained when the conditions $N \leq L$ and $N_d < N_r$ hold. Otherwise, RS MIMO NCC with RAS at relays is more preferable due to the lower complexity.
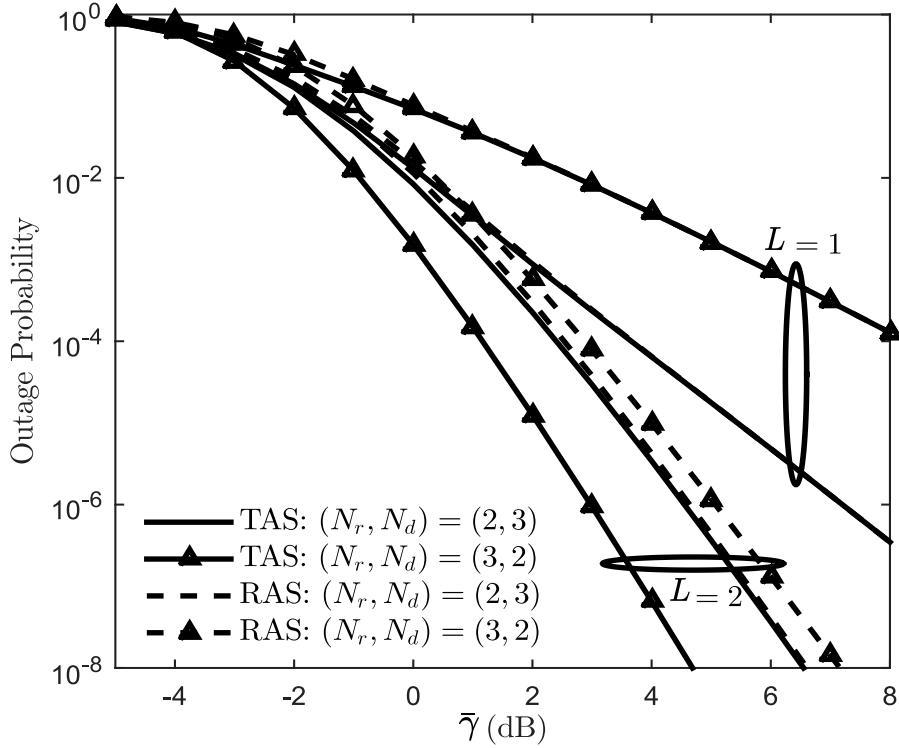
Fig. 4.9: OP versus $\bar{\gamma}$ for Strategy $\mathcal{A}$ ($\mathcal{B}_2$) using TAS and RAS at relays. $N = 2$, $M = 4$, $N_r = 2, 3$, $N_d = 2, 3$, and $L = 1, 2$.

4.5.2   i.n.i.d. Fading Channels

Here, we consider i.n.i.d. Rayleigh fading channels that take into account the effect of nodes' locations. In particular, we assume that the nodes are located in a 2-D plane where $d_{S_n R_m}$, $d_{S_n D}$, and $d_{R_m D}$ ($\forall n, m$) respectively denote the distances of source-to-relay, source-to-destination, and relay-to-destination links. The so-called "geometric gain" for $S_n \to R_m$ link with respect to $S_1 \to D$ link can then be defined as[4]

$$g_{n,m} = \left(\frac{d_{S_n R_m}}{d_{S_1 D}}\right)^{-\alpha}, \qquad \forall n, m \tag{4.88}$$

where α being the path-loss exponent.

Similarly, the geometric gain of $S_n \to D$ and $R_m \to D$ links with respect to $S_1 \to D$

---

[4]We assume that S_1 is the most distant source to the destination.

link are respectively given by

$$g_n = \left(\frac{d_{S_n D}}{d_{S_1 D}}\right)^{-\alpha}, \qquad \forall n \tag{4.89}$$

and

$$g_m = \left(\frac{d_{R_m D}}{d_{S_1 D}}\right)^{-\alpha}, \qquad \forall m \tag{4.90}$$

In Fig. 4.10, we plot the OP of RS MIMO NCC over i.n.i.d. channels, assuming $N = 3$, $M = 3$, $L = 2$, $N_r = 2$, $N_d = 2$, $\mathcal{R}_0 = 2$, and $\alpha = 3$. The positions of S_1, S_2, S_3, and D are kept fixed and are given by $\mathbf{X}_{S_1} = \{0, 300 \text{ m}\}$, $\mathbf{X}_{S_2} = \{100 \text{ m}, -100 \text{ m}\}$, $\mathbf{X}_{S_3} = \{0, -200 \text{ m}\}$, $\mathbf{X}_D = \{1000 \text{ m}, 0\}$. The positions of the relays, however, vary along the x axis and are given by $\mathbf{X}_{R_1} = \{300 + \Delta \text{ m}, 200 \text{ m}\}$, $\mathbf{X}_{R_2} = \{200 + \Delta \text{ m}, \ 0\}$, and $\mathbf{X}_{R_3} = \{300 + \Delta \text{ m}, -300 \text{ m}\}$, where $\Delta \in \{0, 300, 600\}$ denotes the amount of the relay position shift. As can be seen the analytical results perfectly match simulations. In addition, the best outage performance occurs when the relays are in the vicinity of the sources i.e., $\Delta \approx 0$. However, as relays move towards the destination the outage performance deteriorates. We also observe that as SNR goes to infinity, the outage curves converge and the diversity for all curves is identical and equal to $(L+1)\tilde{N} = 6$.

4.6 Conclusions

For NCC systems, we developed a new RS strategy with the same performance as the "*max-min*" criterion but does not need global CSI. We first had to analyze MIMO NCC (which did not exist in the literature). In particular, we considered N single-antenna sources, M multiple-antenna relays, and a single multiple-antenna destination. Considering the general case of i.n.i.d. fading channels, closed-form expressions for the OP, asymptotic OP, the diversity order, and the coding gain were derived and confirmed by Monte-Carlo simulations.
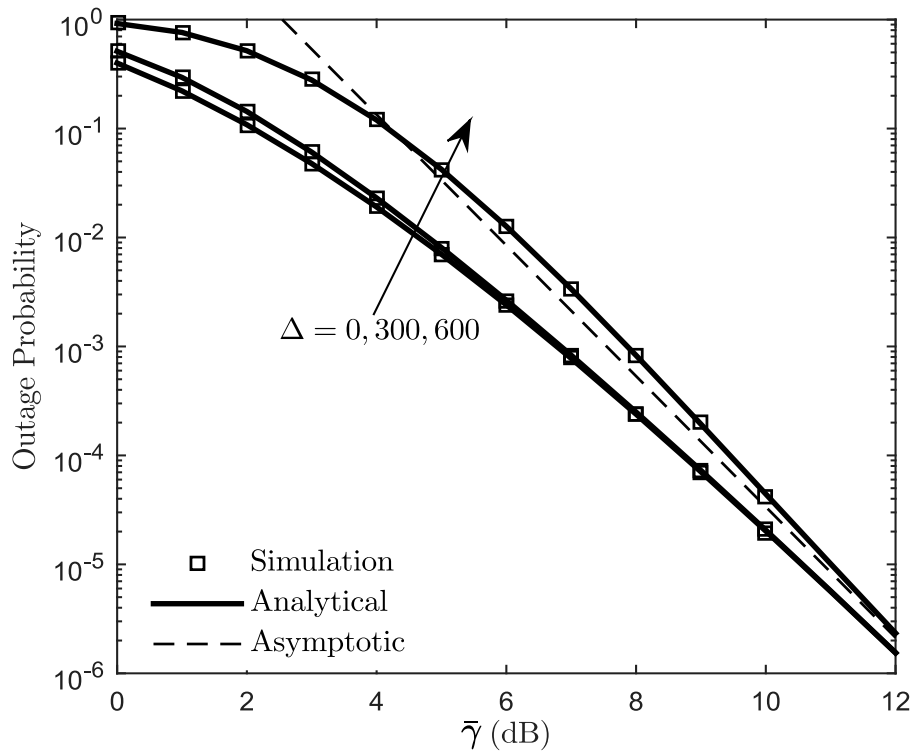
Fig. 4.10: OP versus $\bar{\gamma}$ for RS Strategy $\mathcal{A}$ ($\mathcal{B}_2$) over i.n.i.d. fading channels when $N = 3$, $M = 3$, $L = 2$, $N_r = 2$, $N_d = 2$, $R_0 = 2$, and $\alpha = 3$.

90

Chapter 5

Network-Coded Cooperative MIMO With Outdated CSI and CCI

In this chapter, we consider a dual-hop cooperative network that consists of $N > 1$ single-antenna sources, $M \geq 1$ DF multiple-antenna relays and a single multiple-antenna destination. The destination selects L best relays that maximize the SNR of relay-destination channels. The selected relays apply NC on the received sources' symbols using network code coefficients based on MDS codes. In our system setup, the relays use one transmit antenna to forward encoded signals to the destination. On the other hand, both the destination and relays employ selection combining (SC) for signal reception.[1] For this system, we derive the exact OP in closed-form. To obtain further insights into the system-design parameters, the asymptotic high-SNR OP is also derived, through which the diversity order and the coding gain are quantified. Valuable insights and guidelines are provided to help the design of practical RS MIMO NCC.

This chapter is as follows: Section 5.1 explains the system and channel models. The

---

[1]In Chapter 4, we assume that the relays and the destination employ MRC for the signal reception. MRC reception, however, requires a separate receiver chain for each receive antenna leading to the increase in the cost, energy consumption, and complexity. In this chapter, we assume SC at the relays and the destination to gain MIMO diversity benefits while keeping the costs/complexity as low as possible.

exact OP and asymptotic analyses are presented in Section 5.2. Numerical results are given in Section 5.3. Finally, we conclude in Section 5.4.

5.1 System and Channel Models

Let us consider a dual-hop multi-source multi-relay cooperative network where N single-antenna sources $\mathcal{S} = \{S_n\}_{n=1}^N$ communicate with the destination D, equipped with $N_d \geq 1$ antennas, with the help of M DF relays $\mathcal{R} = \{R_m\}_{m=1}^M$. Each relay has $N_r \geq 1$ receive antennas and uses only one antenna for transmission. We assume the direct links from the sources to the destination are not reliable and the sources' packets are transmitted only through the relays. This can happen due to propagation impairments such as shadowing and path-loss. The channels are assumed to follow a flat Rayleigh fading model. Let $\mathbf{h}_{S_n R_m} \in \mathbb{C}^{N_r \times 1}$ and $\mathbf{h}_{R_m D} \in \mathbb{C}^{N_d \times 1}$, respectively, denote the single-input multiple-output (SIMO) channel vectors for the source-relay and relay-destination links whose elements are modeled as $\sim \mathcal{CN}(0, 1)$. The jth and the ℓth elements of $\mathbf{h}_{S_n R_m}$ and $\mathbf{h}_{R_m D}$ are denoted by $h_{S_n R_m}^{(j,1)}$ and $h_{R_m D}^{(\ell,1)}$. Further, the channels include independent AWGN terms with mean zero and variance one. We assume that the number of CCI signals impairing the relays and the destination are I_1 and I_2, respectively, and that the received interference signals at the relays and destination have identical average energy.[2]

    The transmission of the sources and the relays occurs in non-overlapping time-slots and a complete round of cooperation takes place in two phases.

5.1.1 First Phase: Source-Relay Transmission

In the first phase, the sources transmit their messages to the relays in N orthogonal time-slots. The relays employ SC to exploit receiver diversity. In particular, the best receiver antenna providing the maximum SNR between source S_n and relay R_m is selected for data reception. At the same time, relay R_m receives I_1 CCI signals. The

---

[2]This assumption is made for the sake of analytical tractability. Extension to general unequal power and i.n.i.d channels can easily be made from our work.

instantaneous SINR for $S_n \to R_m$ $(\forall n, m)$ link can then be written as

$$\gamma_{nm} = \frac{\gamma_{nm}^*}{1 + \gamma_{I_1}}. \tag{5.1}$$

In (5.1) $\gamma_{I_1} = \sum_{i=1}^{I_1} \mu_1 |g_{m,i}|^2$ where μ_1 is the interference transmit SNR and $g_{m,i}$ is the channel coefficient of the ith interference at R_m. Also, $\gamma_{nm}^* = \bar{\gamma} |h_{nm}^*|^2$ where $\bar{\gamma}$ is the transmit SNR and $|h_{nm}^*|$ is given by

$$|h_{nm}^*| = \max_{1 \leqslant j \leqslant N_r} \{|h_{S_n R_m}^{(j,1)}|\}. \tag{5.2}$$

At the end of the first phase, the relays which successfully decode all N sources' packets, send a flag packet to the destination, indicating that they are ready for cooperation. Let $\mathcal{D}$ denote the set of decodable relays with the cardinality of l. Mathematically speaking, this can be written as

$$\mathcal{D} \triangleq \{R_m \in \mathcal{R} : \gamma_{nm} > \gamma_{th}, \ \forall n\}, \tag{5.3}$$

where γ_{th} is the predefined SINR threshold.

It is clear that the number of relays in $\mathcal{D}$, l, is upper bounded by the total number of available relays M, i.e., $l \leq M$. Note that $\mathcal{D}$ is a random set and l is thus a RV.

5.1.2 Second Phase: Relay-Destination Transmission

The second phase lasts for L time-slots. At the beginning of each time-slot a relay in $\mathcal{D}$ which maximizes the SNR of relay-destination channels is selected for transmission. This procedure continues until L relays transmit. In particular, the selected relay R_{m^*} linearly combines the received sources' packets using a non-binary q-ary GF NC based on MDS codes. The resulting network-coded packet is then forwarded to the destination by a single antenna at R_{m^*}. At the same time, the received signal at the destination is impaired by I_2 CCI signals. Since the destination employs SC, the SNR of relay-destination channel at selection instant t is given by

$$\hat{\gamma}_{m^*} = \bar{\gamma} |\hat{h}_{m^*}| = \bar{\gamma} \max_{R_m \in \mathcal{D}} \left\{ \max_{1 \leqslant \ell \leqslant N_d} \{|h_{R_m D}^{(\ell,1)}|\} \right\}, \tag{5.4}$$

which may differ from the actual SNR $\gamma_{m^*} = \bar{\gamma} |h_{m^*}|^2$ during transmission time $t + \tau$ due to feedback delay. $\hat{h}_{m^*}$ and h_{m^*} are joint complex Gaussian distributions with

correlation coefficients $0 \leqslant \rho \leqslant 1$. When $\rho = 1$, then the channels are perfectly correlated and RS is based on the perfect CSI. On the other hand, when $\rho = 0$, the channels are perfectly uncorrelated and RS is equivalent to random selection of relays from decoding set $\mathcal{D}$.

The SINR of $R_{m^*} \to D$ link can be expressed as

$$\gamma_m = \frac{\gamma_{m^*}}{1 + \gamma_{I_2}}, \tag{5.5}$$

where $\gamma_{I_2} = \sum_{i=1}^{I_2} \mu_2 |g_i|^2$, μ_2 is the interference transmit SNR, and g_i is the channel coefficient of the ith CCI at D.

5.2 Performance Analysis

5.2.1 CDF of Intermediate Links

To evaluate overall RS MIMO NCC outage, we must compute the CDF of the SINR in the first hop ($S \to R$ links) and in the second hop ($R \to D$ links).

Lemma 5.1. *The CDF of γ_{nm} (5.1) and γ_m (5.5) are, respectively, given by*

$$F_{\gamma_{nm}}(\gamma) = \sum_{k=0}^{N_r} \frac{\binom{N_r}{k}(-1)^k}{\mu_1^{I_1}} \left(\frac{\bar{\gamma}\mu_1}{\bar{\gamma} + \gamma k \mu_1} \right)^{I_1} e^{-\frac{k\gamma}{\bar{\gamma}}}, \tag{5.6}$$

$$F_{\gamma_m}(\gamma) = 1 - \sum_{k=0}^{lN_d-1} \frac{\binom{lN_d-1}{k}(-1)^k lN_d}{1+k} \left(\frac{\bar{\gamma}(1+(1-\rho)k)}{(1+k)\mu_2\gamma + \bar{\gamma}(1+(1-\rho)k)} \right)^{I_2} e^{-\frac{(1+k)\gamma}{(1+(1-\rho)k)\bar{\gamma}}}. \tag{5.7}$$

Proof. We first proceed to determine the CDF of (5.1). The CDF of γ_{nm}^* in (5.1) is given by $F_{\gamma_{nm}^*}(\gamma) = (1 - e^{-\frac{\gamma}{\bar{\gamma}}})^{N_r}$. Applying binomial expansion, we have

$$F_{\gamma_{nm}^*}(\gamma) = \sum_{k=0}^{N_r} \binom{N_r}{k} (-1)^k e^{-\frac{k\gamma}{\bar{\gamma}}}. \tag{5.8}$$

On the other hand, the PDF of γ_{I_1} in (5.1) is given by

$$f_{\gamma_{I_1}}(y) = \frac{y^{I_1-1}}{\Gamma(I_1)\mu_1^{I_1}} e^{-\frac{y}{\mu_1}}, \tag{5.9}$$

where $\Gamma(\cdot)$ is the Gamma function.

The CDF of γ_{nm} can then be obtained as

$$F_{\gamma_{nm}}(\gamma) = \int_0^\infty F_{\gamma_{nm}^*}\big((1+y)\gamma\big) f_{\gamma_{I_1}}(y) dy. \tag{5.10}$$

Inserting (5.8) and (5.9) into (5.10), we have

$$F_{\gamma_{nm}}(\gamma) = \sum_{k=0}^{N_r} \frac{\binom{N_r}{k}(-1)^k}{\Gamma(I_1)\mu_1^{I_1}} e^{-\frac{\gamma k}{\bar{\gamma}}} \int_0^\infty e^{-\left(\frac{\gamma k}{\bar{\gamma}} + \frac{1}{\mu_1}\right)y} y^{I_1-1} dy. \tag{5.11}$$

Using $\int_0^\infty y^{\upsilon-1} e^{-\varphi y} dy = \varphi^{-\upsilon}\Gamma(\upsilon)$ [68], $F_{\gamma_{nm}}(\gamma)$ can be derived as (5.6).

Furthermore, the PDF of γ_{m^*} in (5.5) can be obtained by taking the average of the conditional PDF $f_{\gamma_{m^*}|\hat{\gamma}_{m^*}}(\gamma|\hat{\gamma})$ over the PDF of $\hat{\gamma}_{m^*}$. This can be written as

$$f_{\gamma_{m^*}}(\gamma) = \int_0^\infty f_{\gamma_{m^*}|\hat{\gamma}_{m^*}}(\gamma|\hat{\gamma}) f_{\hat{\gamma}_{m^*}}(\hat{\gamma}) d\hat{\gamma}. \tag{5.12}$$

The conditional PDF is given by [69]

$$f_{\gamma_{m^*}|\hat{\gamma}_{m^*}}(\gamma|\hat{\gamma}) = \frac{1}{(1-\rho)\bar{\gamma}} e^{-\frac{\rho\hat{\gamma}+\gamma}{(1-\rho)\bar{\gamma}}} \mathcal{I}_0\left(\frac{2\sqrt{\rho\gamma\hat{\gamma}}}{(1-\rho)\bar{\gamma}}\right), \tag{5.13}$$

where $\mathcal{I}_0(\cdot)$ is the zeroth-order modified Bessel function of the first kind. Furthermore, the CDF of $\hat{\gamma}_{m^*}$ is given by $F_{\hat{\gamma}_{m^*}}(\hat{\gamma}) = (1-e^{-\frac{\hat{\gamma}}{\bar{\gamma}}})^{lN_d}$. Thus, the PDF of $\hat{\gamma}_{m^*}$ can be written as

$$f_{\hat{\gamma}_{m^*}}(\hat{\gamma}) = \sum_{k=0}^{lN_d-1} \frac{\binom{lN_d-1}{k}(-1)^k lN_d}{\bar{\gamma}} e^{-\frac{(1+k)\hat{\gamma}}{\bar{\gamma}}}. \tag{5.14}$$

Substituting (5.13) and (5.14) into (5.12), we have

$$f_{\gamma_{m^*}}(\gamma) = \sum_{k=0}^{lN_d-1} \frac{\binom{lN_d-1}{k}(-1)^k lN_d}{(1-\rho)\bar{\gamma}^2} e^{-\frac{\gamma}{(1-\rho)\bar{\gamma}}} \int_0^\infty e^{-\upsilon\hat{\gamma}} \mathcal{I}_0(2\sqrt{\varphi\hat{\gamma}}) d\hat{\gamma}, \tag{5.15}$$

where $\upsilon = \frac{1+(1-\rho)k}{(1-\rho)\bar{\gamma}}$ and $\varphi = \frac{\rho\gamma}{(1-\rho)^2\bar{\gamma}^2}$. Finally, solving the integral by using $\int_0^\infty e^{-\upsilon x} \mathcal{I}_0(2\sqrt{\varphi x}) dx = \frac{1}{\upsilon} e^{\frac{\varphi}{\upsilon}}$ [68], $f_{\gamma_{m^*}}(\gamma)$ can be derived as

$$f_{\gamma_{m^*}}(\gamma) = \sum_{k=0}^{lN_d-1} \frac{\binom{lN_d-1}{k}(-1)^k lN_d}{(1+(1-\rho)k)\bar{\gamma}} e^{-\frac{(1+k)\gamma}{(1+(1-\rho)k)\bar{\gamma}}}. \tag{5.16}$$

From (5.16), the CDF of γ_{m^*} can be obtained as

$$F_{\gamma_{m^*}}(\gamma) = 1 - \sum_{k=0}^{lN_d-1} \frac{\binom{lN_d-1}{k}(-1)^k lN_d}{1+k} e^{-\frac{(1+k)\gamma}{(1+(1-\rho)k)\bar{\gamma}}}. \tag{5.17}$$

95

Therefore, $F_{\gamma_m}(\gamma)$ can be formulated as

$$F_{\gamma_m}(\gamma) = 1 - \frac{lN_d}{\Gamma(I_2)\mu_2^{I_2}} \sum_{k=0}^{lN_d-1} \frac{\binom{lN_d-1}{k}(-1)^k}{1+k}$$
$$\times e^{-\frac{(1+k)\gamma}{(1+(1-\rho)k)\bar{\gamma}}} \int_0^\infty y^{I_2-1} e^{-\frac{((1+k)\mu_2\gamma+\bar{\gamma}(1+(1-\rho)k))y}{\bar{\gamma}(1+(1-\rho)k)\mu_2}} \, dy. \tag{5.18}$$

Solving the integral in (5.18), one can obtain (5.7). This completes the proof. $\quad\square$

5.2.2 Overall Outage Probability

The probability that l relays succeed to recover all sources' messages can be written as

$$\mathsf{Pr}\{|\mathcal{D}| = l\} = \binom{M}{l} \mathsf{P}_s^l (1 - \mathsf{P}_s)^{M-l}, \tag{5.19}$$

where $\mathsf{P}_s = \left(1 - F_{\gamma_{nm}}(\gamma_{th})\right)^N$.

Also, the probability that ζ relays (out of L selected relays) are not in outage given that $|\mathcal{D}| = l$ is computed as

$$\mathsf{Pr}\{|\mathcal{E}| = \zeta|l\} = \binom{L}{\zeta} \left(F_{\gamma_m}(\gamma_{th})\right)^{L-\zeta} \left(1 - F_{\gamma_m}(\gamma_{th})\right)^\zeta. \tag{5.20}$$

In NCC, at least N successful transmissions are required. Since direct source-destination links are not available, the number of selected relays L must be at least equal to the number of sources N i.e., $N \leqslant L$. An outage occurs if fewer than N network-coded packets are received by the destination. The overall OP can then be obtained using the law of total probability and is given by

$$\mathcal{P}_{\mathrm{out}} = \sum_{l=0}^M \sum_{\zeta=0}^{N-1} \mathsf{Pr}\{|\mathcal{E}| = \zeta|l\} \mathsf{Pr}\{|\mathcal{D}| = l\}. \tag{5.21}$$

5.2.3 Asymptotic Analysis

Although the OP expression in (5.21) is exact, direct insights into the effect of the feedback delays and CCI on the system performance are desirable. In this subsection, we thus derive the asymptotic outage expression.

Theorem 5.1. *For perfect CSI ($\rho = 1$), the diversity order G_{d_1} and the coding gain $\mathcal{C}_1$ are, respectively, given by*

$$G_{d_1} = M\min\{N_r, (L-N+1)N_d\}, \tag{5.22}$$

$$\mathcal{C}_1 = \begin{cases} \dfrac{\varpi_1^{(1)\,-\frac{1}{MN_r}}}{\gamma_{th}} & L-N+1 > \dfrac{N_r}{N_d} \\[3ex] \dfrac{\varpi_1^{(2)\,-\frac{1}{M(L-N+1)N_d}}}{\gamma_{th}} & L-N+1 < \dfrac{N_r}{N_d} \\[3ex] \dfrac{\varpi_1^{(3)\,-\frac{1}{MN_r}}}{\gamma_{th}} & L-N+1 = \dfrac{N_r}{N_d} \end{cases} \tag{5.23}$$

in which $\varpi_1^{(1)} = (N\mathcal{H}_1(N_r))^M$, $\varpi_1^{(2)} = \binom{L}{N-1}(\mathcal{H}_2(MN_d))^{L-N+1}$, $\varpi_1^{(3)} = (N\mathcal{H}_1(N_r))^M + \sum_{l=1}^{M}\binom{M}{l}(N\mathcal{H}_1(N_r))^{M-l}\binom{L}{N-1}(\mathcal{H}_2(lN_d))^{L-N+1}$, *and*

$$\mathcal{H}_i(a) = \sum_{k=0}^{a} \frac{\binom{a}{k}\mu_i^k\Gamma(I_i+k)}{\Gamma(I_i)}. \tag{5.24}$$

Further, for outdated CSI ($\rho \neq 1$), we have

$$G_{d_2} = \min\{MN_r, L-N+1\}, \tag{5.25}$$

$$\mathcal{C}_2 = \begin{cases} \dfrac{\varpi_2^{(1)\,-\frac{1}{MN_r}}}{\gamma_{th}} & L-N+1 > MN_r \\[3ex] \dfrac{\varpi_2^{(2)\,-\frac{1}{L-N+1}}}{\gamma_{th}} & L-N+1 < MN_r \\[3ex] \dfrac{\left(\varpi_2^{(1)}+\varpi_2^{(2)}\right)^{-\frac{1}{L-N+1}}}{\gamma_{th}} & L-N+1 = MN_r \end{cases} \tag{5.26}$$

with $\varpi_2^{(1)} = (N\mathcal{H}_1(N_r))^M$, $\varpi_2^{(2)} = \binom{L}{N-1}\mathcal{T}^{L-N+1}$, *and*

$$\mathcal{T} = \sum_{k=0}^{MN_d-1} \frac{MN_d\left(\Gamma(I_2)+\mu_2\Gamma(I_2+1)\right)\binom{MN_d-1}{k}(-1)^k}{\left(1+(1-\rho)k\right)\Gamma(I_2)}. \tag{5.27}$$

Proof. In high-SNR regime i.e., $\bar{\gamma} \to \infty$, we have $F_{\gamma_{nm}^*}^{\infty}(\gamma_{th}) = (\gamma_{th}/\bar{\gamma})^{N_r}$. Then by substituting this expression and (5.9) into (5.10), we have

$$F_{\gamma_{nm}}^{\infty}(\gamma_{th}) = \int_0^{\infty} \frac{\gamma_{th}^{N_r}(1+y)^{N_r}y^{I_1-1}}{\bar{\gamma}^{N_r}\Gamma(I_1)\mu_1^{I_1}}e^{\frac{-y}{\mu_1}}\,dy. \tag{5.28}$$

Finally, by performing binomial expansion and solving the integral, we obtain

$$F_{\gamma_{nm}}^{\infty}(\gamma_{th}) = \sum_{k=0}^{N_r} \frac{\binom{N_r}{k}\mu_1^k\Gamma(I_1+k)}{\Gamma(I_1)}\left(\frac{\gamma_{th}}{\bar{\gamma}}\right)^{N_r}. \tag{5.29}$$

Similarly, the asymptotic expression for $F_{\gamma_m}(\gamma_{th})$ when $\rho = 1$ can be derived as

$$F_{\gamma_m}^{\infty}(\gamma_{th}) = \sum_{k=0}^{lN_d} \frac{\binom{lN_d}{k}\mu_2^k\Gamma(I_2+k)}{\Gamma(I_2)} \left(\frac{\gamma_{th}}{\bar{\gamma}}\right)^{lN_d}. \tag{5.30}$$

on the other hand, when $\rho \neq 1$, $F_{\gamma_{m^*}}^{\infty}(\gamma_{th})$ can be well approximated as

$$F_{\gamma_{m^*}}^{\infty}(\gamma_{th}) = \sum_{k=0}^{lN_d-1} \frac{\binom{lN_d-1}{k}(-1)^k lN_d}{1+(1-\rho)k} \left(\frac{\gamma_{th}}{\bar{\gamma}}\right). \tag{5.31}$$

Using (5.31), we obtain

$$F_{\gamma_m}^{\infty}(\gamma_{th}) = lN_d \left(\Gamma(I_2) + \mu_2\Gamma(I_2+1)\right) \sum_{k=0}^{lN_d-1} \frac{\binom{lN_d-1}{k}(-1)^k}{(1+(1-\rho)k)\Gamma(I_2)} \left(\frac{\gamma_{th}}{\bar{\gamma}}\right). \tag{5.32}$$

Plugging these expressions in (5.21) and considering the dominant terms, one can obtain the diversity order and coding gain. □

5.2.4 Remarks and Guidelines

The following remarks can be drawn from (5.22) and (5.23):

Remark 5.1. *The maximum achievable diversity is given by (5.22). It is either equal to MN_r or $M(L-N+1)N_d$. If $L-N+1 > N_r/N_d$, then the diversity is determined by $G_{d_1} = MN_r$ which is a function of M and N_r and is independent of other system parameters N, L, N_d. This implies that adding more antennas at the destination N_d, and selecting more relays L not only do not change the diversity but also increase the complexity and decrease the system throughput. On the other hand, if $L-N+1 < N_r/N_d$, then the diversity is given by $G_{d_1} = M(L-N+1)N_d$ which is a function of all system parameters except the number of antennas at relays N_r. Here, increasing the number of sources N decreases the diversity.*

Remark 5.2. *The optimal number of selected relays that maximizes the achievable diversity is a function of N_r, N_d, and N and is equal to (5.33). It can be seen that L_{opt_1} is inversely proportional to N_d. Therefore, by adding more antennas at the destination (i.e., increasing the complexity), the number of relays to be selected for achieving the*

maximum diversity can be decreased (i.e., reducing the relay transmissions). This clearly shows a trade-off between the system complexity and system throughput.

$$L_{\text{opt}_1} = \lceil \tfrac{N_r}{N_d} + N - 1 \rceil. \tag{5.33}$$

Remark 5.3. *In our proposed system model, the relay uses only one transmit antenna for data transmission. TAS, which maximizes the relay-destination SNR, can also be employed at the relays. If TAS is used, then the diversity in (5.22) changes to*

$$G_d^{\text{TAS}} = M\min\{N_r, (L-N+1)N_rN_d\} = MN_r. \tag{5.34}$$

Thus, TAS improves the diversity only when $L - N + 1 < N_r/N_d$. However, when $L - N + 1 > N_r/N_d$, the system with TAS provides coding gain without diversity advantages.

Remark 5.4. *Although CCI does not impact diversity order (for fixed interference powers), it degrades the coding gain. When $L - N + 1 > N_r/N_d$, the system parameters of the first hop (i.e., N_r, I_1, μ_1) impact the coding gain. When $L - N + 1 < N_r/N_d$, the coding gain is determined by N_d, I_2 and μ_2. For $L - N + 1 = N_r/N_d$, the coding gain is affected by the system parameters associated with both hops.*

Remark 5.5. *For single-antenna NCC i.e., when $N_d = N_r = 1$, the diversity in (5.22) is reduced to $G_{d_1} = M$. Thus, the proposed RS strategy increases the diversity from $M - N + 1$ (earlier reported in [18]) to M. Based on (5.33), the optimal number of relays to be selected is $L_{\text{opt}_1} = N$.*

On the other hand, from (5.25) and (5.26), we have the following remarks:

Remark 5.6. *Outdated CSI degrades diversity order from G_{d_1} (5.22) to G_{d_2} (5.25). Thus, if ρ is not equal to one, the diversity is independent of number of antennas at the destination. Further, if TAS is used at the relays, the diversity does not change and is equal to (5.25), meaning that in the case of outdated CSI, TAS does not provide any diversity advantages. Also, the optimal number of selected relays that maximizes the diversity is*

$$L_{\text{opt}_2} = MN_r + N - 1. \tag{5.35}$$

Remark 5.7. *The coding gain is determined by the system parameters in the first hop, second hop, and both hops when* $L - N + 1 > MN_r$, $L - N + 1 < MN_r$, *and* $L - N + 1 = MN_r$, *respectively.*

5.3   Numerical Results and Discussions

In this section, we present Monte-Carlo simulations to validate the derived analytical expressions. Unless otherwise stated, we assume $N = 5$, $I_1 = 2$, $I_2 = 3$, $\mu_1 = 0$ dB, $\mu_2 = 0$ dB and $\gamma_{th} = 0$ dB.

Fig. 5.1 depicts the outage and asymptotic curves for different values of ρ and L when $M = 4$, $N_r = 3$, and $N_d = 2$. It can be readily checked that when $\rho = 1$ the optimal number of relays to be selected is $L_{\mathrm{opt}_1} = 6$ (5.33). Therefore, as L increases from five to six the diversity increases from $G_{d_1} = M(L - N + 1)N_d = 8$ to its maximum value $G_{d_1} = MN_r = 12$. However, the diversity for $L = 7$ is identical to that of $L_{\mathrm{opt}_1} = 6$. This implies that selecting more than L_{opt_1} relays does not increase the diversity, confirming the statements in Remark 5.2. Also, the slope of the asymptotic curves reveals that for $\rho = 0.8$ the diversity significantly reduces to $G_{d_2} = L - N + 1$ (5.25) and is equal to one, two, and three for $L = 5$, 6, and 7.

Fig. 5.2 illustrates the effect of CCI on the OP of RS MIMO NCC, assuming different values of N_d and μ_1 when $M = 4$, $L = 5$, $N_r = 3$, and $\rho = 1$. As can be seen, CCI degrades the coding gain, rather than the diversity. Also, when $N_d = 2$ (which satisfies $L - N + 1 < N_r/N_d$), the value of μ_1 does not change the system performance as $\bar{\gamma} \to \infty$ and the curve corresponding to $\mu_1 = 5$ dB converges to that of $\mu_1 = 0$ dB, confirming Remark 5.4.

Fig. 5.3 compares the outage performance of RS MIMO NCC with TAS and without TAS (SIMO) at the relays when $M = 3$, $L = 6$, $N_d = 2$, $N_r = 3$, 5, and $\rho = 1$. It is observed that TAS improves the diversity from $G_{d_1} = M(L - N + 1)N_d = 12$ (5.22) to $G_d^{\mathrm{TAS}} = MN_r = 15$ (5.34) when $N_r = 5$ ($L - N + 1 < N_r/N_d$). When $N_r = 3$ ($L - N + 1 > N_r/N_d$), however, TAS provides the diversity of nine which is identical to that of without TAS. This confirms the statements in Remark 5.3.
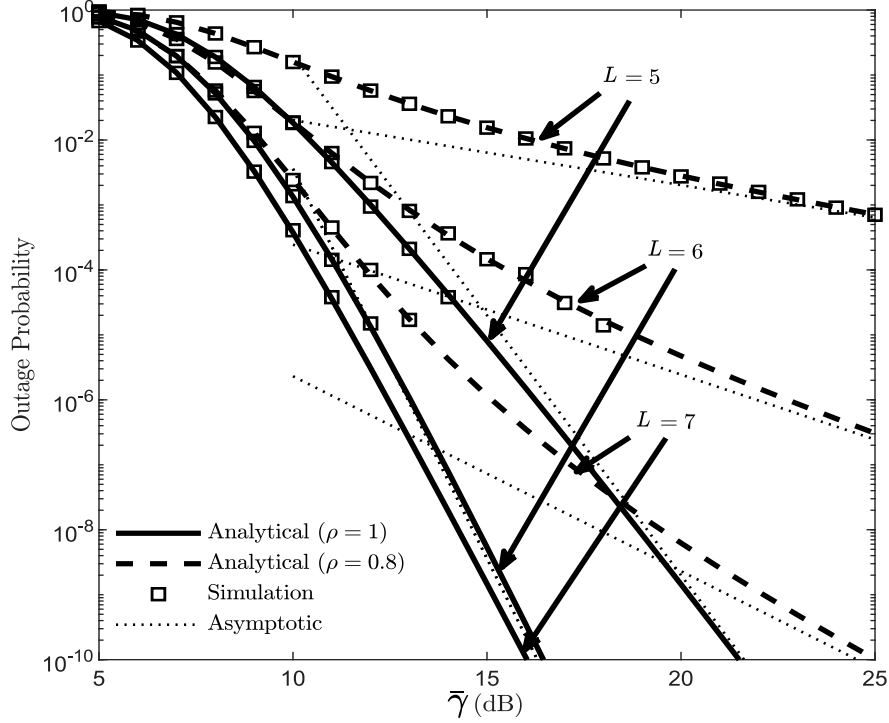
Fig. 5.1: OP versus $\bar{\gamma}$ for different values of ρ and L when $M = 4$, $N_r = 3$, and $N_d = 2$.

5.4   Conclusions

We proposed a RS MIMO NCC which provides most of the MIMO benefits while employing only one transmit/receive chain at the relays and destination. Our analysis revealed that RS MIMO NCC incurs substantial performance losses with outdated CSI and CCI. These had not been analyzed before. Several design guidelines for practical RS MIMO NCC systems were provided. A future research area is to study the performance of RS MIMO NCC with other antenna strategies.
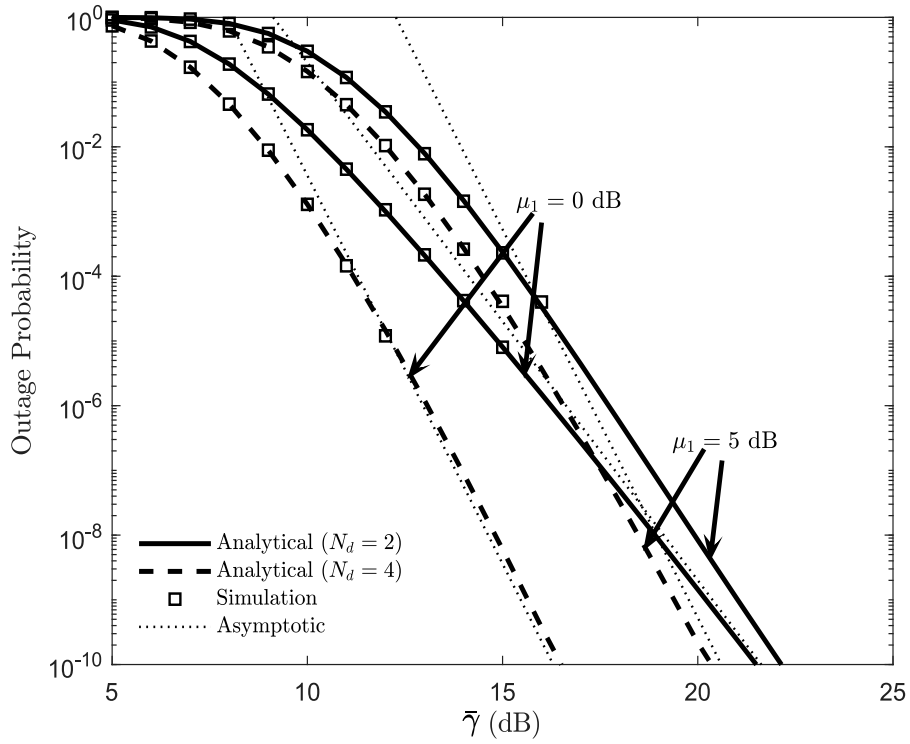
Fig. 5.2: OP versus $\bar{\gamma}$ for different values of N_d and μ_1 when $M = 4$, $L = 5$, $N_r = 3$, and $\rho = 1$.
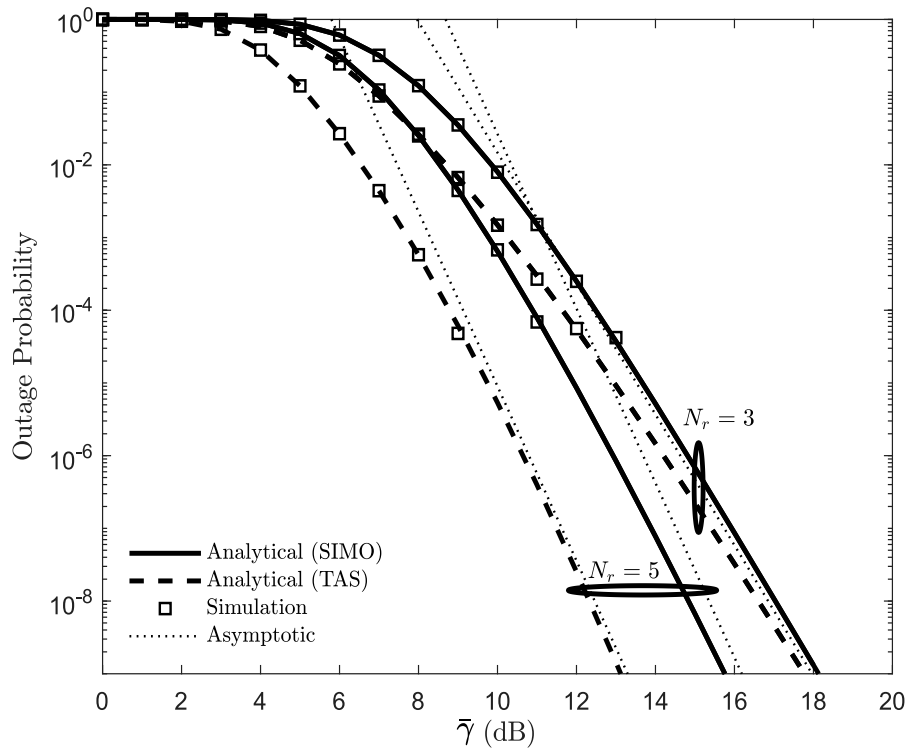
Fig. 5.3: Comparison between SIMO/SC and TAS/SC when $M = 3$, $L = 6$, $N_d = 2$, $N_r = 3, 5$, and $\rho = 1$.

Chapter 6

Summary and Future Work

In this chapter, we first highlight the important contributions discussed in the thesis, and then, we describe possible research directions for future work.

6.1   Summary

Relaying technology is an effective means to improve the spectral and power efficiency of wireless communications. In conventional CC systems, relays forward the sources' packets to the destination with no combining operation. This method becomes prohibitive as the size of the network grows. By combining multiple sources' packets into one packet algebraically at the relays, before forwarding to the destination, NCC exploits the benefits of NC in CC systems and provides excellent advantages in offering high system throughput and reliability.

In this thesis, we proposed and analyzed new transmission strategies for NCC networks. Our goal was to exploit the diversity gains available among distributed single-antenna and/or multiple-antenna terminals in NCC systems and study NCC performance under practical implementation issues.

In Chapter 2, we proposed MUD-based NCC to exploit both MUD and CD in a multiuser multirelay NCC system. We studied the most GURS scheme in the literature where the destination selects K (out of N) users, the i_1^{th}, i_2^{th}, ..., i_K^{th} best users, and L (out of M) relays, the j_1^{th}, j_2^{th},..., j_L^{th} best relays, subject to practical constraints

such as load balancing conditions and scheduling policy. Our analytical results and design guidelines generalize and subsume all existing results as special cases. To this end, we derived a new closed-form OP expression, assuming i.n.i.d. Rayleigh fading channels. The asymptotic outage expression at high-SNR regime was further derived, based on which, the achievable diversity order and coding gain were quantified. Our results revealed that if $K > L$, $G_{d_1} = N - i_{K-1} + 1$, and the set of selected relays does not include the lowest-SNR relay i.e., $j_L \neq M$, the coding gain of any arbitrary RS is identical to that of the best RS. On the other hand, when $K \leq L$ and the RSs include K highest-SNR relays, GURS NCC has the minimum diversity of $G_{d_2} = M + 1$ when the lowest-SNR user is in the sets of selected users i.e., $i_K = N$. Similarly, the worst RS has the minimum diversity of $G_{d_2}^{\min} = L + 1$ if $i_K = N$. Our results clearly provide useful design insights and guidelines for practical cooperative systems with user-relay selection protocols.

In Chapter 3, we studied the performance of an underlay cognitive NCC. In particular, we assumed that the PN consists of a single transmitter-receiver pair, while the SN NCC is composed of N sources, a single destination, and M DF relays. In this light, we derived the exact and asymptotic OP expressions of the SN over i.n.i.d. Nakagami-m fading channels, assuming maximum transmit power at the SN, S2P and P2S interference links. Based on the asymptotic OP expression, the SN diversity order was further quantified. We observed that the diversity is independent of Q (when $Q = \mu\rho$) and the fading severity parameters $\{m_{\alpha_i}\}_{i=1}^N$, $\{m_{\alpha_j}\}_{j=1}^M$, $\{m_{v_j}\}_{j=1}^M$, and m_{v_0}. On there other hand, the diversity is a function of N, M, L, and the fading severity parameters in the SN $\{m_{f_i}\}_{i=1}^N$ and $\{m_j\}_{j=1}^M$. Further, when Q is fixed, an error floor occurs, leading to a diversity order of zero. Our analysis can be applied to many network settings, and more importantly, subsumes the case of generalized channels, ranging from i.i.d. Rayleigh fading to i.n.i.d. Nakagami-m fading.

NCC has been studied for single-antenna terminals only. Employing MIMO techniques can significantly improve the performance of NCC systems. Furthermore, the existing RS strategies for NCC utilize the "*max-min*" E2E criterion. This selection strategy (called Strategy $\mathcal{A}$) is complicated even for a network with single-antenna

terminals as it requires global CSI. This requirement makes it hard to implement RS-based NCC. To counter this issue, in Chapter 4, we introduced a new RS strategy (Strategy $\mathcal{B}$), which utilizes only the local CSI (not global CSI), reducing the signaling overhead significantly without sacrificing the performance. The performance of MIMO NCC under Strategy $\mathcal{A}$ and $\mathcal{B}$ was studied over i.n.i.d. Rayleigh fading channels. We assumed that the relays and the destination are equipped with multiple antennas, whereas sources have single antenna. The exact OP expressions of the system under consideration were derived. The asymptotic outage expressions were further provided to obtain valuable insights into the practical system-design parameters such as the diversity order and coding gain. Our results showed that, RS Strategy $\mathcal{B}_2$ is capable of achieving diversity order similar to Strategy $\mathcal{A}$. Furthermore, although the outage expressions for RS Strategy $\mathcal{A}$ and $\mathcal{B}_2$ are completely different, the OP values are exactly the same for all SNR regime. Therefore, the proposed RS strategy has the same outage performance as that of RS $\mathcal{A}$, while it significantly reduces signaling overhead. Further, we showed that the diversity order of RS MIMO NCC is unpredictable and highly dependent on the system configuration. In particular, our results interestingly demonstrated that increasing the number of relays and the number of antennas at relays does not necessarily improve the diversity order. Further, in contrast to single-antenna RS NCC system, increasing the number of sources may decrease the diversity order of the RS MIMO NCC for some values of system parameters.

In Chapter 5, we studied the effect of outdated CSI and CCI on the performance of RS MIMO NCC systems. Specifically, we considered a RS MIMO NCC system where N single-antenna sources communicate with one multiple-antenna destination using M DF multiple-antenna relays. The destination selects L best relays according to the quality of relay-destination channels. The exact closed-form OP of the system was derived. The asymptotic high-SNR OP was also obtained, through which the diversity order and the coding gain were found. Our results revealed that outdated CSI significantly decreases the diversity order, while CCI degrades the coding gain.

6.2 Future Work

In the following, we provide some future research problems which can be considered as the extension of this work.

6.2.1 Millimeter-Wave

5G wireless communication systems use two main frequency bands, namely the traditional sub-6 GHz band (< 6 GHz) and millimeter-wave (mm-wave) band (30-300 GHz). This thesis considered sub-6 GHz 5G and assumed Rayleigh/Nakagam-m fading channels to model multipath fading environments. Therefore, our analyses cannot be directly applied to the mm-wave band due to poor scattering propagation and mm-wave signals' significant attenuation. Investigating the performance of NCC systems in mm-wave networks will be interesting future work.

6.2.2 Energy Harvesting

Energy harvesting (EH) has been envisioned as a promising technique to prolong the lifetime of energy-limited wireless networks. Simultaneous wireless information and power transfer (SWIPT) is a new emerging EH technology that enables the usage of ambient radio frequency (RF) signals [70–72]. The basic premise of SWIPT is that the wireless devices and relays in wireless relay networks can harvest energy and decode information from their received observations simultaneously. On the other hand, NCC is a promising approach to improve the spectral efficiency of relay networks. Thus, the common use of NCC and SWIPT in relay networks offers an efficient way in terms of both energy and spectral efficiency and hence is an exciting research direction.

6.2.3 Non-Orthogonal Multiple Access

Non-orthogonal multiple access (NOMA) has emerged as a key enabling multiple access technology for 5G and beyond [73–75]. Unlike orthogonal multiple access (OMA) techniques, where communication resources (frequency, time, or code) are allocated to different users orthogonally, NOMA serves multiple users simultaneously to

share the same resource block, hence dramatically improves the network capacity and outperforms conventional OMA schemes. The hybrid of NOMA and NCC offers a great potential to meet massive connectivity, low latency, and high throughput requirements of the next-generation wireless networks. Thus, integrating NOMA with NCC may reap further gains and is a crucial future research topic.

Bibliography

[1] K. Sultan, "Best relay selection schemes for NOMA based cognitive relay networks in underlay spectrum sharing," *IEEE Access*, vol. 8, pp. 190 160–190 172, 2020.

[2] L. Zhu, Z. Xiao, X. Xia, and D. Oliver Wu, "Millimeter-wave communications with non-orthogonal multiple access for B5G/6G," *IEEE Access*, vol. 7, pp. 116 123–116 132, 2019.

[3] M. Series, "IMT vision–framework and overall objectives of the future development of IMT for 2020 and beyond," Tech. Rep. Recommendation ITU-R M.2083-0, 2015.

[4] K. B. Letaief, W. Chen, Y. Shi, J. Zhang, and Y. A. Zhang, "The roadmap to 6G: AI empowered wireless networks," *IEEE Commun. Mag.*, vol. 57, no. 8, pp. 84–90, 2019.

[5] J. N. Laneman, D. N. C. Tse, and G. W. Wornell, "Cooperative diversity in wireless networks: Efficient protocols and outage behavior," *IEEE Trans. Inf. Theory*, vol. 50, no. 12, pp. 3062–3080, Dec. 2004.

[6] J. N. Laneman and G. W. Wornell, "Distributed space-time-coded protocols for exploiting cooperative diversity in wireless networks," *IEEE Trans. Inf. Theory*, vol. 49, no. 10, pp. 2415–2425, Oct. 2003.

[7] Q. Li, R. Q. Hu, Y. Qian, and G. Wu, "Cooperative communications for wireless networks: techniques and applications in LTE-advanced systems," *IEEE Wireless Commun.*, vol. 19, no. 2, pp. 22–29, Apr. 2012.

[8] F. Boccardi, R. W. Heath, A. Lozano, T. L. Marzetta, and P. Popovski, "Five disruptive technology directions for 5G," *IEEE Commun. Mag.*, vol. 52, no. 2, pp. 74–80, Feb. 2014.

[9] R. Ahlswede, N. Cai, S. Y. R. Li, and R. W. Yeung, "Network information flow," *IEEE Trans. Inf. Theory*, vol. 46, no. 4, pp. 1204–1216, Jul. 2000.

[10] Y. Chen, S. Kishore, and J. Li, "Wireless diversity through network coding," in *Proc. IEEE Wireless Commun. and Network. Conf. (WCNC)*, vol. 3, 2006, pp. 1681–1686.

[11] M. Yu, J. Li, and R. S. Blum, "User cooperation through network coding," in *Proc. IEEE Int. Conf. on Commun. (ICC)*, 2007, pp. 4064–4069.

[12] Z. Ding and K. K. Leung, "On the combination of cooperative diversity and network coding for wireless uplink transmissions," *IEEE Trans. Veh. Technol.*, vol. 60, no. 4, pp. 1590–1601, May 2011.

[13] S. Katti, H. Rahul, W. Hu, D. Katabi, M. Medard, and J. Crowcroft, "XORs in the air: Practical wireless network coding," *EEE/ACM Transactions on Networking*, vol. 16, no. 3, pp. 497–510, Jun. 2008.

[14] S. Katti, S. Gollakota, , and D. Katabi, "Embracing wireless interference: Analog network coding," in *Proc. ACM SIGCOMM*, 2007, pp. 397–408.

[15] L. Song, G. Hong, B. Jiao, and M. Debbah, "Joint relay selection and analog network coding using differential modulation in two-way relay channels," *IEEE Trans. Veh. Technol.*, vol. 59, no. 6, pp. 2932–2939, Jul 2010.

[16] Z. Li, X. . Xia, and B. Li, "Achieving full diversity and fast ML decoding via simple analog network coding for asynchronous two-way relay networks," *IEEE Trans. on Commun.*, vol. 57, no. 12, pp. 3672–3681, Dec. 2009.

[17] P. K. Upadhyay and S. Prakriya, "Performance of analog network coding with asymmetric traffic requirements," *IEEE Commun. Lett.*, vol. 15, no. 6, pp. 647–649, Jun. 2011.

[18] M. Xiao, J. Kliewer, and M. Skoglund, "Design of network codes for multiple-user multiple-relay wireless networks," *IEEE Trans. Commun.*, vol. 60, no. 12, pp. 3755–3766, Dec. 2012.

[19] D. Tse and P. Viswanath, *Fundamentals of Wireless Communication*, 2005.

[20] H. Topakkaya and Z. Wang, "Wireless network code design and performance analysis using diversity-multiplexing tradeoff," *IEEE Trans. Commun.*, vol. 59, no. 2, pp. 488–496, Feb. 2011.

[21] A. Bletsas, A. Khisti, D. P. Reed, and A. Lippman, "A simple cooperative diversity method based on network path selection," *IEEE J. Sel. Areas Commun.*, vol. 24, no. 3, pp. 659–672, Mar. 2006.

[22] A. R. Heidarpour, G. K. Kurt, and M. Uysal, "Finite-SNR DMT analysis for multisource multirelay NCC systems with imperfect CSI," in *Proc. IEEE 84th Veh. Technol. Conf. (VTC-Fall)*, Sept. 2016, pp. 1–5.

[23] ——, "Finite-SNR diversity-multiplexing tradeoff for network coded cooperative OFDMA systems," *IEEE Trans. Wireless Commun.*, vol. 16, no. 3, pp. 1385–1396, Mar. 2017.

[24] Z. C. Pereira, T. H. Ton, J. L. Rebelatto, R. D. Souza, and B. F. Uchôa-Filho, "Generalized network-coded cooperation in OFDMA communications," *IEEE Access*, vol. 6, pp. 6550–6559, 2018.

[25] A. R. Heidarpour, G. K. Kurt, and M. Uysal, "On the performance of NCC-OFDMA systems in the presence of carrier frequency offset," in *Proc. IEEE Int. Conf. on Commun. (ICC)*, May 2017, pp. 1–6.

[26] M. D. Renzo, M. Iezzi, and F. Graziosi, "On diversity order and coding gain of multisource multirelay cooperative wireless networks with binary network coding," *IEEE Trans. Veh. Technol.*, vol. 62, no. 3, pp. 1138–1157, Mar. 2013.

[27] ——, "Error performance and diversity analysis of multi-source multi-relay wireless networks with binary network coding and cooperative MRC," *IEEE Trans. Wireless Commun.*, vol. 12, no. 6, pp. 2883–2903, 2013.

[28] C. Peng, Q. Zhang, M. Zhao, Y. Yao, and W. Jia, "On the performance analysis of network-coded cooperation in wireless networks," *IEEE Trans. Wireless Commun.*, vol. 7, no. 8, pp. 3090–3097, Aug. 2008.

[29] M. D. Renzo, "On the achievable diversity of repetition-based and relay selection network-coded cooperation," *IEEE Trans. Commun.*, vol. 62, no. 7, pp. 2296–2313, Jul. 2014.

[30] T. X. Vu, P. Duhamel, and M. D. Renzo, "On the diversity of network-coded cooperation with decode-and-forward relay selection," *IEEE Trans. Wireless Commun.*, vol. 14, no. 8, pp. 4369–4378, Aug. 2015.

[31] E. Beres and R. Adve, "Selection cooperation in multi-source cooperative networks," *IEEE Trans. on Wireless Commun.*, vol. 7, no. 1, pp. 118–127, Jan. 2008.

[32] H. Ding, J. Ge, D. B. da Costa, and Z. Jiang, "A new efficient low-complexity scheme for multi-source multi-relay cooperative networks," *IEEE Trans. Veh. Technol.*, vol. 60, no. 2, pp. 716–722, Feb. 2011.

[33] L. Sun, T. Zhang, L. Lu, and H. Niu, "On the combination of cooperative diversity and multiuser diversity in multi-source multi-relay wireless networks," *IEEE Signal Process. Lett.*, vol. 17, no. 6, pp. 535–538, Jun. 2010.

[34] S. Chen, W. Wang, and X. Zhang, "Performance analysis of multiuser diversity in cooperative multi-relay networks under Rayleigh-fading channels," *IEEE Trans. Wireless Commun.*, vol. 8, no. 7, pp. 3415–3419, Jul. 2009.

[35] A. R. Heidarpour, M. Ardakani, and C. Tellambura, "Multiuser diversity in network-coded cooperation: Outage and diversity analysis," *IEEE Commun. Lett.*, vol. 23, no. 3, pp. 550–553, Mar. 2019.

[36] A. R. Heidarpour, M. Ardakani, and C. Tellambura, "Opportunistic scheduling in network-coded cooperative systems," in *Proc. IEEE 30th Annual International Symposium on Personal, Indoor and Mobile Radio Communications (PIMRC)*, sept. 2019, pp. 1–6.

[37] L. Fan, X. Lei, P. Fan, and R. Q. Hu, "Outage probability analysis and power allocation for two-way relay networks with user selection and outdated channel state information," *IEEE Comm. Lett.*, vol. 16, no. 5, pp. 638–641, May 2012.

[38] P. K. Sharma and P. K. Upadhyay, "Performance analysis of cooperative spectrum sharing with multiuser two-way relaying over fading channels," *IEEE Trans. Veh. Technol.*, vol. 66, no. 2, pp. 1324–1333, Feb. 2017.

[39] A. M. Salhab and S. A. Zummo, "Multiuser cognitive networks with Nth-best user selection and imperfect channel estimation," *Arab. J. Sci. Eng.*, vol. 39, no. 12, p. 8979–8987, Dec. 2014.

[40] S. S. Ikki and M. H. Ahmed, "On the performance of cooperative-diversity networks with the Nth best-relay selection scheme," *IEEE Trans. Commun*, vol. 58, no. 11, pp. 3062–3069, Nov. 2010.

[41] L. Yang, K. Qaraqe, E. Serpedin, and X. Gao, "Performance analysis of two-way relaying networks with the Nth worst relay selection over various fading channels," *IEEE Trans. Veh. Technol.*, vol. 64, no. 7, pp. 3321–3327, Jul. 2015.

[42] S.-I. Chu, "SER and PER performance of packet decode-and-forward relaying with generalized order selection combining," *IEEE Wireless Commun. Lett.*, vol. 3, no. 5, pp. 449–452, Oct. 2014.

[43] A. R. Heidarpour, M. Ardakani, C. Tellambura, M. Di Renzo, and M. Uysal, "Network-coded cooperative systems with generalized user-relay selection," *IEEE Trans. Wireless Commun.*, vol. 19, no. 11, pp. 7251–7264, Nov. 2020.

[44] A. R. Heidarpour, M. Ardakani, C. Tellambura, and M. Di Renzo, "Generalized user-relay selection in network-coded cooperation systems," in *Proc. IEEE Int. Conf. on Commun. (ICC)*, May 2019, pp. 1–6.

[45] A. Goldsmith, S. A. Jafar, I. Maric, and S. Srinivasa, "Breaking spectrum gridlock with cognitive radios: An information theoretic perspective," *Proc. IEEE*, vol. 97, no. 5, pp. 894–914, May 2009.

[46] L. Luo, P. Zhang, G. Zhang, and J. Qin, "Outage performance for cognitive relay networks with underlay spectrum sharing," *IEEE Commun. Lett.*, vol. 15, no. 7, pp. 710–712, 2011.

[47] X. Zhang, Y. Zhang, Z. Yan, J. Xing, and W. Wang, "Performance analysis of cognitive relay networks over Nakagami-*m* fading channels," *IEEE J. Sel. Areas Commun.*, vol. 33, no. 5, pp. 865–877, 2015.

[48] W. Xu, J. Zhang, P. Zhang, and C. Tellambura, "Outage probability of decode-and-forward cognitive relay in presence of primary user's interference," *IEEE Commun. Lett.*, vol. 16, no. 8, pp. 1252–1255, 2012.

[49] V. N. Q. Bao, T. Q. Duong, and C. Tellambura, "On the performance of cognitive underlay multihop networks with imperfect channel state information," *IEEE Trans. Commun.*, vol. 61, no. 12, pp. 4864–4873, 2013.

[50] Y. J. Chun, M. O. Hasna, and A. Ghrayeb, "Adaptive network coding for spectrum sharing systems," *IEEE Trans. Wireless Commun.*, vol. 14, no. 2, pp. 639–654, Feb. 2015.

[51] R. Bordón, S. Montejo Sánchez, S. Baraldi Mafra, R. Demo Souza, J. L. Rebelatto, and E. M. Garcia Fernandez, "Energy efficient power allocation schemes for a two-user network-coded cooperative cognitive radio network," *IEEE Trans. Signal Process.*, vol. 64, no. 7, pp. 1654–1667, Apr. 2016.

[52] S. Mafra, R. Souza, J. Rebelatto, G. Brante, and O. Rayel, "Outage performance of a network coding aided multi-user cooperative secondary network," *Trans. Emerg. Telecommun. Technol*, vol. 28, no. 2, p. e2943, May 2017.

[53] W. Liang, H. V. Nguyen, S. X. Ng, and L. Hanzo, "Adaptive-TTCM-aided near-instantaneously adaptive dynamic network coding for cooperative cognitive radio networks," *IEEE Trans. Veh. Technol.*, vol. 65, no. 3, pp. 1314–1325, Mar. 2016.

[54] G. Amarasuriya, C. Tellambura, and M. Ardakani, "Two-way amplify-and-forward multiple-input multiple-output relay networks with antenna selection," *IEEE J. Sel. Areas Commun.*, vol. 30, no. 8, pp. 1513–1529, Sept. 2012.

[55] A. Adinoyi and H. Yanikomeroglu, "Cooperative relaying in multi-antenna fixed relay networks," *IEEE Trans. Wireless Commun.*, vol. 6, no. 2, pp. 533–544, Feb. 2007.

[56] G. Amarasuriya, C. Tellambura, and M. Ardakani, "Performance analysis framework for transmit antenna selection strategies of cooperative MIMO AF relay networks," *IEEE Trans. Veh. Technol.*, vol. 60, no. 7, pp. 3030–3044, Sept. 2011.

[57] H. A. Suraweera, G. K. Karagiannidis, Y. Li, H. K. Garg, A. Nallanathan, and B. Vucetic, "Amplify-and-forward relay transmission with end-to-end antenna selection," in *Proc. IEEE Wireless Commun. and Network. Conf. (WCNC)*, Apr. 2010, pp. 1–6.

[58] A. R. Heidarpour, M. Ardakani, C. Tellambura, and M. Di Renzo, "Relay selection in network-coded cooperative MIMO systems," *IEEE Trans. Commun.*, vol. 67, no. 8, pp. 5346–5361, Aug. 2019.

[59] A. R. Heidarpour, M. Ardakani, and C. Tellambura, "Network-coded cooperation with outdated CSI," *IEEE Commun. Lett.*, vol. 22, no. 8, pp. 1720–1723, Aug. 2018.

[60] A. R. Heidarpour, M. Ardakani, and C. Tellambura, "Network-coded cooperative MIMO with outdated CSI and CCI," in *Proc. IEEE 92nd Veh. Technol. Conf. (VTC-Fall)*, Nov. 2020, pp. 1–5.

[61] ——, "Generalized relay selection for network-coded cooperation systems," *IEEE Comm. Lett.*, vol. 21, no. 12, pp. 2742–2745, Dec. 2017.

[62] ——, "Network coded cooperation based on relay selection with imperfect CSI," in *Proc. IEEE 86th Veh. Technol. Conf. (VTC-Fall)*, Sept. 2017, pp. 1–5.

[63] F. Xu, F. C. M. Lau, Q. F. Zhou, and D. Yue, "Outage performance of cooperative communication systems using opportunistic relaying and selection combining receiver," *IEEE Signal Process. Lett.*, vol. 16, no. 4, pp. 237–240, Apr. 2009.

[64] S. Chu, "Performance of amplify-and-forward cooperative communications with the Nth best-relay selection scheme over Nakagami-m fading channels," *IEEE Commun. Lett.*, vol. 15, no. 2, pp. 172–174, Feb. 2011.

[65] Y. Kim and H. Liu, "Infrastructure relay transmission with cooperative MIMO," *IEEE Trans. Veh. Technol.*, vol. 57, no. 4, pp. 2180–2188, Jul. 2008.

[66] S. Thoen, L. V. der Perre, B. Gyselinckx, and M. Engels, "Performance analysis of combined transmit-SC/receive-MRC," *IEEE Trans. Commun.*, vol. 49, no. 1, pp. 5–8, Jan. 2001.

[67] A. R. Heidarpour and M. Ardakani, "Diversity analysis of MIMO network coded cooperation systems with relay selection," in *Proc. IEEE 86th Veh. Technol. Conf. (VTC-Fall)*, Sept. 2017, pp. 1–6.

[68] I. Gradshteyn, I. Ryzhik, and A. Jeffrey, *Table of Integrals, Series, and Products.* Academic Press, 2007.

[69] J. L. Vicario, A. Bel, J. A. Lopez-salcedo, and G. Seco, "Opportunistic relay selection with outdated CSI: outage probability and diversity analysis," *IEEE Trans. Wireless Commun.*, vol. 8, no. 6, pp. 2872–2876, Jun. 2009.

[70] L. Liu, R. Zhang, and K. Chua, "Wireless information transfer with opportunistic energy harvesting," *IEEE Trans. on Wireless Commun.*, vol. 12, no. 1, pp. 288–300, 2013.

[71] X. Zhou, R. Zhang, and C. K. Ho, "Wireless information and power transfer: Architecture design and rate-energy tradeoff," *IEEE Trans. on Commun.*, vol. 61, no. 11, pp. 4754–4767, 2013.

[72] L. R. Varshney, "Transporting information and energy simultaneously," in *Proc. IEEE Int. Symp. Inf. Theory (ISIT)*, 2008, pp. 1612–1616.

[73] L. Dai, B. Wang, Y. Yuan, S. Han, I. Chih-lin, and Z. Wang, "Non-orthogonal multiple access for 5G: solutions, challenges, opportunities, and future research trends," *IEEE Commun. Mag.*, vol. 53, no. 9, pp. 74–81, 2015.

[74] Z. Ding, X. Lei, G. K. Karagiannidis, R. Schober, J. Yuan, and V. K. Bhargava, "A survey on non-orthogonal multiple access for 5G networks: Research challenges and future trends," *EEE J. Sel. Areas Commun.*, vol. 35, no. 10, pp. 2181–2195, 2017.

[75] Z. Ding, Y. Liu, J. Choi, Q. Sun, M. Elkashlan, I. Chih-Lin, and H. V. Poor, "Application of non-orthogonal multiple access in LTE and 5G networks," *IEEE Commun. Mag.*, vol. 55, no. 2, pp. 185–191, 2017.